

---

# ARE GRAPH NEURAL NETWORKS OPTIMAL APPROXIMATION ALGORITHMS?

**Morris Yau**  
MIT CSAIL  
morrisy@mit.edu

**Eric Lu\***  
Harvard  
ericlu01@g.harvard.edu

**Nikolaos Karalias\***  
MIT CSAIL  
stalence@mit.edu

**Jessica Xu\***  
Reverie Labs  
jessica.peng.xu@gmail.com

**Stefanie Jegelka**  
MIT CSAIL  
stefje@mit.edu

## ABSTRACT

In this work we design graph neural network architectures that capture optimal approximation algorithms for a large class of combinatorial optimization problems, using powerful algorithmic tools from semidefinite programming (SDP). Concretely, we prove that polynomial-sized message-passing algorithms can represent the most powerful polynomial time algorithms for Max Constraint Satisfaction Problems assuming the Unique Games Conjecture. We leverage this result to construct efficient graph neural network architectures, OptGNN, that obtain high-quality approximate solutions on landmark combinatorial optimization problems such as Max-Cut, Min-Vertex-Cover, and Max-3-SAT. Our approach achieves strong empirical results across a wide range of real-world and synthetic datasets against solvers and neural baselines. Finally, we take advantage of OptGNN’s ability to capture convex relaxations to design an algorithm for producing bounds on the optimal solution from the learned embeddings of OptGNN.

## 1 INTRODUCTION

Combinatorial Optimization (CO) is the class of problems that optimize functions subject to constraints over discrete search spaces. They are often NP-hard to solve and to approximate, owing to their typically exponential search spaces over nonconvex domains. Nevertheless, their important applications in science and engineering (Gardiner et al., 2000; Zaki et al., 1997; Smith et al., 2004; Du et al., 2017) has engendered a long history of study rooted in the following simple insight. In practice, CO instances are endowed with domain-specific structure that can be exploited by specialized algorithms (Hespe et al., 2020; Walteros & Buchanan, 2019; Ganesh & Vardi, 2020). In this context, neural networks are natural candidates for learning and then exploiting patterns in the data distribution over CO instances.

The emerging field at the intersection of machine learning (ML) and combinatorial optimization (CO) has led to novel algorithms with promising empirical results for several CO problems. However, similar to classical approaches to CO, ML pipelines have to manage a tradeoff between efficiency and optimality. Indeed, prominent works in this line of research forego optimality and focus on parametrizing heuristics (Li et al., 2018; Khalil et al., 2017; Yolcu & Póczos, 2019; Chen & Tian, 2019) or by employing specialized models (Zhang et al., 2023; Nazari et al., 2018; Toenshoff et al., 2019; Xu et al., 2021; Min et al., 2022) and task-specific loss functions (Amizadeh et al., 2018; Karalias & Loukas, 2020; Wang et al., 2022; Karalias et al., 2022; Sun et al., 2022). Exact ML solvers that can guarantee optimality often leverage general techniques like branch and bound (Gasse et al., 2019; Paulus et al., 2022) and constraint programming (Parjadis et al., 2021; Cappart et al., 2019), which offer the additional benefit of providing approximate solutions together with a bound on the distance to the optimal solution. The downside of those methods is their exponential worst-case time complexity. Striking the right balance between efficiency and optimality is quite challenging, which leads us to the central question of this paper:

---

\*Equal Contribution.

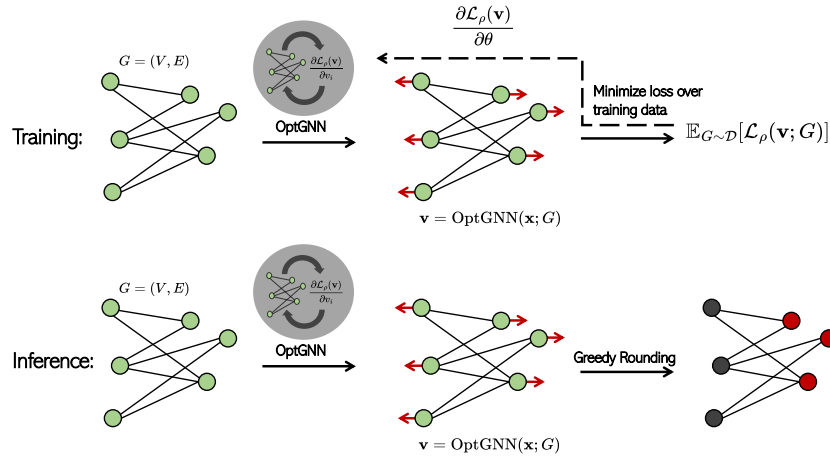


Figure 1: Schematic representation of OptGNN. During training, OptGNN produces node embeddings  $\mathbf{v}$  using message passing updates on the graph  $G$ . These embeddings are used to compute the penalized objective  $\mathcal{L}_p(\mathbf{v}; G)$ . OptGNN is trained by minimizing the average loss over the training set. At inference time, the fractional solutions (embeddings)  $\mathbf{v}$  for an input graph  $G$  produced by OptGNN are rounded using randomized rounding.

*Are there neural architectures for efficient combinatorial optimization that can learn to adapt to a data distribution over instances yet capture algorithms with **optimal** worst-case approximation guarantees?*

To answer this question, we build on the extensive literature on approximation algorithms and semidefinite programming. Convex relaxations of CO problems via semidefinite programming are the fundamental building block for breakthrough results in the design of efficient algorithms for NP-hard combinatorial problems, such as the Goemans-Williamson approximation algorithm for Max-Cut (Goemans & Williamson, 1995) and the use of the Lovász theta function to find the maximum independent set on perfect graphs (Lovász, 1979; Grötschel et al., 1981). For several problems, it is known that if the Unique Games Conjecture (UGC) is true, then the approximation guarantees obtained through semidefinite programming relaxations are indeed the best that can be achieved (Raghavendra, 2008; Barak & Steurer, 2014). We will leverage these results to provide an affirmative answer to our question. Our contributions can be organized into theory and experiments.

The theoretical contribution of this work is to show that a polynomial time message-passing algorithm approximates the solution of an SDP with the optimal integrality gap for the class of Maximum Constraint Satisfaction Problems (Max-CSP), assuming the UGC. Max-CSP is the problem of given a set of constraints over variables satisfy as many as possible. The key theoretical insight is that a message-passing algorithm can be used to compute gradient updates for the penalized Lagrangian of an overparameterized reformulation of the SDP in (Raghavendra, 2008). This in turn leads to our main contribution, OptGNN, a GNN architecture that generalizes our message-passing algorithm and therefore captures its approximation guarantee. Leveraging this result, we provide a perturbation analysis demonstrating OptGNN is efficiently PAC-learnable.

Our second contribution is empirical. We show that our theoretical construction can be used directly to design efficient graph neural network pipelines for CO that are easy to implement and train. By training with the SDP objective as a loss function, OptGNN learns embeddings that can be regarded as feasible fractional solutions of an overparameterized low-rank SDP, which are subsequently rounded to feasible integral solutions. We show OptGNN achieves strong empirical results against solvers and neural baselines across a broad battery of datasets for landmark CO problems such as Max-Cut, Vertex-Cover, and Max-3-SAT.

---

Finally, to underscore the fact that OptGNN captures powerful convex relaxations, we construct dual certificates of optimality, i.e. bounds that are provably correct, from OptGNN embeddings for the Max-Cut problem that are virtually tight for small synthetic instances. See our discussion on general neural certification schemes for extracting dual certificates from OptGNN networks in Appendix C.2. To summarize, the contribution of this paper is twofold:

- We construct a polynomial time message passing algorithm for solving the SDP of Raghavendra (2008) for the broad class of maximum constraint satisfaction problems (including Max-Cut, Max-SAT, etc.), that is optimal barring the possibility of significant breakthroughs in the foundations of algorithms.
- We construct a graph neural architecture to capture this message-passing algorithm and show that it achieves strong results against solvers and neural baselines.

## 2 BACKGROUND AND RELATED WORK

**Optimal Approximation Algorithms.** It is typically difficult to prove that an algorithm achieves the best approximation guarantee for a given problem, as it is hard to rule out the existence of a more powerful algorithm. The Unique Games Conjecture (UGC) (Khot, 2002) is a striking development in the theory of approximation algorithms because it can circumvent precisely this obstacle. If true, it implies approximation hardness results which often match the approximation guarantees of the best-known algorithms (Raghavendra & Steurer, 2009b; Raghavendra et al., 2012). For that reason, those algorithms are also sometimes referred to as UGC-optimal. More importantly, the UGC implies something even stronger: there is a *general* algorithm based on semidefinite programming that achieves the best possible approximation guarantees for the broad class of Max Constraint Satisfaction Problems (Raghavendra, 2008). For a complete exposition on the topic of UGC and approximation algorithms, we refer the reader to Barak & Steurer (2014). Our theoretical contribution builds on these ideas to construct a neural architecture that is a candidate optimal approximation algorithm.

**Neural approximation algorithms and their limitations.** The design of neural approximation algorithms typically involves the use of state of the art architectures like graph neural networks (GNN). There has been important progress in characterizing the combinatorial capabilities of those architectures, including bounds on the approximation guarantees achievable by GNNs on bounded degree graphs (Sato et al., 2019; 2021) and conditional impossibility results for solving classic combinatorial problems such as Max-Independent-Set and Min-Spanning-Tree (Loukas, 2019). It has been shown that a GNN can implement a distributed local algorithm that straightforwardly obtains a 1/2-approximation for Max-SAT (Liu et al., 2021), which is also achievable through a simple randomized algorithm (Johnson, 1973). Recent work proves there are barriers to the approximation power of GNNs for combinatorial problems including Max-Cut and Min-Vertex-Cover (Gamarnik, 2023) for constant depth GNNs. Other approaches to obtaining approximation guarantees propose avoiding the dependence of the model on the size of the instance with a divide-and-conquer strategy. This is done by partitioning the input into smaller subproblems of bounded size and using the neural network to solve each subproblem (McCarty et al., 2021; Kahng et al., 2023).

**Convex Relaxations and Machine Learning.** Convex relaxations are the workhorse of approximation algorithms; a discrete problem is first relaxed, solved, and then rounded to produce a high quality solution. SDPs are a particularly powerful tool in this context, as they often yield the strongest approximation guarantees for combinatorial problems.

In this work we show how SDP-based approximation algorithms can be incorporated into the architecture of neural networks. Efficient methods have been developed for solving low rank SDPs Burer & Monteiro (2003); Wang et al. (2017); Wang & Kolter (2019); Boumal et al. (2020). Building on these ideas, we design and then embed a UGC-optimal message passing algorithm within a GNN architecture. Beyond approximation algorithms, there is work on designing differentiable Max-SAT solvers via SDPs to facilitate symbolic reasoning in neural architectures (Wang et al., 2019). This approach uses a fixed algorithm for solving a novel SDP relaxation for Max-SAT, and aims to learn the structure of the SAT instance. In our case, the instance is given, but our algorithm is learnable, and we seek to predict the solution.

Semidefinite programming has a myriad of applications in machine learning including the design of high-dimensional differentiable extensions of discrete functions (Karalias et al., 2022) for neural CO, the use of neural networks to solve feasibility SDPs in quantum information tasks Kriváchy

et al. (2021), global minimization of functions via a kernel approach to semidefinite programming (Rudi et al., 2020), and leveraging the connection between SVMs and the Lovász theta function to efficiently find the largest common dense subgraph among a collection of graphs (Jethava et al., 2013).

Convex relaxations are also instrumental in Mixed Integer Programming. Convex relaxation guided branch-and-bound tree search is guaranteed to terminate with optimal integral solutions to Mixed Integer Linear Programs (MILP). Proposals for incorporating neural networks into the MILP pipeline include providing a “warm start” (Benidis et al., 2023) to the solver, learning branching heuristics (Gasse et al., 2019; Nair et al., 2020; Gupta et al., 2020; Paulus et al., 2022), and learning cutting plane protocols Paulus et al. (2022). A recent line of work studies the capabilities of neural networks to solve linear programs (Chen et al., 2022; Qian et al., 2023). It is shown that GNN’s can represent LP solvers, which may in turn explain the success of learning branching heuristics (Qian et al., 2023). In a similar line of work, neural nets are used to learn branching heuristics for CDCL SAT solvers (Selsam & Bjørner, 2019; Kurin et al., 2020; Wang et al., 2021). Finally, convex optimization has also found applications Numeroso et al. (2023) in the neural algorithmic reasoning paradigm (Veličković et al.; 2022) where neural networks are trained to solve problems by learning to emulate discrete algorithms in higher dimensional spaces.

**Learning frameworks for CO.** There are numerous viable design paradigms when it comes to developing effective neural CO architectures. Some works employ a supervised approach and rely on learning from execution traces of expert algorithms or labeled solutions to the problem they are trying to solve (Li et al., 2018; Selsam et al., 2018; Prates et al., 2019; Vinyals et al., 2015; Joshi et al., 2019; 2020; Gasse et al., 2019; Ibarz et al., 2022; Georgiev et al., 2023). Obtaining labels for combinatorial problems can be computationally costly. Consequently, a broad class of algorithms for neural CO involves training without any access to labels or partial solutions. This includes approaches based on Reinforcement Learning (Ahn et al., 2020; Böther et al., 2022; Barrett et al., 2020; 2022; Bello et al., 2016; Khalil et al., 2017; Yolcu & Póczos, 2019; Chen & Tian, 2019), and other self-supervised methods (Brusca et al., 2023; Karalias et al., 2022; Karalias & Loukas, 2020; Tönshoff et al., 2022; Schuetz et al., 2022a;b; Amizadeh et al., 2019; Dai et al., 2020; Sun et al., 2022; Wang et al., 2022; Amizadeh et al., 2018; Gaile et al., 2022). For a complete overview of the field, we refer the reader to the relevant survey papers (Cappart et al., 2023; Bengio et al., 2021). Our work falls into the latter category since only the problem instance is sufficient for training and supervision signals are not required.

### 3 OPTIMAL APPROXIMATION ALGORITHMS WITH NEURAL NETWORKS

We begin by showing that solving the Max-Cut problem using a vector (low-rank SDP) relaxation and a simple projected gradient descent scheme amounts to executing a message-passing algorithm on a graph. This sets the stage for our main result for the class of maximum constraint satisfaction problems (Max-CSP), which generalizes this insight. We reformulate the UGC-optimal SDP for Max-CSP in (SDP 1 top of pg. 19). Our main Theorem 3.1 exhibits a message passing algorithm (Algorithm 1) for solving SDP 1. We then capture Algorithm 1 via a message passing architecture (OptGNN) with learnable weights. Thus, by construction OptGNN captures algorithms with UGC-optimal approximation guarantees for Max-CSP. Furthermore, we prove that OptGNN is efficiently PAC-learnable (see Lemma 3.1) as a step towards explaining its empirical performance.

#### 3.1 SOLVING COMBINATORIAL OPTIMIZATION PROBLEMS WITH MESSAGE PASSING

In the Max-Cut problem, we are given a graph  $G = (V, E)$  with  $N$  vertices  $V$  and edges  $E$ . The goal is to divide the vertices into two sets that maximize the number of edges going between them. This corresponds to the following quadratic integer program.

$$\begin{aligned} \max_{(x_1, x_2, \dots, x_N)} \quad & \sum_{(i,j) \in E} \frac{1}{2}(1 - x_i x_j) \\ \text{subject to:} \quad & x_i^2 = 1 \quad \forall i \in [N] \end{aligned}$$

The global optimum of the integer program is the Max-Cut. Noting that discrete variables are not amenable to the tools of continuous optimization, a standard technique is to ‘lift’ the quadratic integer problem and solve it with a rank constrained SDP. Here we introduce a matrix  $X \in \mathbb{R}^{N \times N}$  of

variables, where we index the  $i$ 'th row and  $j$ 'th column entry as  $X_{ij}$ .

$$\begin{aligned} \max_X \quad & \sum_{(i,j) \in E} \frac{1}{2} (1 - X_{ij}) \\ \text{subject to:} \quad & X_{ii} = 1 \quad \forall i \in [N] \\ & X \succeq 0 \\ & \text{rank}(X) = r \end{aligned} \tag{1}$$

The intuition is that a rank  $r = 1$  solution to Problem 1 is equivalent to solving the integer program. A common approach is to replace the integer variables  $x_i$  with vectors  $v_i \in \mathbb{R}^r$  and constrain  $v_i$  to lie on the unit sphere.

$$\begin{aligned} \min_{v_1, v_2, \dots, v_N} \quad & - \sum_{(i,j) \in E} \frac{1}{2} (1 - \langle v_i, v_j \rangle) \\ \text{subject to:} \quad & \|v_i\| = 1 \quad \forall i \in [N] \\ & v_i \in \mathbb{R}^r \end{aligned} \tag{2}$$

This problem can be solved with a fast iterative algorithm Burer & Monteiro (2003). The landscape of this nonconvex optimization can be benign in that all local minima are approximately global minima (Ge et al., 2016) and variations on stochastic gradient descent converge to its optimum (Bhojanapalli et al., 2018; Jin et al., 2017) under a variety of smoothness and compactness assumptions. Specifically, for large enough  $r$  Boumal et al. (2020); O'Carroll et al. (2022), simple algorithms such as block coordinate descent (Erdogdu et al., 2019) can find an approximate global optimum of the objective. Projected gradient descent is a natural approach for solving the minimization problem in equation 2. In iteration  $t$  (for  $T$  iterations), update vector  $v_i$  as

$$\hat{v}_i^{t+1} = v_i^t - \eta \sum_{j \in N(i)} v_j^t \tag{4}$$

$$v_i^{t+1} = \hat{v}_i^{t+1} / \|\hat{v}_i^{t+1}\|, \tag{5}$$

where  $\eta \in \mathbb{R}^+$  is an adjustable step size and  $N(i)$  the neighborhood of node  $i$ . The gradient updates to the vectors are local, i.e., each vector is updated by aggregating information from its neighboring vectors. Hence, projected gradient descent can be implemented as a message-passing algorithm (See our precise definition of message passing algorithm in Definition C.1). Subsequently, the vectors can be rounded to an integral solution by taking a random projection with a hyperplane or any of a variety of rounding methods.

**OptGNN for Max-Cut.** Our main contribution in this paper builds on the following observation. We may generalize the dynamics described above by considering an overparametrized version of the gradient descent updates in equations 4 and 5. Let  $M_1, M_2, \dots, M_T \in \mathbb{R}^{r \times 2r}$  be a set of  $T$  learnable matrices corresponding to  $T$  layers of a neural network. Then for layer  $t$  and embedding  $v_i$  we have

$$\hat{v}_i^{t+1} := M_t \left( \begin{bmatrix} v_i^t \\ \sum_{j \in N(i)} v_j^t \end{bmatrix} \right) \tag{6}$$

$$v_i^{t+1} := \hat{v}_i^{t+1} / \|\hat{v}_i^{t+1}\|, \tag{7}$$

More generally, we can write the dynamics as

$$\hat{v}_i^{t+1} := M_t (\text{AGG}(v_i^t, \{v_j^t\}_{j \in N(i)})) \tag{8}$$

$$v_i^{t+1} := \text{NONLINEAR}(\hat{v}_i^{t+1}), \tag{9}$$

where AGG is a function of the node embedding and its neighboring embeddings. It is straightforward to see that these update dynamics can be captured by a Graph Neural Network (GNN). For a Max-Cut instance  $\Lambda$  specified by a graph  $G_\Lambda$ , we refer to equation 6 and equation 7 as the OptGNN for Max-Cut with learnable parameters  $M = \{M_t\}_{t \in [T]}$  over a constraint graph  $G_\Lambda$  denoted  $\text{OptGNN}_{(M, \Lambda)}$  (for formal definition see Definition 3.3). Furthermore, we exhibit a message passing algorithm 2 that generalizes the dynamics of 4 and 5 to the entire class of Max-CSPs, which provably converges in polynomial iterations for a reformulation of the canonical SDP relaxation of Raghavendra (2008) (see SDP 1 top of pg. 19 for reformulated SDP). For our main theorem on convergence see the informal statement Theorem 3.1 and formal statement Theorem C.1. For ease of reading, we suggest the reader first inspect the informal description of algorithm 1 before the formal description in algorithm 2. We also extend our OptGNN construction to the Min-Vertex-Cover problem and Max-3-SAT (see derivation in Appendix A and Appendix B).

### 3.2 MESSAGE PASSING FOR MAX-CSPs

Given a set of constraints over variables, Max-CSP asks to find a variable assignment that maximizes the number of satisfied constraints. Formally, a Constraint Satisfaction Problem  $\Lambda = (\mathcal{V}, \mathcal{P}, q)$  consists of a set of  $N$  variables  $\mathcal{V} := \{x_i\}_{i \in [N]}$  each taking values in an alphabet  $[q]$  and a set of predicates  $\mathcal{P} := \{P_z\}_{z \subseteq \mathcal{V}}$  where each predicate is a payoff function over  $k$  variables  $X_z = \{x_{i_1}, x_{i_2}, \dots, x_{i_k}\}$ . Here we refer to  $k$  as the arity of the Max- $k$ -CSP. We adopt the normalization that each predicate  $P_z$  returns outputs in  $[0, 1]$ . We index each predicate  $P_z$  by its domain  $z$ . The goal of Max- $k$ -CSP is to maximize the payoff of the predicates.

$$\text{OPT}(\Lambda) := \max_{(x_1, \dots, x_N) \in [q]^N} \frac{1}{|\mathcal{P}|} \sum_{P_z \in \mathcal{P}} P_z(X_z), \quad (10)$$

where we normalize by the number of constraints so that the total payoff is in  $[0, 1]$ . Therefore we can unambiguously define an  $\epsilon$ -approximate assignment as an assignment achieving a payoff of  $\text{OPT} - \epsilon$ . Since our result depends on a message-passing algorithm, we will need to define an appropriate graph structure over which messages will be propagated. To that end, we will leverage the constraint graph of the CSP instance: Given a Max- $k$ -CSP instance  $\Lambda = (\mathcal{V}, \mathcal{P}, q)$  a *constraint graph*  $G_\Lambda = (V, E)$  is comprised of vertices  $V = \{v_{\phi, \zeta}\}$  for every subset of variables  $\phi \subseteq z$  for every predicate  $P_z \in \mathcal{P}$  and every assignment  $\zeta \in [q]^{|\phi|}$  to the variables in  $z$ . The edges  $E$  are between any pair of vectors  $v_{\phi, \zeta}$  and  $v_{\phi', \zeta'}$  such that the variables in  $\phi$  and  $\phi'$  appear in a predicate together. For instance, for a SAT clause  $(x_1 \vee x_2) \wedge x_1 \wedge x_3$  there are four nodes  $v_1, v_{12}, v_3$  and  $v_\emptyset$  with a complete graph between  $\{v_1, v_{12}, v_\emptyset\}$  and  $v_3$  an isolated node.

We construct our message passing algorithm as follows. We formulate SDP 1, a general SDP for Max-CSPs that is equivalent to the UGC-optimal SDP of Raghavendra (2008). Concretely, let  $\text{SDP}(\Lambda)$  be the optimal value of the SDP 1 on instance  $\Lambda$ . Then, the *approximation ratio* for the Max- $k$ -CSP problem achieved by the SDP 1 is

$$\text{Approximation Ratio} := \min_{\Lambda \in \text{Max-}k\text{-CSP}} \frac{\text{OPT}(\Lambda)}{\text{SDP}(\Lambda)},$$

where the minimization is taken over all instances  $\Lambda$  with arity  $k$ . Note the approximation ratio is always smaller than one. Then, there is no polynomial time algorithm that can achieve a superior (larger) approximation ratio assuming the truth of the UGC. Next, based on SDP 1 we form a quadratically penalized Lagrangian  $\mathcal{L}_p(\mathbf{v}) = \mathcal{L}_o(\mathbf{v}) + \rho \mathcal{L}_c(\mathbf{v})^2$ . We then show that gradient descent on this Lagrangian takes the form of a message-passing algorithm that can provably converge to an approximate global optimum for the SDP. A simplified version of the algorithm is provided in algorithm 1. To emphasize the conceptual point, we abuse notation in algorithm 1 and use  $\mathcal{L}_o(v_i, v_j), \mathcal{L}_c(v_i, v_j)$  to denote the terms involving  $v_i$  and its neighbors  $v_j$  in the objective and the constraints of the Lagrangian respectively. See equation 61 and algorithm 2 for the detailed version of the Max-CSP message passing update. See appendix A and B for Min-Vertex-Cover and Max-3-SAT message passing updates.

Our main theorem is the following.

**Theorem 3.1.** (Informal) *Given a Max- $k$ -CSP instance  $\Lambda$ , there exists a message passing Algorithm 2 on constraint graph  $G_\Lambda$  with a per iteration update time of  $\text{poly}(|\mathcal{P}|q^k)$  that computes in  $\text{poly}(\epsilon^{-1}, |\mathcal{P}|q^k, \log(\delta^{-1}))$  iterations an  $\epsilon$ -approximate solution to SDP 1 with probability  $1 - \delta$ . That is to say, Algorithm 2 computes a set of vectors  $\mathbf{v}$  satisfying constraints of SDP 1 to error  $\epsilon$  with objective value denoted  $\text{OBJ}(\mathbf{v})$  satisfying  $|\text{OBJ}(\mathbf{v}) - \text{SDP}(\Lambda)| \leq \epsilon$  where  $\text{SDP}(\Lambda)$  is the optimum of SDP 1*

For the formal theorem and proof see Theorem C.1.

### 3.3 OPTGNN FOR MAX-CSP

The message-passing form of algorithm 1 allows us to define OptGNN, a natural GNN generalization that captures this gradient iteration.

**Definition** (OptGNN for Max-CSP). Let  $\Lambda$  be a Max-CSP instance on a constraint graph  $G_\Lambda$  with  $N$  nodes. Let  $U$  be an input matrix of dimension  $r \times N$  for the  $N$  nodes with embedding dimension  $r$ . Let  $\mathcal{L}_\rho$  be the loss defined as in equation 61 associated with the Max-CSP instance  $\Lambda$ . Let  $M$

be the OptGNN weights which are a set of matrices  $M := \{M_1, M_2, \dots, M_T\} \in \mathbb{R}^{r \times 2r}$ . We define  $\text{OptGNN}_{(M, \Lambda)} : \mathbb{R}^{r \times N} \rightarrow \mathbb{R}$  to be the function

$$\begin{aligned} \text{OptGNN}_{(M, \Lambda)}(U) = & \quad (11) \\ \mathcal{L}_\rho \circ \text{LAYER}_{M_T} \circ \dots \circ \text{LAYER}_{M_2} \circ \text{LAYER}_{M_1}(U). \end{aligned}$$

Here we define  $\text{LAYER}_{M_i} : \mathbb{R}^{r \times N} \rightarrow \mathbb{R}^{r \times N}$  to be the function  $\text{LAYER}_{M_i}(U) = M_i(\text{AGG}(U))$ , where  $\text{AGG} : \mathbb{R}^{r \times N} \rightarrow \mathbb{R}^{2r \times N}$  is the aggregation function:

$$\text{AGG}(U) := \begin{bmatrix} U \\ \nabla \mathcal{L}_\rho(U) \end{bmatrix}.$$

To update the parameters of OptGNN, We feed the output of the final layer  $\text{LAYER}_{M_T}$  to the Lagrangian  $\mathcal{L}_\rho : \mathbb{R}^{r \times N} \rightarrow \mathbb{R}$  and backpropagate its derivatives. It is important to emphasize that the data is the instance  $\Lambda$  and not the collection of vectors  $U$  which can be chosen entirely at random. The form of the gradient  $\nabla \mathcal{L}_\rho$  is a message passing algorithm over the nodes of the constraint graph  $G_\Lambda$ . Therefore, OptGNN is a message passing GNN over  $G_\Lambda$ . This point is of practical importance as it is what informs out implementation of the OptGNN architecture. To make the theoretical connection between OptGNN and SDP solving precise, we must ensure that a small amount of additive stochastic noise  $\{b_t\}_{t \in [T]}$  is added at each layer for the sake of theoretical convergence Jin et al. (2017) as  $\mathcal{L}_\rho$  has exponential saddle points. We then arrive at the following corollary.

**Corollary 1.** Given a Max-k-CSP instance  $\Lambda$ , there is an  $\text{OptGNN}_{(M, \Lambda)}$  with  $T = \text{poly}(\log(\delta^{-1}), \epsilon^{-1}, |\mathcal{P}|q^k)$  layers, and embeddings of dimension  $r = |\mathcal{P}|q^k$  such that there is an instantiation of learnable parameters  $M = \{M_t\}_{t \in [T]}$  and random perturbations  $b = \{b_t\}_{t \in [T]}$  that outputs a set of vectors  $\mathbf{v}$  satisfying the constraints of SDP 1 and approximating its optimum,  $\text{SDP}(\Lambda)$ , to error  $\epsilon$  with probability  $1 - \delta$  over the randomness in  $b$ .

Moving on from our result on representing approximation algorithms, it is natural to ask whether OptGNN is even learnable. That is to say, does OptGNN approximate the value of  $\text{SDP}(\Lambda)$  when given a polynomial amount of data? We provide a perturbation analysis to establish the polynomial sample complexity of PAC-learning OptGNN. The key idea is to bound the smoothness of the polynomial circuit AGG used in the OptGNN layer. We state the informal version below. For the formal version see Lemma E.5

**Lemma 3.1** (PAC learning (informal)). Let  $\Lambda$  be a dataset of Max-k-CSP instances over an alphabet of size  $[q]$ . Here the dataset  $\Lambda := \Lambda_1, \Lambda_2, \dots, \Lambda_\Gamma \sim \mathcal{D}$  is drawn i.i.d from a distribution over instances  $\mathcal{D}$  with no more than  $|\mathcal{P}|$  predicates. Let  $M$  be a set of parameters  $M = \{M_1, M_2, \dots, M_T\}$  in a parameter space  $\Theta$ . Then for  $T = O(|\mathcal{P}|^4 q^{4k})$ , for  $\Gamma = O(\frac{1}{\epsilon^4} |\mathcal{P}|^6 q^{6k} \log^4(\delta^{-1}))$ , let  $\hat{M}$  be the empirical loss minimizer for arbitrary choice of initial embeddings  $U$ .

$$\hat{M} := \arg \min_{M \in \Theta} \frac{1}{\Gamma} \sum_{i \in [\Gamma]} \text{OptGNN}_{(M, \Lambda_i)}(U)$$

Let the empirical loss be denoted

$$\text{EMP}(\Lambda) := \frac{1}{\Gamma} \sum_{i \in [\Gamma]} \text{OptGNN}_{(\hat{M}, \Lambda_i)}(U)$$

Then we have that OptGNN is  $(\Gamma, \epsilon, \delta)$ -PAC learnable. That is to say the empirical loss is within  $\epsilon$  from the optimal distributional loss with probability greater than  $1 - \delta$ :

$$\Pr[|\text{EMP}(\Lambda) - \mathbb{E}_{\Lambda \sim \mathcal{D}}[\text{SDP}(\Lambda)]| \leq \epsilon] \geq 1 - \delta.$$

We note that this style of perturbation analysis is akin to the VC theory on neural networks adapted to our unsupervised setting. As such, our analysis does not provide an explanation for why deep neural networks can learn with fewer samples than parameters which is a notorious challenge in learning theory Bartlett et al. (2021). Nevertheless, our analysis sheds light on how architectures that capture gradient iterations can successfully generalize.

**Obtaining neural certificates.** The goal of OptGNN is to find high-quality solutions to CO problems by capturing powerful convex relaxations. To underscore this point, we construct dual certificates of optimality from the embeddings of OptGNN. The certificates provide a bound on the optimal

---

**Algorithm 1** Message Passing for Max-CSP (informal).

---

**Input: Max-CSP Instance**  $\Lambda$   
{ $\rho$ : penalty for the constraint}  
{ $\mathcal{L}_o$ : objective component of the penalized objective}  
{ $\mathcal{L}_c$ : constraint component of the penalized objective}  
 $\mathbf{v}^0 \leftarrow \text{Uniform}(\mathcal{S}^{n-1})$  {Initialize vectors to uniform on the unit sphere}  
**for**  $t = 1, 2, \dots, T$  **do**  
  **what**  
  **for**  $v_w^t \in \mathbf{v}^t$  {message passing on the constraint graph} **do**  
    **what**  
      
$$\frac{\partial \mathcal{L}(\mathbf{v}^t)}{\partial v_i} = \sum_{j \in \mathcal{N}(i)} \frac{\partial (\mathcal{L}_o(v_i, v_j) + \rho \mathcal{L}_c(v_i, v_j)^2)}{\partial v_i}$$
  
      
$$v_i^{t+1} \leftarrow v_i^t - \eta \frac{\partial \mathcal{L}(\mathbf{v})}{\partial v_i}$$
  
      **if**  $\|v_i^{t+1} - v_i^t\| \leq \psi$  **then**  
         $v_i^{t+1} \leftarrow v_i^{t+1} + \mathcal{N}(0, \sigma I)$   
      **end if**  
    **end for**  
  **end for**  
  **return**  $\mathbf{v}^t$   
**Output: vector solution for SDP 1**

---

solution of the SDP and can be computed directly from the embeddings produced by OptGNN. The key idea is to estimate the dual variables of SDP 1 from the output embeddings/SDP solution  $\mathbf{v}$ . Since we use a quadratic penalty for constraints, the natural dual estimate is one step of the augmented method of Lagrange multipliers on the SDP solution which can be obtained straightforwardly from the overparameterized primal problem variables  $\mathbf{v}$ . Of course, this estimate need not be dual feasible. To handle this problem we analytically bound the error in satisfying the KKT conditions of SDP 1. See C.2 for derivations and extended discussion, and 4.2 for an experimental demonstration.

### 3.4 OPTGNN IN PRACTICE

Figure 1 summarizes the OptGNN pipeline for solving CO problems. To run the forward pass, the first step is message passing. Given a graph  $G$  with  $N$  nodes, from some initial features as input, OptGNN computes the node embeddings  $\mathbf{v} \in \mathbb{R}^{N \times r}$  using message passing per equation 11. Please refer to the pseudocode for Max-Cut in 3 and for general SDPs in 4.

After message passing, we compute  $\mathcal{L}(\mathbf{v}; G)$ . For Max-Cut, this is  $-\sum_{(i,j) \in E} \frac{1}{2}(1 - \langle v_i, v_j \rangle)$ . In training, we treat this as the loss and call the backward pass to calculate gradients. We use Adam (Kingma & Ba, 2014) to update the parameter matrices  $M$ . The same approach is used for other problems; see Appendix A for examples of other loss functions. Given a training distribution  $\mathcal{D}$ , the network is trained in a completely unsupervised fashion by minimizing  $\mathbb{E}_{G \sim \mathcal{D}}[\mathcal{L}(\mathbf{v}; G)]$  with a standard automatic differentiation package like PyTorch (Paszke et al., 2019).

A practical benefit of our approach is that users do not need to reimplement the network to handle each new problem. Users need only implement the appropriate Lagrangian, and our implementation uses automatic differentiation to compute the messages in the forward pass.

To obtain a discrete solution at inference time, the vectors solving the SDP must be rounded. To do this, we select a random hyperplane vector  $y \in \mathbb{R}^r$ , and for each node with embedding vector  $v_i$ , we calculate its discrete assignment  $x_i \in \{-1, 1\}$  as  $x_i = \text{sign}(v_i^\top y)$ . We use multiple hyperplanes and pick the best resulting solution.

## 4 EXPERIMENTS

This section is organized as follows. First, we provide a comprehensive experimental evaluation of the OptGNN pipeline on several problems and datasets and compare it against solvers and neural baselines. We then describe a model ablation study, an out-of-distribution performance (OOD) study, and an experiment with our neural certification scheme.



Dataset	OptGNN	Greedy	Gurobi 0.1s	Gurobi 1.0s
BA <sup>a</sup> (400,500)	2197.99 (66)	1255.22	2208.11	2208.11
ER <sup>a</sup> (400,500)	16387.46 (225)	8622.34	16476.72	16491.60
HK <sup>a</sup> (400,500)	2159.90 (61)	1230.98	2169.46	2169.46
WC <sup>a</sup> (400,500)	1166.47 (78)	690.19	1173.45	1175.97
ENZYMES <sup>b</sup>	81.37 (14)	48.53	81.45	81.45
COLLAB <sup>b</sup>	2622.41 (22)	1345.70	2624.32	2624.57
REDDIT-M-12K <sup>c</sup>	568.00 (89)	358.40	567.71	568.91
REDDIT-M-5K <sup>c</sup>	786.09 (133)	495.02	785.44	787.48

Table 1: Performance of OptGNN, Greedy, and Gurobi 0.1s, 1s, and 8s on Maximum Cut. For each approach and dataset, we report the average cut size measured on the test slice. Here, higher score is better. In parentheses, we include the average runtime in *milliseconds* for OptGNN.

Dataset	$r = 4.00$	$r = 4.15$	$r = 4.30$
ErdősGNN	$5.46^{\pm 1.91}$ (0.01)	$6.14^{\pm 2.01}$ (0.01)	$6.79^{\pm 2.03}$ (0.01)
Walksat100	$0.14^{\pm 0.36}$ (0.12)	$0.36^{\pm 0.52}$ (0.25)	$0.68^{\pm 0.65}$ (0.40)
Walksat1	$0.94^{\pm 0.92}$ (0.01)	$1.46^{\pm 1.11}$ (0.01)	$1.97^{\pm 1.28}$ (0.01)
OptGNN	$4.46^{\pm 1.68}$ (0.01)	$5.15^{\pm 1.76}$ (0.01)	$5.84^{\pm 2.18}$ (0.01)
Autograd	$6.85^{\pm 2.33}$ (6.80)	$7.52^{\pm 2.38}$ (6.75)	$8.32^{\pm 2.50}$ (6.77)

Table 2: Average number of unsatisfied clauses for Max-3-SAT on random instances with  $N = 100$  variables and clause ratios  $r = 4.00, 4.15, 4.30$ . Standard deviation is reported in superscript. In parentheses, we report the average time per instance on the test set in seconds. The number next to Walksat indicates the number of restarts.

#### 4.1 COMPARISONS WITH CLASSICAL ALGORITHMS

We report experimental measurements of the performance of the OptGNN approach on NP-Hard combinatorial optimization problems: *Maximum Cut*, *Minimum Vertex Cover*, and *Maximum 3-SAT*. We obtain results for several datasets and compare against greedy algorithms, local search, a state-of-the-art MIP solver (Gurobi), and various neural baselines. For Max-3-SAT and Min-Vertex-Cover we derive a quadratically penalized loss based on the SDP formulation of those problems. For details of the experimental setup see Appendix D.

Method	RB200	RB500
CMP	1.031 $\pm 0.006$	1.015 $\pm 0.004$
ErdősGNN	1.031 $\pm 0.004$	1.021 $\pm 0.002$
Meta-EGN	1.028 $\pm 0.005$	1.016 $\pm 0.002$
RUN-CSP	1.124 $\pm 0.001$	1.062 $\pm 0.005$
OptGNN	1.012 $\pm 0.006$	1.013 $\pm 0.003$
Greedy MVC	1.027 $\pm 0.007$	1.014 $\pm 0.003$
Gurobi 10.0 (0.5s)	1.009 $\pm 0.006$	1.013 $\pm 0.004$
Gurobi 10.0 (1s)	1.002 $\pm 0.003$	1.012 $\pm 0.003$
Gurobi 10.0 (5s)	1.000 $\pm 0.001$	1.004 $\pm 0.003$

Table 3: Average approximation ratio for vertex covers on forced RB instances, with standard deviations reported in superscript. Here, lower is better, and a ratio of 1.000 represents finding the minimum vertex cover.

Method	$N = 800$	$N = 1000$	$N = 2000$	$N \geq 3000$
Greedy	411.44	359.11	737.00	774.25
SDP	245.44	229.22	-	-
RUNCSP	185.89	156.56	357.33	401.00
ECO-DQN	65.11	54.67	157.00	428.25
ECORD	8.67	8.78	39.22	187.75
ANYCSP	1.22	2.44	13.11	51.63
OptGNN	109.22	125.00	284.67	549.38

Table 4: Comparison on GSET instances for Max-Cut against state of the art neural baselines. Numbers reported are the mean deviations from the best known Max-Cut values, reported as  $f_{\text{best}}$  in table 2 of Benlic & Hao (2013). Lower is better.

**Min-Vertex-Cover experiments.** We evaluated OptGNN on forced RB instances, which are hard vertex cover instances from the RB random CSP model that contain hidden optimal solutions (Xu et al., 2007). We considered two forced RB distributions, RB200 and RB500, as specified in prior work (Wang & Li, 2023). The results are in Table 3, which also includes the performance of several neural and classical baselines as reported in (Wang & Li, 2023; Brusca et al., 2023). OptGNN consistently outperforms state-of-the-art unsupervised baselines on this task and is even able to match the performance of Gurobi with a 0.5s time limit.

**Max-3-SAT experiment and ablation.** The purpose of this experiment is twofold: to demonstrate the viability of OptGNN on the Max-3-SAT problem and to examine the role of overparameterization in OptGNN. We generate 3-SAT formulae on the fly with 100 variables and a random number of clauses in the  $[400, 430]$  interval, and train OptGNN for 100,000 iterations. We then test on instances with 100 variables and  $\{400, 415, 430\}$  clauses. The results are in Table 2. We compare with WalkSAT, a classic local search algorithm for SAT, and ErdosGNN Karalias & Loukas (2020), a neural baseline trained in the same way. Furthermore, we compare with a simple baseline reported as ‘‘Autograd’’ that implements gradient descent directly on the Lagrangian. For details see D.1. OptGNN is able to outperform ErdosGNN consistently and improves significantly over Autograd, which supports the overparameterized message passing of OptGNN.

**Max-Cut experiments.** Table 6 presents a comparison between OptGNN, a greedy algorithm, and Gurobi for Max-Cut. OptGNN is competitive with Gurobi when run on a similar time budget and clearly outperforms greedy on all datasets. For results on more datasets see D.2. We generated Erdos-Renyi graphs  $\mathcal{G}_{n,p}$  for  $n \in [400, 500]$  and  $p = 0.15$  on the fly and trained an OptGNN for 20k iterations. Table 4 shows test results on GSET benchmark instances (Benlic & Hao, 2013). Furthermore, we report the performance for several other baselines, including a greedy algorithm, the Goemans-Williamson SDP, and neural baselines. We can see that OptGNN consistently outperforms the SDP and the greedy algorithm, while also being competitive with the neural baselines. However, OptGNN is not able to outperform ANYCSP, which to the best of our knowledge achieves the current state-of-the-art results.

**Out of distribution generalization.** We tested OptGNN’s ability to perform well on data distributions (for the same optimization problem) that it was not trained on. We test this using a collection of different datasets. The results can be seen in table 9 and subsection D.5. Overall, the results show that the model is capable of performing well even on datasets it has not been trained on.

**Model ablation.** We train modern GNN architectures from the literature with the same loss function and compare them against OptGNN. Please see D.3 for more details and results on multiple datasets for two different problems. Overall, OptGNN is the best performing model on both problems across all datasets.

## 4.2 EXPERIMENTAL DEMONSTRATION OF NEURAL CERTIFICATES.

In this section, we provide a simple experimental example of our neural certificate scheme on small synthetic instances. Deploying this scheme on Max-Cut on random graphs, we find this dual certificate to be remarkably tight. An example can be seen in figure 2. For 100 node graphs with 1000 edges our certificates deviate from the SDP certificate by about 20 nodes but are dramatically faster to produce. The runtime is dominated by the feedforward of OptGNN which is 0.02 seconds vs.

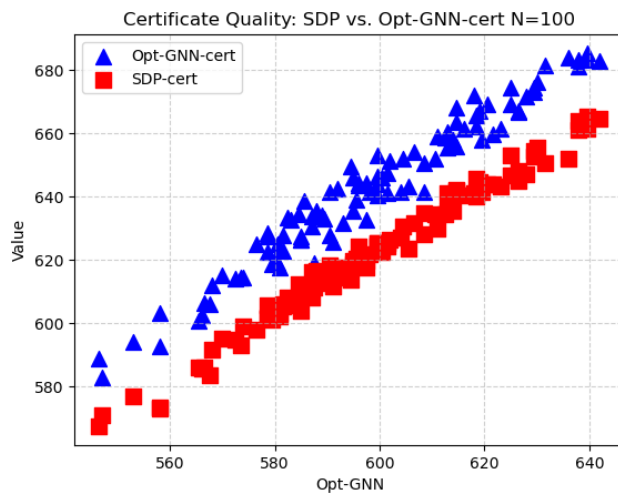


Figure 2: Experimental comparison of SDP versus OptGNN Dual Certificates on random graphs of 100 nodes for the Max-Cut problem. Our OptGNN certificates track closely with the SDP certificates while taking considerably less time to generate.

the SDP solve time which is 0.5 seconds on cvxpy. See C.2 for extensive discussion and additional results.

## 5 CONCLUSION

We have presented OptGNN, a GNN that can capture provably optimal message passing algorithms for a large class of combinatorial optimization problems. OptGNN achieves the appealing combination of obtaining approximation guarantees while also being able to adapt to the data to achieve improved results. Empirically, we observed that the OptGNN architecture achieves strong performance on a wide range of datasets and on multiple problems. OptGNN opens up several directions for future exploration, such as the design of more powerful and sound (neural) rounding procedures that can secure approximation guarantees, the construction of neural certificates that improve upon the ones we described in Appendix C.2, and the design of neural SDP-based branch and bound solvers.

## 6 IMPACT STATEMENT

This paper presents work whose goal is to advance the field of Machine Learning. There are many potential societal consequences of our work, none of which we feel must be specifically highlighted here.

---

## REFERENCES

- Sungsoo Ahn, Younggyo Seo, and Jinwoo Shin. Learning what to defer for maximum independent sets. In *International Conference on Machine Learning*, pp. 134–144. PMLR, 2020.
- Saeed Amizadeh, Sergiy Matushevych, and Markus Weimer. Learning to solve circuit-sat: An unsupervised differentiable approach. 2018.
- Saeed Amizadeh, Sergiy Matushevych, and Markus Weimer. Pdp: A general neural framework for learning constraint satisfaction solvers, 2019.
- Boaz Barak and David Steurer. Sum-of-squares proofs and the quest toward optimal algorithms. *arXiv preprint arXiv:1404.5236*, 2014.
- Thomas Barrett, William Clements, Jakob Foerster, and Alex Lvovsky. Exploratory combinatorial optimization with reinforcement learning. In *Proceedings of the AAAI conference on artificial intelligence*, volume 34, pp. 3243–3250, 2020.
- Thomas D Barrett, Christopher WF Parsonson, and Alexandre Laterre. Learning to solve combinatorial graph partitioning problems via efficient exploration. *arXiv preprint arXiv:2205.14105*, 2022.
- Peter L. Bartlett, Andrea Montanari, and Alexander Rakhlin. Deep learning: a statistical viewpoint, 2021.
- Irwan Bello, Hieu Pham, Quoc V Le, Mohammad Norouzi, and Samy Bengio. Neural combinatorial optimization with reinforcement learning. *arXiv preprint arXiv:1611.09940*, 2016.
- Yoshua Bengio, Andrea Lodi, and Antoine Prouvost. Machine learning for combinatorial optimization: a methodological tour d’horizon. *European Journal of Operational Research*, 290(2):405–421, 2021.
- Konstantinos Benidis, Ugo Rosolia, Syama Rangapuram, George Iosifidis, and Georgios Paschos. Solving recurrent mips with semi-supervised graph neural networks. *arXiv preprint arXiv:2302.11992*, 2023.
- Una Benlic and Jin-Kao Hao. Breakout local search for the max-cut problem. *Engineering Applications of Artificial Intelligence*, 26(3):1162–1173, 2013.
- Srinadh Bhojanapalli, Nicolas Boumal, Prateek Jain, and Praneeth Netrapalli. Smoothed analysis for low-rank solutions to semidefinite programs in quadratic penalty form, 2018.
- Maximilian Böther, Otto Kißig, Martin Taraz, Sarel Cohen, Karen Seidel, and Tobias Friedrich. What’s wrong with deep learning in tree search for combinatorial optimization. *arXiv preprint arXiv:2201.10494*, 2022.
- Nicolas Boumal, Vladislav Voroninski, and Afonso S Bandeira. Deterministic guarantees for burer-monteiro factorizations of smooth semidefinite programs. *Communications on Pure and Applied Mathematics*, 73(3):581–608, 2020.
- Lorenzo Brusca, Lars CPM Quaedvlieg, Stratis Skoulakis, Grigorios G Chrysos, and Volkan Cevher. Maximum independent set: Self-training through dynamic programming. In *Advances in neural information processing systems (NeurIPS)*, 2023.
- Samuel Burer and Renato Monteiro. A nonlinear programming algorithm for solving semidefinite programs via low-rank factorization. *Mathematical Programming, Series B*, 95:329–357, 02 2003. doi: 10.1007/s10107-002-0352-8.
- Quentin Cappart, Emmanuel Goutierre, David Bergman, and Louis-Martin Rousseau. Improving optimization bounds using machine learning: decision diagrams meet deep reinforcement learning. In *Proceedings of the AAAI Conference on Artificial Intelligence*, volume 33, pp. 1443–1451, 2019.
- Quentin Cappart, Didier Chételat, Elias B Khalil, Andrea Lodi, Christopher Morris, and Petar Velickovic. Combinatorial optimization and reasoning with graph neural networks. *J. Mach. Learn. Res.*, 24:130–1, 2023.

- 
- Xinyun Chen and Yuandong Tian. Learning to perform local rewriting for combinatorial optimization. In *Advances in Neural Information Processing Systems*, pp. 6278–6289, 2019.
- Ziang Chen, Jialin Liu, Xinshang Wang, Jianfeng Lu, and Wotao Yin. On representing linear programs by graph neural networks. *arXiv preprint arXiv:2209.12288*, 2022.
- Hanjun Dai, Xinshi Chen, Yu Li, Xin Gao, and Le Song. A framework for differentiable discovery of graph algorithms. 2020.
- Jiaoman Du, Xiang Li, Lean Yu, Ralescu Dan, and Jiandong Zhou. Multi-depot vehicle routing problem for hazardous materials transportation: A fuzzy bilevel programming. *Information sciences*, 399:201–218, 2017.
- Vijay Prakash Dwivedi, Chaitanya K Joshi, Anh Tuan Luu, Thomas Laurent, Yoshua Bengio, and Xavier Bresson. Benchmarking graph neural networks. *arXiv preprint arXiv:2003.00982*, 2020.
- Vijay Prakash Dwivedi, Anh Tuan Luu, Thomas Laurent, Yoshua Bengio, and Xavier Bresson. Graph neural networks with learnable structural and positional representations. *arXiv preprint arXiv:2110.07875*, 2021.
- Murat A. Erdogdu, Asuman Ozdaglar, Pablo A. Parrilo, and Nuri Denizcan Vanli. Convergence rate of block-coordinate maximization burer-monteiro method for solving large sdps, 2019.
- Elīza Gaile, Andis Draguns, Emīls Ozoliņš, and Kārlis Freivalds. Unsupervised training for neural tsp solver. In *International Conference on Learning and Intelligent Optimization*, pp. 334–346. Springer, 2022.
- David Gamarnik. Barriers for the performance of graph neural networks (gnn) in discrete random structures. *Proceedings of the National Academy of Sciences*, 120(46):e2314092120, 2023.
- Vijay Ganesh and Moshe Y Vardi. On the unreasonable effectiveness of sat solvers. *Beyond the Worst-Case Analysis of Algorithms*, pp. 547–566, 2020.
- Eleanor J Gardiner, Peter Willett, and Peter J Artymiuk. Graph-theoretic techniques for macromolecular docking. *Journal of Chemical Information and Computer Sciences*, 40(2):273–279, 2000.
- Maxime Gasse, Didier Chételat, Nicola Ferroni, Laurent Charlin, and Andrea Lodi. Exact combinatorial optimization with graph convolutional neural networks. *arXiv preprint arXiv:1906.01629*, 2019.
- Rong Ge, Jason D. Lee, and Tengyu Ma. Matrix completion has no spurious local minimum. *CoRR*, abs/1605.07272, 2016. URL <http://arxiv.org/abs/1605.07272>.
- Dobrik Georgiev, Danilo Numeroso, Davide Bacciu, and Pietro Liò. Neural algorithmic reasoning for combinatorial optimisation. *arXiv preprint arXiv:2306.06064*, 2023.
- Michel X Goemans and David P Williamson. Improved approximation algorithms for maximum cut and satisfiability problems using semidefinite programming. *Journal of the ACM (JACM)*, 42(6): 1115–1145, 1995.
- Martin Grötschel, László Lovász, and Alexander Schrijver. The ellipsoid method and its consequences in combinatorial optimization. *Combinatorica*, 1:169–197, 1981.
- Prateek Gupta, Maxime Gasse, Elias Khalil, Pawan Mudigonda, Andrea Lodi, and Yoshua Bengio. Hybrid models for learning to branch. *Advances in neural information processing systems*, 33: 18087–18097, 2020.
- Aric A. Hagberg, Daniel A. Schult, and Pieter J. Swart. Exploring network structure, dynamics, and function using networkx. In Gaël Varoquaux, Travis Vaught, and Jarrod Millman (eds.), *Proceedings of the 7th Python in Science Conference*, pp. 11 – 15, Pasadena, CA USA, 2008.
- Demian Hespe, Sebastian Lamm, Christian Schulz, and Darren Strash. Wegotyoucovered: The winning solver from the pace 2019 challenge, vertex cover track. In *2020 Proceedings of the SIAM Workshop on Combinatorial Scientific Computing*, pp. 1–11. SIAM, 2020.

- 
- Borja Ibarz, Vitaly Kurin, George Papamakarios, Kyriacos Nikiforou, Mehdi Bennani, Róbert Csordás, Andrew Joseph Dudzik, Matko Bošnjak, Alex Vitvitskyi, Yulia Rubanova, et al. A generalist neural algorithmic learner. In *Learning on Graphs Conference*, pp. 2–1. PMLR, 2022.
- Vinay Jethava, Anders Martinsson, Chiranjib Bhattacharyya, and Devdatt Dubhashi. Lovász  $\vartheta$  function, svms and finding dense subgraphs. *The Journal of Machine Learning Research*, 14(1): 3495–3536, 2013.
- Chi Jin, Rong Ge, Praneeth Netrapalli, Sham M. Kakade, and Michael I. Jordan. How to escape saddle points efficiently, 2017.
- David S Johnson. Approximation algorithms for combinatorial problems. In *Proceedings of the fifth annual ACM symposium on Theory of computing*, pp. 38–49, 1973.
- Chaitanya K Joshi, Thomas Laurent, and Xavier Bresson. An efficient graph convolutional network technique for the travelling salesman problem. *arXiv preprint arXiv:1906.01227*, 2019.
- Chaitanya K Joshi, Quentin Cappart, Louis-Martin Rousseau, and Thomas Laurent. Learning tsp requires rethinking generalization. *arXiv preprint arXiv:2006.07054*, 2020.
- Andrew B Kahng, Robert R Nerem, Yusu Wang, and Chien-Yi Yang. Nn-steiner: A mixed neural-algorithmic approach for the rectilinear steiner minimum tree problem. *arXiv preprint arXiv:2312.10589*, 2023.
- Nikolaos Karalias. Probabilistic methods for neural combinatorial optimization. Technical report, EPFL, 2023.
- Nikolaos Karalias and Andreas Loukas. Erdos goes neural: an unsupervised learning framework for combinatorial optimization on graphs. *arXiv preprint arXiv:2006.10643*, 2020.
- Nikolaos Karalias, Joshua Robinson, Andreas Loukas, and Stefanie Jegelka. Neural set function extensions: Learning with discrete functions in high dimensions. *Advances in Neural Information Processing Systems*, 35:15338–15352, 2022.
- Elias Khalil, Hanjun Dai, Yuyu Zhang, Bistra Dilkina, and Le Song. Learning combinatorial optimization algorithms over graphs. In *Advances in Neural Information Processing Systems*, pp. 6348–6358, 2017.
- Subhash Khot. On the power of unique 2-prover 1-round games. In *Proceedings of the thirty-fourth annual ACM symposium on Theory of computing*, pp. 767–775, 2002.
- Diederik P Kingma and Jimmy Ba. Adam: A method for stochastic optimization. *arXiv preprint arXiv:1412.6980*, 2014.
- Tamás Kriváchy, Yu Cai, Joseph Bowles, Daniel Cavalcanti, and Nicolas Brunner. High-speed batch processing of semidefinite programs with feedforward neural networks. *New Journal of Physics*, 23(10):103034, 2021.
- Vitaly Kurin, Saad Godil, Shimon Whiteson, and Bryan Catanzaro. Can q-learning with graph networks learn a generalizable branching heuristic for a sat solver? *Advances in Neural Information Processing Systems*, 33:9608–9621, 2020.
- Yujia Li, Daniel Tarlow, Marc Brockschmidt, and Richard Zemel. Gated graph sequence neural networks. *arXiv preprint arXiv:1511.05493*, 2015.
- Zhuwen Li, Qifeng Chen, and Vladlen Koltun. Combinatorial optimization with graph convolutional networks and guided tree search. In *Advances in Neural Information Processing Systems*, pp. 539–548, 2018.
- Minghao Liu, Fuqi Jia, Pei Huang, Fan Zhang, Yuchen Sun, Shaowei Cai, Feifei Ma, and Jian Zhang. Can graph neural networks learn to solve maxsat problem? *arXiv preprint arXiv:2111.07568*, 2021.
- Andreas Loukas. What graph neural networks cannot learn: depth vs width, 2019.

- 
- László Lovász. On the shannon capacity of a graph. *IEEE Transactions on Information theory*, 25(1): 1–7, 1979.
- Evan McCarty, Qi Zhao, Anastasios Sidiropoulos, and Yusu Wang. Nn-baker: A neural-network infused algorithmic framework for optimization problems on geometric intersection graphs. *Advances in Neural Information Processing Systems*, 34:23023–23035, 2021.
- Yimeng Min, Frederik Wenkel, Michael Perlmutter, and Guy Wolf. Can hybrid geometric scattering networks help solve the maximum clique problem? *Advances in Neural Information Processing Systems*, 35:22713–22724, 2022.
- Christopher Morris, Martin Ritzert, Matthias Fey, William L Hamilton, Jan Eric Lenssen, Gaurav Rattan, and Martin Grohe. Weisfeiler and leman go neural: Higher-order graph neural networks. In *Proceedings of the AAAI conference on artificial intelligence*, volume 33, pp. 4602–4609, 2019.
- Vinod Nair, Sergey Bartunov, Felix Gimeno, Ingrid Von Glehn, Pawel Lichocki, Ivan Lobov, Brendan O’Donoghue, Nicolas Sonnerat, Christian Tjandraatmadja, Pengming Wang, et al. Solving mixed integer programs using neural networks. *arXiv preprint arXiv:2012.13349*, 2020.
- Mohammadreza Nazari, Afshin Oroojlooy, Lawrence Snyder, and Martin Takác. Reinforcement learning for solving the vehicle routing problem. In *Advances in Neural Information Processing Systems*, pp. 9839–9849, 2018.
- Danilo Numeroso, Davide Bacciu, and Petar Veličković. Dual algorithmic reasoning. *arXiv preprint arXiv:2302.04496*, 2023.
- Liam O’Carroll, Vaidehi Srinivas, and Aravindan Vijayaraghavan. The burer-monteiro sdp method can fail even above the barvinok-pataki bound. *Advances in Neural Information Processing Systems*, 35:31254–31264, 2022.
- Augustin Parjadis, Quentin Cappart, Louis-Martin Rousseau, and David Bergman. Improving branch-and-bound using decision diagrams and reinforcement learning. In *Integration of Constraint Programming, Artificial Intelligence, and Operations Research: 18th International Conference, CPAIOR 2021, Vienna, Austria, July 5–8, 2021, Proceedings 18*, pp. 446–455. Springer, 2021.
- Adam Paszke, Sam Gross, Francisco Massa, Adam Lerer, James Bradbury, Gregory Chanan, Trevor Killeen, Zeming Lin, Natalia Gimelshein, Luca Antiga, et al. Pytorch: An imperative style, high-performance deep learning library. *Advances in neural information processing systems*, 32, 2019.
- Max B Paulus, Giulia Zarpellon, Andreas Krause, Laurent Charlin, and Chris Maddison. Learning to cut by looking ahead: Cutting plane selection via imitation learning. In *International conference on machine learning*, pp. 17584–17600. PMLR, 2022.
- Marcelo Prates, Pedro HC Avelar, Henrique Lemos, Luis C Lamb, and Moshe Y Vardi. Learning to solve np-complete problems: A graph neural network for decision tsp. In *Proceedings of the AAAI Conference on Artificial Intelligence*, volume 33, pp. 4731–4738, 2019.
- Chendi Qian, Didier Chételat, and Christopher Morris. Exploring the power of graph neural networks in solving linear optimization problems. *arXiv preprint arXiv:2310.10603*, 2023.
- Prasad Raghavendra. Optimal algorithms and inapproximability results for every csp? In *Proceedings of the fortieth annual ACM symposium on Theory of computing*, pp. 245–254, 2008.
- Prasad Raghavendra and David Steurer. How to round any csp. In *2009 50th Annual IEEE Symposium on Foundations of Computer Science*, pp. 586–594, 2009a. doi: 10.1109/FOCS.2009.74.
- Prasad Raghavendra and David Steurer. Towards computing the grothendieck constant. In *Proceedings of the Twentieth Annual ACM-SIAM Symposium on Discrete Algorithms*, pp. 525–534. SIAM, 2009b.
- Prasad Raghavendra, David Steurer, and Madhur Tulsiani. Reductions between expansion problems. In *2012 IEEE 27th Conference on Computational Complexity*, pp. 64–73. IEEE, 2012.

- 
- Alessandro Rudi, Ulysse Marteau-Ferey, and Francis Bach. Finding global minima via kernel approximations. *arXiv preprint arXiv:2012.11978*, 2020.
- Ryoma Sato, Makoto Yamada, and Hisashi Kashima. Approximation ratios of graph neural networks for combinatorial problems, 2019.
- Ryoma Sato, Makoto Yamada, and Hisashi Kashima. Random features strengthen graph neural networks. In *Proceedings of the 2021 SIAM international conference on data mining (SDM)*, pp. 333–341. SIAM, 2021.
- Martin JA Schuetz, J Kyle Brubaker, and Helmut G Katzgraber. Combinatorial optimization with physics-inspired graph neural networks. *Nature Machine Intelligence*, 4(4):367–377, 2022a.
- Martin JA Schuetz, J Kyle Brubaker, Zhihuai Zhu, and Helmut G Katzgraber. Graph coloring with physics-inspired graph neural networks. *Physical Review Research*, 4(4):043131, 2022b.
- Daniel Selsam and Nikolaj Bjørner. Guiding high-performance sat solvers with unsat-core predictions. In *Theory and Applications of Satisfiability Testing–SAT 2019: 22nd International Conference, SAT 2019, Lisbon, Portugal, July 9–12, 2019, Proceedings 22*, pp. 336–353. Springer, 2019.
- Daniel Selsam, Matthew Lamm, Benedikt Bünz, Percy Liang, Leonardo de Moura, and David L. Dill. Learning a sat solver from single-bit supervision, 2018.
- Alexander Smith, Andreas Veneris, and Anastasios Viglas. Design diagnosis using boolean satisfiability. In *ASP-DAC 2004: Asia and South Pacific Design Automation Conference 2004 (IEEE Cat. No. 04EX753)*, pp. 218–223. IEEE, 2004.
- Haoran Sun, Etash K Guha, and Hanjun Dai. Annealed training for combinatorial optimization on graphs. *arXiv preprint arXiv:2207.11542*, 2022.
- Jan Toenshoff, Martin Ritzert, Hinrikus Wolf, and Martin Grohe. Run-csp: Unsupervised learning of message passing networks for binary constraint satisfaction problems. *arXiv preprint arXiv:1909.08387*, 2019.
- Jan Tönshoff, Berke Kisin, Jakob Lindner, and Martin Grohe. One model, any csp: Graph neural networks as fast global search heuristics for constraint satisfaction. *arXiv preprint arXiv:2208.10227*, 2022.
- Petar Veličković, Rex Ying, Matilde Padovano, Raia Hadsell, and Charles Blundell. Neural execution of graph algorithms. In *International Conference on Learning Representations*.
- Petar Veličković, Guillem Cucurull, Arantxa Casanova, Adriana Romero, Pietro Liò, and Yoshua Bengio. Graph attention networks. In *International Conference on Learning Representations*, 2018.
- Petar Veličković, Adrià Puigdomènech Badia, David Budden, Razvan Pascanu, Andrea Banino, Misha Dashevskiy, Raia Hadsell, and Charles Blundell. The clrs algorithmic reasoning benchmark. In *International Conference on Machine Learning*, pp. 22084–22102. PMLR, 2022.
- Oriol Vinyals, Meire Fortunato, and Navdeep Jaitly. Pointer networks. In *Advances in Neural Information Processing Systems*, pp. 2692–2700, 2015.
- Jose L Walteros and Austin Buchanan. Why is maximum clique often easy in practice. *Oper. Res.*, 2019.
- Haoyu Wang and Pan Li. Unsupervised learning for combinatorial optimization needs meta-learning. *International Conference on Learning Representations*, 2023.
- Haoyu Peter Wang, Nan Wu, Hang Yang, Cong Hao, and Pan Li. Unsupervised learning for combinatorial optimization with principled objective relaxation. In *Advances in Neural Information Processing Systems*, 2022.
- Po-Wei Wang and J Zico Kolter. Low-rank semidefinite programming for the max2sat problem. In *Proceedings of the AAAI Conference on Artificial Intelligence*, volume 33, pp. 1641–1649, 2019.



- 
- Po-Wei Wang, Priya Donti, Bryan Wilder, and Zico Kolter. Satnet: Bridging deep learning and logical reasoning using a differentiable satisfiability solver. In *International Conference on Machine Learning*, pp. 6545–6554. PMLR, 2019.
- Wenxi Wang, Yang Hu, Mohit Tiwari, Sarfraz Khurshid, Kenneth McMillan, and Risto Miikkulainen. Neurocomb: Improving sat solving with graph neural networks. *arXiv preprint arXiv:2110.14053*, 2021.
- Yiming Wang, Austin Buchanan, and Sergiy Butenko. On imposing connectivity constraints in integer programs. *Mathematical Programming*, 166(1-2):241–271, 2017.
- Ke Xu, Frédéric Boussemart, Fred Hemery, and Christophe Lecoutre. Random constraint satisfaction: Easy generation of hard (satisfiable) instances. *Artificial intelligence*, 171(8-9):514–534, 2007.
- Keyulu Xu, Weihua Hu, Jure Leskovec, and Stefanie Jegelka. How powerful are graph neural networks? In *International Conference on Learning Representations*, 2019. URL <https://openreview.net/forum?id=ryGs6iA5Km>.
- Yunqiu Xu, Meng Fang, Ling Chen, Gangyan Xu, Yali Du, and Chengqi Zhang. Reinforcement learning with multiple relational attention for solving vehicle routing problems. *IEEE Transactions on Cybernetics*, 52(10):11107–11120, 2021.
- Emre Yolcu and Barnabás Póczos. Learning local search heuristics for boolean satisfiability. *Advances in Neural Information Processing Systems*, 32, 2019.
- Mohammed Javeed Zaki, Srinivasan Parthasarathy, Mitsunori Ogihara, Wei Li, et al. New algorithms for fast discovery of association rules. In *KDD*, volume 97, pp. 283–286, 1997.
- Dinghuai Zhang, Hanjun Dai, Nikolay Malkin, Aaron Courville, Yoshua Bengio, and Ling Pan. Let the flows tell: Solving graph combinatorial optimization problems with gflownets. *arXiv preprint arXiv:2305.17010*, 2023.

## A MIN-VERTEX-COVER OPTGNN

Min-Vertex-Cover can be written as the following integer program

$$\text{Minimize: } \sum_{i \in [N]} \frac{1 + x_i}{2} \quad (12)$$

$$\text{Subject to: } (1 - x_i)(1 - x_j) = 0 \quad \forall (i, j) \in E \quad (13)$$

$$x_i^2 = 1 \quad \forall i \in [N] \quad (14)$$

To deal with the constraint on the edges  $(1 - x_i)(1 - x_j) = 0$ , we add a quadratic penalty to the objective with a penalty parameter  $\rho > 0$  yielding

$$\text{Minimize: } \sum_{i \in [N]} \frac{1 + x_i}{2} + \rho \sum_{(i, j) \in E} (1 - x_i - x_j + x_i x_j)^2 \quad (15)$$

$$\text{Subject to: } x_i^2 = 1 \quad \forall i \in [N] \quad (16)$$

Analogously to Max-Cut, we adopt a natural low rank vector formulation for vectors  $\mathbf{v} = \{v_i\}_{i \in [N]}$  in  $r$  dimensions.

$$\text{Minimize: } \sum_{i \in [N]} \frac{1 + \langle v_i, v_\emptyset \rangle}{2} + \rho \sum_{(i, j) \in E} (1 - \langle v_i, v_\emptyset \rangle - \langle v_j, v_\emptyset \rangle + \langle v_i, v_j \rangle)^2 \quad (17)$$

$$\text{Subject to: } \|v_i\| = 1 \quad v_i \in \mathbb{R}^r \quad \forall i \in [N] \quad (18)$$

Now we can design a simple projected gradient descent scheme as follows. For iteration  $t$  in max iterations  $T$ , and for vector  $v_i$  in  $\mathbf{v}$  we perform the following update.

$$\hat{v}_i^{t+1} := v_i^t - \eta(v_\emptyset + 2\rho \sum_{j \in N(i)} (1 - \langle v_i^t, v_\emptyset \rangle - \langle v_j^t, v_\emptyset \rangle + \langle v_i^t, v_j^t \rangle)(-v_\emptyset + v_j^t)) \quad (19)$$

$$v_i^{t+1} := \frac{\hat{v}_i^{t+1}}{\|\hat{v}_i^{t+1}\|} \quad (20)$$

We can then define a OptGNN $_{(M, G)}$  analogously with learnable matrices  $M = \{M_t\}_{t \in [T]} \in \mathbb{R}^{r \times 2r}$  which are each sets of  $T$  learnable matrices corresponding to  $T$  layers of neural network. Let the message from node  $v_j$  to node  $v_i$  be

$$\text{MESSAGE}[v_j \rightarrow v_i] := 2\rho(1 - \langle v_i^t, v_\emptyset \rangle - \langle v_j^t, v_\emptyset \rangle + \langle v_i^t, v_j^t \rangle)(-v_\emptyset + v_j^t)$$

Let the aggregation function AGG be defined as

$$\text{AGG}(\{v_j^t\}_{j \in N(i)}) := \left[ \sum_{j \in N(i)} \text{MESSAGE}[v_j \rightarrow v_i] \right]$$

Then for layer  $t$  in max iterations  $T$ , for  $v_i$  in  $\mathbf{v}$ , we have

$$\hat{v}_i^{t+1} := M(\text{AGG}(v_i^t)) \quad (21)$$

$$v_i^{t+1} := \frac{\hat{v}_i^{t+1}}{\|\hat{v}_i^{t+1}\|} \quad (22)$$

This approach can be straightforwardly adopted to compute the maximum clique and the maximum independent set.

## B MAX-3-SAT OPTGNN

Our formulation for Max 3-SAT directly translates the OptGNN architecture from Definition 3.3. Let  $\Lambda$  be a 3-SAT instance with a set of clauses  $\mathcal{P}$  over a set of binary literals  $\mathcal{V} = \{x_1, x_2, \dots, x_N\} \in \{-1, 1\}$ . Here  $-1$  corresponds to assigning the literal to False whilst  $1$  corresponds to True. Each clause  $P_z \in \mathcal{P}$  can be specified by three literals  $(x_i, x_j, x_k)$  and a set of three 'tokens'  $(\tau_i, \tau_j, \tau_k) \in \{-1, 1\}^3$  which correspond to whether the variable  $x_i, x_j, x_k$  are negated in the clause. For instance the clause  $(x_1 \vee \neg x_2 \vee x_3)$  is translated into three literals  $(x_1, x_2, x_3)$  and tokens  $(1, -1, 1)$ .

The 3-SAT problem on instance  $\Lambda$  is equivalent to maximizing the following polynomial

$$\sum_{(x_i, x_j, x_k, \tau_i, \tau_j, \tau_k) \in \mathcal{P}} \left(1 - \frac{1}{8}(1 + \tau_i x_i)(1 + \tau_j x_j)(1 + \tau_k x_k)\right) \quad (23)$$

Subject to the constraint  $x_1, x_2, \dots, x_N \in \{1, -1\}$ . Now we're reading to define the OptGNN for 3-SAT

**Objective:** First we define the set of vector embeddings. For every literal  $x_i$  we associate an embedding  $v_i \in \mathbb{R}^r$ . For every pair of literals that appear in a clause  $(x_i, x_j)$  we associate a variable  $v_{ij} \in \mathbb{R}^r$ . Finally we associate a vector  $v_\emptyset$  to represent 1. Then the unconstrained objective SAT is defined as

$$\begin{aligned} \text{SAT}(\Lambda) := & \sum_{(x_i, x_j, x_k, \tau_i, \tau_j, \tau_k) \in \mathcal{P}} \frac{1}{8} \left( -\tau_i \tau_j \tau_k \frac{1}{3} [\langle v_i, v_{jk} \rangle + \langle v_j, v_{ik} \rangle + \langle v_k, v_{ij} \rangle] \right. \\ & - \tau_i \tau_j \frac{1}{2} [\langle v_i, v_j \rangle + \langle v_{ij}, v_\emptyset \rangle] - \tau_i \tau_k \frac{1}{2} [\langle v_i, v_k \rangle + \langle v_{ik}, v_\emptyset \rangle] - \tau_j \tau_k \frac{1}{2} [\langle v_j, v_k \rangle + \langle v_{jk}, v_\emptyset \rangle] \\ & \left. - \tau_i \langle v_i, v_\emptyset \rangle - \tau_j \langle v_j, v_\emptyset \rangle - \tau_k \langle v_k, v_\emptyset \rangle + 7 \right) \quad (24) \end{aligned}$$

**Constraints:** The constraints are then as follows. For every clause involving variables  $(x_i, x_j, x_k)$  we impose the following constraints on  $v_i, v_j, v_k, v_{ij}, v_{ik}, v_{jk}$  and  $v_\emptyset$ . Note that these constraints are exactly the ones listed in algorithm 1 which we organize here for convenience. The naming convention is the degree of the polynomial on the left to the degree of the polynomial on the right.

### 1. pair-to-pair

$$\langle v_i, v_j \rangle = \langle v_{ij}, v_\emptyset \rangle \quad (25)$$

$$\langle v_i, v_k \rangle = \langle v_{ik}, v_\emptyset \rangle \quad (26)$$

$$\langle v_j, v_k \rangle = \langle v_{jk}, v_\emptyset \rangle \quad (27)$$

### 2. triplets-to-triplet

$$\langle v_{ij}, v_k \rangle = \langle v_{ik}, v_j \rangle = \langle v_{jk}, v_i \rangle \quad (28)$$

### 3. triplet-to-single

$$\langle v_i, v_{ij} \rangle = \langle v_j, v_\emptyset \rangle \quad (29)$$

$$\langle v_j, v_{ij} \rangle = \langle v_i, v_\emptyset \rangle \quad (30)$$

$$\langle v_j, v_{jk} \rangle = \langle v_k, v_\emptyset \rangle \quad (31)$$

$$\langle v_k, v_{jk} \rangle = \langle v_j, v_\emptyset \rangle \quad (32)$$

$$\langle v_i, v_{ik} \rangle = \langle v_k, v_\emptyset \rangle \quad (33)$$

$$\langle v_k, v_{ik} \rangle = \langle v_i, v_\emptyset \rangle \quad (34)$$

$$(35)$$

### 4. quad-to-pair

$$\langle v_{ij}, v_{jk} \rangle = \langle v_i, v_k \rangle \quad (36)$$

$$\langle v_{ij}, v_{ik} \rangle = \langle v_j, v_k \rangle \quad (37)$$

$$\langle v_{ik}, v_{jk} \rangle = \langle v_i, v_j \rangle \quad (38)$$

$$(39)$$

## 5. unit norm

$$\|v_i\| = \|v_j\| = \|v_k\| = \|v_{ij}\| = \|v_{ik}\| = \|v_{jk}\| = \|v_\emptyset\| = 1 \quad (40)$$

Then for completeness we write out the full penalized objective. We perform this exercise in such great detail to inform the reader of how this could be set up for other Max-CSP's.

**Definition** (OptGNN for 3-SAT). Let  $\Lambda$  be a 3-SAT instance. Let  $\mathcal{L}_\rho$  be defined as

$$\begin{aligned} \mathcal{L}_\rho(V) := & \sum_{(x_i, x_j, x_k, \tau_i, \tau_j, \tau_k) \in \mathcal{P}} \left[ -\frac{1}{8} \left( -\tau_i \tau_j \tau_k \frac{1}{3} [\langle v_i, v_{jk} \rangle + \langle v_j, v_{ik} \rangle + \langle v_k, v_{ij} \rangle] \right. \right. \\ & - \tau_i \tau_j \frac{1}{2} [\langle v_i, v_j \rangle + \langle v_{ij}, v_\emptyset \rangle] - \tau_i \tau_k \frac{1}{2} [\langle v_i, v_k \rangle + \langle v_{ik}, v_\emptyset \rangle] - \tau_j \tau_k \frac{1}{2} [\langle v_j, v_k \rangle + \langle v_{jk}, v_\emptyset \rangle] \\ & \left. \left. - \tau_i \langle v_i, v_\emptyset \rangle - \tau_j \langle v_j, v_\emptyset \rangle - \tau_k \langle v_k, v_\emptyset \rangle + 7 \right) \right. \\ & + \rho [(\langle v_i, v_j \rangle - \langle v_{ij}, v_\emptyset \rangle)^2 + (\langle v_i, v_k \rangle - \langle v_{ik}, v_\emptyset \rangle)^2 + (\langle v_j, v_k \rangle - \langle v_{jk}, v_\emptyset \rangle)^2] \\ & + \rho [(\langle v_{ij}, v_k \rangle - \langle v_{ik}, v_j \rangle)^2 + (\langle v_{ik}, v_j \rangle - \langle v_{jk}, v_i \rangle)^2 + (\langle v_{jk}, v_i \rangle - \langle v_{ij}, v_k \rangle)^2] \\ & + \rho [(\langle v_{ij}, v_{jk} \rangle - \langle v_i, v_k \rangle)^2 + (\langle v_{ij}, v_{ik} \rangle - \langle v_j, v_k \rangle)^2 + (\langle v_{ik}, v_{jk} \rangle - \langle v_i, v_j \rangle)^2] \\ & \rho [(\langle v_i, v_{ij} \rangle - \langle v_j, v_\emptyset \rangle)^2 + (\langle v_j, v_{ij} \rangle - \langle v_i, v_\emptyset \rangle)^2 + (\langle v_j, v_{jk} \rangle - \langle v_k, v_\emptyset \rangle)^2 + (\langle v_k, v_{jk} \rangle - \langle v_j, v_\emptyset \rangle)^2 \\ & + (\langle v_i, v_{ik} \rangle - \langle v_k, v_\emptyset \rangle)^2 + (\langle v_k, v_{ik} \rangle - \langle v_i, v_\emptyset \rangle)^2] \\ & \left. + \rho [(\|v_i\| - 1)^2 + (\|v_j\| - 1)^2 + (\|v_k\| - 1)^2 + (\|v_{ij}\| - 1)^2 + (\|v_{ik}\| - 1)^2 + (\|v_{jk}\| - 1)^2 + (\|v_\emptyset\| - 1)^2] \right] \quad (41) \end{aligned}$$

Then taking the gradient of  $\mathcal{L}$  gives us the precise form of the message passing. We list the forms of the messages from adjacent nodes in the constraint graph  $G_\Lambda$ .

**Message: Pair to Singles for Single in Pair.** This is the message  $\text{MESSAGE}[v_{ij} \rightarrow v_i]$  for each pair node  $v_{ij}$  to a single  $v_i$  node.

$$\text{MESSAGE}[v_{ij} \rightarrow v_i] = |\{c \in \mathcal{P} : x_i, x_j \in c\}| 2\rho (\langle v_i, v_{ij} \rangle - \langle v_j, v_\emptyset \rangle) v_{ij} \quad (42)$$

**Message: Pair to Singles for Single not in Pair.** This is the message  $\text{MESSAGE}[v_{ij} \rightarrow v_k]$  for each pair node  $v_{ij}$  to a single  $v_k$  node.

$$\begin{aligned} \text{MESSAGE}[v_{ij} \rightarrow v_k] = & \sum_{c \in \mathcal{P}: (x_i, x_j, x_k) \in c} \left[ -\frac{1}{8} \left( -\tau_i \tau_j \tau_k \frac{1}{3} v_{ij} \right) \right. \\ & \left. + 2\rho [(\langle v_k, v_{ij} \rangle - \langle v_i, v_{jk} \rangle) v_{ij} + (\langle v_i, v_{jk} \rangle - \langle v_k, v_{ij} \rangle) (-v_{ij})] \right] \quad (43) \end{aligned}$$

**Message: Single to Pair for Single in Pair.** This is the message  $\text{MESSAGE}[v_i \rightarrow v_{ij}]$  for each single node  $v_i$  to a pair  $v_{ij}$

$$\text{MESSAGE}[v_i \rightarrow v_{ij}] = |\{c \in \mathcal{P} : x_i, x_j \in c\}| 2\rho (\langle v_i, v_{ij} \rangle - \langle v_j, v_\emptyset \rangle) v_i \quad (44)$$

**Message: Single to Pair for Single not in Pair.** This is the message  $\text{MESSAGE}[v_{ij} \rightarrow v_k]$  for each pair node  $v_{ij}$  to a single  $v_k$  node.

$$\text{MESSAGE}[v_{ij} \rightarrow v_k] = \sum_{c \in \mathcal{P}: (x_i, x_j, x_k) \in c} \left[ -\frac{1}{8} \left( -\tau_i \tau_j \tau_k \frac{1}{3} v_k \right) \right. \quad (45)$$

$$\left. + 2\rho [(\langle v_k, v_{ij} \rangle - \langle v_i, v_{jk} \rangle) v_k + (\langle v_k, v_{ij} \rangle - \langle v_j, v_{ik} \rangle) v_k] \right] \quad (46)$$

**Message: Single to Single** This is the message  $\text{MESSAGE}[v_i \rightarrow v_j]$  for each single node  $v_i$  to a single  $v_j$  node.

$$\text{MESSAGE}[v_i \rightarrow v_j] = \sum_{c \in \mathcal{P}: (x_i, x_j, x_k) \in c} \left[ -\frac{1}{8} \left( -\tau_i \tau_j \frac{1}{2} v_i \right) \right. \quad (47)$$

$$\left. + 2\rho [(\langle v_i, v_j \rangle - \langle v_{ij}, v_\emptyset \rangle) v_i + (\langle v_{ik}, v_{jk} \rangle - \langle v_i, v_j \rangle)(-v_i)] \right] \quad (48)$$

**Message: Pair to Pair** This is the message  $\text{MESSAGE}[v_{ij} \rightarrow v_{jk}]$  for each pair node  $v_{ij}$  to a pair  $v_{jk}$  node.

$$\text{MESSAGE}[v_{ij} \rightarrow v_{jk}] = |\{c \in \mathcal{P} : x_i, x_j, x_k \in c\}| 2\rho [(\langle v_{ij}, v_{jk} \rangle - \langle v_i, v_k \rangle) v_{ij}] \quad (49)$$

Then the  $\text{OptGNN}_{(M, G_\Lambda)}$  is defined with the following functions  $\text{UPDATE}$ ,  $\text{AGGREGATE}$ , and  $\text{NONLINEAR}$ . For any node  $v$ , the  $\text{OptGNN}$  update is

$$\text{AGGREGATE}(\{v_\zeta\}_{\zeta \in N(v)}) := \sum_{v_\zeta \in N(v)} \text{MESSAGE}[v_\zeta \rightarrow v] \quad (50)$$

$$\text{UPDATE}(v) = M \left( \left[ \text{AGGREGATE}(\{v_\zeta\}_{\zeta \in N(v)}) \right]^v \right) \quad (51)$$

$$\text{NONLINEAR}(v) = \frac{v}{\|v\|} \quad (52)$$

Finally, we note that many of the signs in the forms of messages could have been chosen differently i.e  $\langle v_i, v_j \rangle - \langle v_{ij}, v_\emptyset \rangle$  produces different gradients from  $\langle v_{ij}, v_\emptyset \rangle - \langle v_i, v_j \rangle$ . We leave small choices like this to the reader.

## C OPTIMALITY OF MESSAGE PASSING FOR MAX-CSP

Our primary theoretical result is that a polynomial time message passing algorithm on an appropriately defined constraint graph computes the approximate optimum of SDP 1 which is notable for being an SDP that achieves the Unique Games optimal integrality gap.

Our proof roadmap is simple. First, we design an SDP relaxation SDP 1 for Max-k-CSP that is provably equivalent to the SDP of Raghavendra (2008) and therefore inherits its complexity theoretic optimality. Finally, we design a message passing algorithm to approximately solve SDP 1 in polynomial time to polynomial precision. Our message passing algorithm has the advantage of being formulated on an appropriately defined constraint graph. For a Max-k-CSP instance  $\Lambda$  with  $N$  variables,  $|\mathcal{P}|$  predicates, over an alphabet of size  $q$ , it takes  $|\mathcal{P}|q^k$  space to represent the Max-CSP. To declutter notation, we let  $\Phi$  be the size of the Max-CSP which is equal to  $|\mathcal{P}|q^k$ . Our message passing algorithm achieves an additive  $\epsilon$  approximation in time  $\text{poly}(\epsilon^{-1}, \Phi, \log(\delta^{-1}))$  which is then polynomial in the size of the CSP and inverse polynomial in the precision.

Here we briefly reiterate the definition of Max-k-CSP. A Max-k-CSP instance  $\Lambda = (\mathcal{V}, \mathcal{P}, q)$  consists of a set of  $N$  variables  $\mathcal{V} := \{x_i\}_{i \in [N]}$  each taking values in an alphabet  $[q]$  and a set of predicates  $\mathcal{P} := \{P_z\}_{z \subset \mathcal{V}}$  where each predicate is a payoff function over  $k$  variables denoted  $z = \{x_{i_1}, x_{i_2}, \dots, x_{i_k}\}$ . Here we refer to  $k$  as the arity of the Max-k-CSP, and we adopt the normalization that each predicate  $P_z$  returns outputs in  $[0, 1]$ . We index each predicate  $P_z$  by its domain  $z$  and we will use the notation  $\mathcal{S}(P)$  to denote the domain of a predicate  $P$ . The goal of Max-k-CSP is to maximize the payoff of the predicates.

$$\max_{(x_1, \dots, x_N) \in [q]^N} \frac{1}{|\mathcal{P}|} \sum_{P_z \in \mathcal{P}} P_z(X_z) \quad (53)$$

Where  $X_z$  denotes the assignment of variables  $\{x_i\}_{i \in z}$ .

There is an SDP relaxation of equation 53 that is the "qualitatively most powerful assuming the Unique Games conjecture" Raghavendra (2008). More specifically, the integrality gap of the SDP achieves the Unique Games optimal approximation ratio. Furthermore, there exists a rounding that achieves its integrality gap.

**SDP Reformulation:** Next we will introduce the SDP formulation we adopt in this paper. For the sake of exposition and notational simplicity, we will work with binary Max-k-CSP's where  $q = \{0, 1\}$ . The extension to general  $q$  is straightforward and detailed in the appendix.

We will adopt the standard pseudoexpectation and pseudodistribution formalism in describing our SDP. Let  $\tilde{\mathbb{E}}_\mu[\mathbf{x}]$  be a matrix in dimension  $\mathbb{R}^{(N+1)^{d/2} \times (N+1)^{d/2}}$  of optimization variables defined as follows

$$\tilde{\mathbb{E}}_\mu[\mathbf{x}] := \tilde{\mathbb{E}}_\mu[(1, x_1, x_2, \dots, x_N)^{\otimes d/2} ((1, x_1, x_2, \dots, x_N)^{\otimes d/2})^T] \quad (54)$$

Where we use  $\otimes$  to denote tensor product. It is convenient to think of  $\tilde{\mathbb{E}}_\mu[\mathbf{x}]$  as a matrix of variables denoting the up to  $d$  multilinear moments of a distribution  $\mu$  over the variables  $\mathcal{V}$ . A multilinear polynomial is a polynomial of the form  $X_\phi := \prod_{i \in \phi} x_i$  for some subset of the variables  $\phi \subseteq \mathcal{V}$ . We index the variables of the matrix  $\tilde{\mathbb{E}}_\mu[\mathbf{x}]$  by the multilinear moment that it represents. Notice that this creates repeat copies as there are multiple entries representing the same monomial. This is dealt with by constraining the repeated copies to be equal with linear equality constraints.

Specifically, let  $z$  be a subset of the CSP variables  $z \subset \{x_i\}_{i \in [N]}$  of size  $k$ . Let  $X_z$  denote the multilinear moment  $X_z := \prod_{i \in z} x_i$ . Then  $\tilde{\mathbb{E}}_\mu[X_z]$  denotes the SDP variable corresponding to the multilinear moment  $\mathbb{E}_\mu[X_z]$ . Of course optimizing over the space of distributions  $\mu$  over  $\mathcal{V}$  is intractable, and so we opt for optimizing over the space of low degree pseudodistributions and their associated pseudoexpectation functionals. See Barak & Steurer (2014) for references therein.

In particular, for any subset of variables  $X_z := \{x_{i_1}, \dots, x_{i_k}\} \in \mathcal{V}$  we let  $\tilde{\mathbb{E}}_\mu[\mathbf{x}]|_{z,d}$  denote the matrix of the up to degree up to  $d$  multilinear moments of the variables in  $z$ .

$$\tilde{\mathbb{E}}_\mu[\mathbf{x}]|_{z,d} := \tilde{\mathbb{E}}_\mu[(1, x_{i_1}, x_{i_2}, \dots, x_{i_k})^{\otimes d/2} ((1, x_{i_1}, x_{i_2}, \dots, x_{i_k})^{\otimes d/2})^T] \quad (55)$$

We refer to the above matrix as a degree  $d$  pseudoexpectation functional over  $X_z$ . Subsequently, we describe a pseudoexpectation formulation of our SDP followed by a vector formulation.

**Multilinear Formulation:** A predicate for a boolean Max-k-CSP  $P_z(X_z)$  can be written as a multilinear polynomial

$$P_z(X_z) := \sum_{\tau = (\tau_1, \dots, \tau_k) \in \{-1, 1\}^k} w_{z, \tau} \prod_{x_i \in z} \frac{1 + \tau_i x_i}{2} := \sum_{s \subseteq z} y_s X_s \quad (56)$$

For some real valued weights  $w_{z, \tau}$  and  $y_s$  which are simply the fourier coefficients of the function  $P_z$ . Then the pseudoexpectation formulation of our SDP is as follows

$$\max_{\tilde{\mathbb{E}}_\mu[\mathbf{x}]} \frac{1}{|\mathcal{P}|} \sum_{P_z \in \mathcal{P}} \tilde{\mathbb{E}}_\mu[P_z(X_z)] \quad (57)$$

subject to the following constraints

1. **Unit:**  $\tilde{\mathbb{E}}_\mu[1] = 1$ ,  $\tilde{\mathbb{E}}_\mu[x_i^2] = 1$  for all  $x_i \in \mathcal{V}$ , and  $\tilde{\mathbb{E}}_\mu[\prod_{i \in s} x_i^2 \prod_{j \in s'} x_j] = \tilde{\mathbb{E}}_\mu[\prod_{j \in s'} x_j]$  for all  $s, s' \subseteq \mathcal{S}(P)$  for every predicate  $P \in \mathcal{P}$  such that  $2s + s' \leq k$ . In expectation, the squares of all multilinear polynomials are equal to 1.
2. **Positive Semidefinite:**  $\tilde{\mathbb{E}}_\mu[\mathbf{x}]|_{\mathcal{V}, 2} \succeq 0$  i.e the degree two pseudoexpectation is positive semidefinite.  $\tilde{\mathbb{E}}_\mu[\mathbf{x}]|_{z, 2k} \succeq 0$  for all  $z = \mathcal{S}(P)$  for all  $P \in \mathcal{P}$ . The moment matrix for the multilinear polynomials corresponding to every predicate is positive semidefinite.

Equivalently we can view the SDP in terms of the vectors in the cholesky decomposition of  $\tilde{\mathbb{E}}_\mu[\mathbf{x}]$ . We rewrite the above SDP accordingly. For this purpose it is useful to introduce the notation  $\zeta(A, B) := A \cup B / A \cap B$ . It is also useful to introduce the notation  $\mathcal{C}(s)$  for the size of the set  $\{g, g' \subseteq s : \zeta(g, g') = s\}$ .

**Lemma C.1.** For Max-k-CSP instance  $\Lambda$ , The SDP of SDP 1 (top of pg.19) is at least as tight as the SDP of Raghavendra (2008).

---

**SDP 1** SDP for Max-k-CSP (Equivalent to UGC-optimal)

---

SDP Vector Formulation  $\Lambda = (\mathcal{V}, \mathcal{P}, \{0, 1\})$ . Multilinear formulation of objective.

$$\min_{x_1, x_2, \dots, x_N} \frac{1}{|\mathcal{P}|} \sum_{P_z \in \mathcal{P}} \tilde{\mathbb{E}}_\mu[-P_z(X_z)] := \sum_{P_z \in \mathcal{P}} \sum_{s \subseteq z} w_s \frac{1}{|\mathcal{C}(s)|} \sum_{g, g' \subseteq s: \zeta(g, g')=s} \langle v_g, v_{g'} \rangle \quad (58)$$

$$\text{subject to: } \|v_s\|^2 = 1 \quad \forall s \subseteq \mathcal{S}(P), \forall P \in \mathcal{P} \quad (59)$$

$$\begin{aligned} \tilde{\mathbb{E}}_\mu[X_{\zeta(g, g')}] &:= \langle v_g, v_{g'} \rangle \\ &= \langle v_h, v_{h'} \rangle \quad \forall \zeta(g, g') = \zeta(h, h') \text{ s.t. } g \cup g' \subseteq \mathcal{S}(P), \forall P \in \mathcal{P} \end{aligned} \quad (60)$$

First constraint is the square of multilinear polynomials are unit.

Second constraint are degree  $2k$  SoS constraints for products of multilinear polynomials.

---

*Proof.* The SDP of Raghavendra (2008) is a degree 2 SoS SDP augmented with  $k$ -local distributions for every predicate  $P \in \mathcal{P}$ . By using the vectors of the cholesky decomposition and constraining them to be unit vectors we automatically capture degree 2 SoS. To capture  $k$  local distributions we simply enforce degree  $2k$  SoS on the boolean hypercube for the domain of every predicate. This can be done with the standard vector formulation written in SDP 1 (top of pg.18). See Barak & Steurer (2014) for background and references.  $\square$

Moving forward, the goal of Algorithm 2 is to minimize the loss  $\mathcal{L}_\rho(\mathbf{v})$  which is a function of the Max-CSP instance  $\Lambda$ .

$$\begin{aligned} \mathcal{L}_\rho(\mathbf{v}) = \frac{1}{|\mathcal{P}|} &\left[ \sum_{P_z \in \mathcal{P}} \sum_{s \subseteq z} y_s \frac{1}{|\mathcal{C}(s)|} \sum_{\substack{g, g' \subseteq s \\ \text{s.t. } \zeta(g, g')=s}} \langle v_g, v_{g'} \rangle \right. \\ &+ \rho \left[ \sum_{P_z \in \mathcal{P}} \sum_{\substack{g, g', h, h' \subseteq z \\ \text{s.t. } \zeta(g, g')=\zeta(h, h')}} (\langle v_g, v_{g'} \rangle - \langle v_h, v_{h'} \rangle)^2 \right. \\ &\left. \left. + \sum_{v_s \in \mathbf{v}} (\|v_s\|^2 - 1)^2 \right] \right] \quad (61) \end{aligned}$$

The loss  $\mathcal{L}_\rho$  has gradient of the form

$$\begin{aligned} \frac{\partial \mathcal{L}_\rho(\mathbf{v})}{\partial v_w} = \frac{1}{|\mathcal{P}|} &\left[ \sum_{P_z \in \mathcal{P}} \sum_{\substack{s \subseteq z \\ \text{s.t. } w \subseteq s}} y_s \frac{1}{|\mathcal{C}(s)|} \sum_{\substack{w' \subseteq s \\ \text{s.t. } \zeta(w, w')=s}} v_{w'} \right. \\ &+ 2\rho \left[ \sum_{P_z \in \mathcal{P}} \sum_{\substack{w', h, h' \subseteq z \\ \text{s.t. } w \subseteq z \text{ s.t. } \zeta(w, w')=\zeta(h, h')}} (\langle v_w, v_{w'} \rangle - \langle v_h, v_{h'} \rangle) v_w' \right. \\ &\left. \left. + (\|v_w\|^2 - 1) v_w \right] \right] \quad (62) \end{aligned}$$

Noticing that the form of the gradient depends only on the vectors in the neighborhood of the constraint graph  $G_\Lambda$  we arrive at our message passing algorithm. The key to our proof is bounding the number of iterations required to optimize equation 61 to sufficient accuracy to be an approximate global optimum of SDP 1.

**Theorem C.1.** *Algorithm 2 computes in  $\text{poly}(\epsilon^{-1}, \Phi, \log(\delta^{-1}))$  iterations a set of vectors  $\mathbf{v} := \{\hat{v}_s\}$  for all  $s \subseteq \mathcal{S}(P)$  for all  $P \in \mathcal{P}$  that satisfy the constraints of SDP 1 to error  $\epsilon$  and approximates the optimum of SDP 1 to error  $\epsilon$  with probability  $1 - \delta$*

$$\left| \sum_{P_z \in \mathcal{P}} \tilde{\mathbb{E}}_\mu[P_z(X_z)] - \text{SDP}(\Lambda) \right| \leq \epsilon$$

---

**Algorithm 2** Message Passing for Max-CSP
 

---

- 1: **Inputs:** Max-CSP instance  $\Lambda$
- 2:  $n \leftarrow \Phi \log(\delta^{-1})$
- 3:  $\eta, \psi, \sigma \leftarrow n^{-100}$  {Initialize step size, noise threshold, and noise variance}
- 4:  $\mathbf{v}^0 = \{v_s\}_{s \subseteq z: P_z \in \mathcal{P}} \leftarrow \text{Uniform}(\mathcal{S}^{n-1})$  {Initialize vectors to uniform on the unit sphere}
- 5: **for**  $t \in [\text{poly}(\epsilon^{-1}, \Phi, \log(\delta^{-1}))]$  **do**
- 6:   **for**  $v_w^t \in \mathbf{v}^t$  {Iterate over vectors and update each vector with neighboring vectors in constraint graph} **do**
- 7:

$$\begin{aligned}
 v_w^{t+1} \leftarrow v_w^t - \eta \frac{1}{|\mathcal{P}|} & \left[ \sum_{\substack{P_z \in \mathcal{P} \\ \text{s.t. } w \subseteq z}} \sum_{\substack{s \subseteq z \\ \text{s.t. } w \subseteq s}} y_s \frac{1}{|\mathcal{C}(s)|} \sum_{\substack{w' \subseteq s \\ \text{s.t. } \zeta(w, w')=s}} v_{w'}^t \right. \\
 & \left. + 2\rho \left[ \sum_{\substack{P_z \in \mathcal{P} \\ \text{s.t. } w \subseteq z}} \sum_{\substack{w', h, h' \subseteq s \\ \text{s.t. } \zeta(w, w')=\zeta(h, h')}} (\langle v_w^t, v_{w'}^t \rangle - \langle v_h^t, v_{h'}^t \rangle) v_w^t + (\|v_w^t\|^2 - 1) v_w^t \right] \right] \quad (63)
 \end{aligned}$$

- 8:   **if**  $\|v_w^{t+1} - v_w^t\| \leq \psi$  **then**
  - 9:      $\zeta \leftarrow N(0, \sigma I)$
  - 10:   **else**
  - 11:      $\zeta \leftarrow 0$
  - 12:   **end if**
  - 13:    $v_w^{t+1} \leftarrow v_w^{t+1} + \zeta$
  - 14:   **end for**
  - 15: **end for**
  - 16: **return**  $\mathbf{v}^t$
  - 17: **Output:** vectors corresponding to solution to SDP 1 (top of pg.18)
- 

where  $SDP(\Lambda)$  is the optimum of SDP 1.

*Proof.* We begin by writing down the objective penalized by a quadratic on the constraints.

$$\begin{aligned}
 \mathcal{L}_\rho(\mathbf{v}) := \frac{1}{|\mathcal{P}|} & \left[ \sum_{P_z \in \mathcal{P}} \tilde{\mathbb{E}}_\mu[P_z(X_z)] \right. \\
 & \left. + \rho \left[ \sum_{P_z \in \mathcal{P}} \sum_{\substack{g, g', h, h' \subseteq z \\ \text{s.t. } \zeta(g, g')=\zeta(h, h')}} (\langle v_g, v_{g'} \rangle - \langle v_h, v_{h'} \rangle)^2 + \sum_{v_s \in \mathbf{v}} (\|v_s\|^2 - 1)^2 \right] \right] \quad (64)
 \end{aligned}$$

For any monomial  $X_s = \prod_{i \in s} x_i$  in  $P_z(X_z)$  we write

$$\tilde{\mathbb{E}}_\mu[X_s] := \frac{1}{|\mathcal{C}(s)|} \sum_{\substack{g, g' \subseteq s \\ \text{s.t. } \zeta(g, g')=s}} \langle v_g, v_{g'} \rangle \quad (65)$$

Where  $\mathcal{C}(s)$  is the size of the set  $\{g, g' \subseteq s : \zeta(g, g') = s\}$ . In a small abuse of notation, we regard this as the definition of  $\tilde{\mathbb{E}}_\mu[X_s]$  but realize that we're referring to the iterates of the algorithm before they've converged to a pseudoexpectation. Now recall equation 56, we can expand the polynomial  $P_z(X_z)$  along its standard monomial basis

$$P_z(X_z) = \sum_{s \subseteq z} y_s X_s \quad (66)$$



where we have defined coefficients  $y_s$  for every monomial in  $P_z(X_z)$ . Plugging equation 65 and equation 66 into equation 64 we obtain

$$\begin{aligned} \mathcal{L}_\rho(\mathbf{v}) = & \frac{1}{|\mathcal{P}|} \left[ \sum_{P_z \in \mathcal{P}} \sum_{s \subseteq z} y_s \frac{1}{|\mathcal{C}(s)|} \sum_{\substack{g, g' \subseteq s \\ \text{s.t. } \zeta(g, g') = s}} \langle v_g, v_{g'} \rangle \right. \\ & + \rho \left[ \sum_{P_z \in \mathcal{P}} \sum_{\substack{g, g', h, h' \subseteq z \\ \text{s.t. } \zeta(g, g') = \zeta(h, h')}} (\langle v_g, v_{g'} \rangle - \langle v_h, v_{h'} \rangle)^2 \right. \\ & \left. \left. + \sum_{v_s \in \mathbf{v}} (\|v_s\|^2 - 1)^2 \right] \right] \quad (67) \end{aligned}$$

Taking the derivative with respect to any  $v_w \in \mathbf{v}$  we obtain

$$\begin{aligned} \frac{\partial \mathcal{L}_\rho(\mathbf{v})}{\partial v_w} = & \frac{1}{|\mathcal{P}|} \left[ \sum_{P_z \in \mathcal{P}} \sum_{\substack{s \subseteq z \\ \text{s.t. } w \subseteq s}} y_s \frac{1}{|\mathcal{C}(s)|} \sum_{\substack{w' \subseteq s \\ \text{s.t. } \zeta(w, w') = s}} v_{w'} \right. \\ & + 2\rho \left[ \sum_{P_z \in \mathcal{P}} \sum_{\substack{w', h, h' \subseteq s \\ \text{s.t. } w \subseteq z, \text{s.t. } \zeta(w, w') = \zeta(h, h')}} (\langle v_w, v_{w'} \rangle - \langle v_h, v_{h'} \rangle) v_{w'} \right. \\ & \left. \left. + (\|v_w\|^2 - 1) v_w \right] \right] \quad (68) \end{aligned}$$

The gradient update is then what is detailed in Algorithm 2

$$v_w^{t+1} = v_w^t - \eta \frac{\partial \mathcal{L}_\rho(\mathbf{v})}{\partial v_w} \quad (69)$$

Thus far we have established the form of the gradient. To prove the gradient iteration converges we reference the literature on convergence of perturbed gradient descent (Jin et al., 2017) which we rewrite in Theorem F.1. First we note that the SDP 1 has  $\ell$  smooth gradient for  $\ell \leq \text{poly}(\rho, B)$  and has  $\gamma$  lipschitz Hessian for  $\gamma = \text{poly}(\rho, B)$  which we arrive at in Lemma E.2 and Lemma F.1. The proofs of Lemma E.2 and Lemma F.1 are technically involved and form the core hurdle in arriving at our proof.

Then by Theorem F.1 the iteration converges to an  $(\epsilon', \gamma^2)$ -SOSP Definition F.1 in no more than  $\tilde{O}(\frac{1}{\epsilon'^2})$  iterations with probability  $1 - \delta$ . Now that we've established that the basic gradient iteration converges to approximate SOSP, we need to then prove that the approximate SOSP are approximate global optimum. We achieve this by using the result of Bhojanapalli et al. (2018) lemma 3 which we restate in Lemma C.2 for convenience.

The subsequent presentation adapts the proof of Lemma C.2 to our setting. To show that  $(\epsilon', \gamma^2)$ -SOSP are approximately global optimum, we have to work with the original SDP loss as opposed to the nonconvex vector loss. For subsequent analysis we need to define the penalized loss which we denote  $\mathcal{H}_\rho(\tilde{\mathbb{E}}[\mathbf{x}])$  in terms of the SDP moment matrix  $\tilde{\mathbb{E}}[\mathbf{x}]$ .

$$\begin{aligned} \mathcal{H}_\rho(\tilde{\mathbb{E}}[\mathbf{x}]) := & \frac{1}{|\mathcal{P}|} \left[ \sum_{P_z \in \mathcal{P}} \tilde{\mathbb{E}}_{\hat{\mu}}[P_z(X_z)] \right. \\ & + \rho \left[ \sum_{P_z \in \mathcal{P}} \sum_{\substack{g, g', h, h' \subseteq z \\ \text{s.t. } \zeta(g, g') = \zeta(h, h')}} (\tilde{\mathbb{E}}_{\hat{\mu}}[X_{\zeta(g, g')}] - \tilde{\mathbb{E}}_{\hat{\mu}}[X_{\zeta(h, h')}] )^2 + \sum_{\substack{X_s \text{ s.t. } s \subseteq \mathcal{S}(P) \\ |s| \leq k, \forall P \in \mathcal{P}}} (\tilde{\mathbb{E}}_{\hat{\mu}}[X_s^2] - 1)^2 \right] \right] \quad (70) \end{aligned}$$

Here we use the notation  $\tilde{\mathbb{E}}_{\hat{\mu}}[X_{\zeta(g, g')}]$  and  $\tilde{\mathbb{E}}_{\hat{\mu}}[X_{\zeta(h, h')}]$  to denote  $\langle v_g, v_{g'} \rangle$  and  $\langle v_h, v_{h'} \rangle$  respectively. Note that although by definition  $\mathcal{H}_\rho(\tilde{\mathbb{E}}[\mathbf{x}]) = \mathcal{L}_\rho(\mathbf{v})$ , their gradients and Hessians are distinct because

$\mathcal{L}_\rho(\mathbf{v})$  is overparameterized. This is the key point. It is straightforward to argue that SOSPs of a convex optimization are approximately global, but we are trying to make this argument for SOSPs of the overparameterized loss  $\mathcal{L}_\rho(\mathbf{v})$ .

Let the global optimum of SDP 1 be denoted  $\tilde{\mathbb{E}}_{\tilde{\mu}}[\tilde{\mathbf{x}}]$  with a cholesky decomposition  $\tilde{\mathbf{v}}$ . Let  $\hat{\mathbf{v}}$  be the set of vectors outputted by Algorithm 2 with associated pseudoexpectation  $\tilde{\mathbb{E}}_{\tilde{\mu}}[\tilde{\mathbf{x}}]$ . Then, we can bound

$$\mathcal{L}_\rho(\hat{\mathbf{v}}) - \mathcal{L}_\rho(\tilde{\mathbf{v}}) = \mathcal{H}_\rho(\tilde{\mathbb{E}}[\tilde{\mathbf{x}}]) - \mathcal{H}_\rho(\tilde{\mathbb{E}}[\tilde{\mathbf{x}}]) \leq \langle \nabla \mathcal{H}_\rho(\tilde{\mathbb{E}}[\tilde{\mathbf{x}}]), \tilde{\mathbb{E}}[\tilde{\mathbf{x}}] - \tilde{\mathbb{E}}[\tilde{\mathbf{x}}] \rangle \quad (71)$$

Here the first equality is by definition, and the inequality is by the convexity of  $\mathcal{H}_\rho$ . Moving on, we use the fact that the min eigenvalue of the hessian of overparameterized loss  $\nabla^2 \mathcal{L}_\rho(\hat{\mathbf{v}}) \succeq -\gamma\sqrt{\epsilon'}$  implies the min eigenvalue of the gradient of the convex loss  $\lambda_{\min}(\nabla \mathcal{H}_\rho(\tilde{\mathbb{E}}[\tilde{\mathbf{x}}])) \geq -\gamma\sqrt{\epsilon'}$ . This fact is invoked in Bhojanapalli et al. (2018) lemma 3 which we adapt to our setting in Lemma C.2. Subsequently, we adapt the lines of their argument in Lemma C.2 most relevant to our analysis which we detail here for the sake of completeness.

$$\begin{aligned} 71 &\leq -\lambda_{\min}(\nabla \mathcal{H}_\rho(\tilde{\mathbb{E}}[\tilde{\mathbf{x}}])) \text{Tr}(\tilde{\mathbb{E}}[\tilde{\mathbf{x}}]) - \langle \nabla \mathcal{H}_\rho(\tilde{\mathbb{E}}[\tilde{\mathbf{x}}]), \tilde{\mathbb{E}}[\tilde{\mathbf{x}}] \rangle \\ &\leq -\lambda_{\min}(\nabla \mathcal{H}_\rho(\tilde{\mathbb{E}}[\tilde{\mathbf{x}}])) \text{Tr}(\tilde{\mathbb{E}}[\tilde{\mathbf{x}}]) + \|\nabla \mathcal{H}_\rho(\tilde{\mathbb{E}}[\tilde{\mathbf{x}}])\|_F \|\tilde{\mathbb{E}}[\tilde{\mathbf{x}}]\|_F \\ &\leq \gamma\sqrt{\epsilon'} \text{Tr}(\tilde{\mathbb{E}}[\tilde{\mathbf{x}}]) + \epsilon' \|\tilde{\mathbf{v}}\|_F \leq \gamma\sqrt{\epsilon'}\Phi + \epsilon'\Phi \leq \epsilon \end{aligned} \quad (72)$$

Here the first inequality follows by a standard inequality of frobenius inner product, the second inequality follows by Cauchy-Schwarz, the third inequality follows by the  $(\epsilon', \gamma^2)$ -SOSP conditions on both the min eigenvalue of the hessian and the norm of the gradient, the final two inequalities follow from knowing the main diagonal of  $\tilde{\mathbb{E}}[\tilde{\mathbf{x}}]$  is the identity and that every vector in  $\tilde{\mathbf{v}}$  is a unit vector up to inverse polynomial error  $\text{poly}(\rho^{-1}, 2^k)$ . For this last point see the proof in Lemma E.1. Therefore if we set  $\epsilon' = \text{poly}(\epsilon, 2^{-k})$  we arrive at any  $\epsilon$  error. Therefore we have established our estimate  $\hat{\mathbf{v}}$  approximates the global optimum of the quadratically penalized objective i.e  $\mathcal{H}_\rho(\tilde{\mathbb{E}}[\tilde{\mathbf{x}}]) - \mathcal{H}_\rho(\tilde{\mathbb{E}}[\tilde{\mathbf{x}}]) \leq \epsilon$ . To finish our proof, we have to bound the distance between the global optimum of the quadratically penalized objective  $\mathcal{H}_\rho(\tilde{\mathbb{E}}[\tilde{\mathbf{x}}])$  and SDP( $\Lambda$ ) the optimum of SDP 1. This is established for  $\rho$  a sufficiently large  $\text{poly}(\epsilon^{-1}, 2^k)$  in Lemma E.1. This concludes our proof that the iterates of Algorithm 2 converge to the solution of SDP 1.  $\square$

In our proof above, the bound on approximate SOSP being approximate global optimum is built on the result of Bhojanapalli et al. (2018) which we rephrase for our setting below.

**Lemma C.2.** [Bhojanapalli et al. (2018) lemma 3 rephrased] Let  $\mathcal{L}_\rho(\cdot)$  be defined as in equation 64 and let  $\mathcal{H}_\rho(\cdot)$  be defined as in equation 70. Let  $U \in \mathbb{R}^{\Phi \times \Phi}$  be an  $(\epsilon, \gamma)$ -SOSP of  $\mathcal{L}_\rho(\cdot)$ , then

$$\lambda_{\min}(\nabla \mathcal{H}_\rho(\tilde{\mathbb{E}}[\tilde{\mathbf{x}}])) \geq -\gamma\sqrt{\epsilon}$$

Furthermore, the global optimum  $\tilde{\mathbf{X}}$  obeys the optimality gap

$$\mathcal{H}_\rho(UU^T) - \mathcal{H}_\rho(\tilde{\mathbf{X}}) \leq \gamma\sqrt{\epsilon} \text{Tr}(\tilde{\mathbf{X}}) + \frac{1}{2}\epsilon \|U\|_F$$

The following Lemma E.1 establishes that for a sufficiently large penalty parameter  $\rho = \text{poly}(\epsilon^{-1}, 2^k)$  the optimum of the penalized problem and the exact solution to SDP 1 are close.

**Lemma C.3.** Let  $\Lambda$  be a Max-k-CSP instance, and let SDP( $\Lambda$ ) be the optimum of SDP 1. Let  $\mathcal{L}_\rho(\mathbf{v})$  be the quadratically penalized objective

$$\mathcal{L}_\rho(\mathbf{v}) := \frac{1}{|\mathcal{P}|} \left[ \sum_{P_z \in \mathcal{P}} \sum_{s \subseteq z} y_s \frac{1}{|\mathcal{C}(s)|} \sum_{\substack{g, g' \subseteq s \\ \text{s.t. } \zeta(g, g') = s}} \langle v_g, v_{g'} \rangle + \rho \left[ \sum_{P_z \in \mathcal{P}} \sum_{\substack{g, g', h, h' \subseteq z \\ \zeta(g, g') = \zeta(h, h')}} (\langle v_g, v_{g'} \rangle - \langle v_h, v_{h'} \rangle)^2 + \sum_{v_s \in \mathbf{v}} (\|v_s\|^2 - 1)^2 \right] \right] \quad (73)$$

Let  $\tilde{v}$  be the argmin of the unconstrained minimization

$$\tilde{v} := \arg \min_{\mathbf{v} \in \mathbb{R}^{|\mathcal{F}|^2 (2^{2k})}} \mathcal{L}_\rho(\mathbf{v})$$

Then we have

$$\mathcal{L}_\rho(\tilde{\mathbf{v}}) - \text{SDP}(\Lambda) \leq \epsilon$$

for  $\rho = \text{poly}(\epsilon^{-1}, 2^k)$

*Proof.* We begin the analysis with the generic equality constrained semidefinite program of the form

$$\text{Minimize: } \langle C, X \rangle \quad (74)$$

$$\text{Subject to: } \langle A_i, X \rangle = b_i \quad \forall i \in \mathcal{F} \quad (75)$$

$$X \succeq 0 \quad (76)$$

$$X \in \mathbb{R}^{d \times d} \quad (77)$$

For an objective matrix  $C$  and constraint matrices  $\{A_i\}_{i \in \mathcal{F}}$  in some constraint set  $\mathcal{F}$ . We will invoke specific properties of SDP 1 to enable our analysis. First we define the penalized objective in this generic form

$$\mathcal{H}_\rho(X) := \langle C, X \rangle + \rho \sum_{i \in \mathcal{F}} (\langle A_i, X \rangle - b_i)^2$$

Let  $\tilde{X}$  be the minimizer of the penalized problem.

$$\tilde{X} := \arg \min_{X \in \mathbb{R}^{d \times d}} \mathcal{L}_\rho(X)$$

Let  $X^*$  be the minimizer of the constrained problem equation 88. Let  $\tau_i$  be the error  $\tilde{X}$  has in satisfying constraint  $\langle A_i, \tilde{X} \rangle = b_i$ .

$$\tau_i := |\langle A_i, \tilde{X} \rangle - b_i|$$

We will show that  $\tau_i$  scales inversely with  $\rho$ . That is,  $\tau_i \leq \text{poly}(k, \rho^{-1})$ . Notice that the quadratic penalty on the violated constraints must be smaller than the decrease in the objective for having violated the constraints. So long as the objective is not too sensitive i.e 'robust' to perturbations in the constraint violations the quadratic penalty should overwhelm the decrease in the objective. To carry out this intuition, we begin with the fact that the constrained minimum is larger than the penalized minimum.

$$\mathcal{H}_\rho(X^*) - \mathcal{H}_\rho(\tilde{X}) \leq 0 \quad (78)$$

Applying the definitions of  $\mathcal{H}_\rho(X^*)$  and  $\mathcal{H}_\rho(\tilde{X})$  we obtain

$$\langle C, X^* \rangle - (\langle C, \tilde{X} \rangle + \rho \sum_{i \in \mathcal{F}} \tau_i^2) \leq 0 \quad (79)$$

Rearranging LHS and RHS and dividing by  $|\mathcal{F}|$  we obtain

$$\rho \frac{1}{|\mathcal{F}|} \sum_{i \in \mathcal{F}} \tau_i^2 \leq \frac{1}{|\mathcal{F}|} \langle C, \tilde{X} - X^* \rangle \quad (80)$$

We upper bound the RHS using the robustness theorem of Raghavendra & Steurer (2009a) restated in the appendix Theorem F.2 which states that an SDP solution that violates the constraints by a small perturbation changes the objective by a small amount. Thus we obtain,

$$\text{RHS} \leq \left( \frac{1}{|\mathcal{F}|} \sum_{i \in \mathcal{F}} \tau_i \right)^{1/2} \text{poly}(k) \quad (81)$$

Therefore combining equation 80 with equation 81 we obtain

$$\rho \frac{1}{|\mathcal{F}|} \sum_i \tau_i^2 \leq \left( \frac{1}{|\mathcal{F}|} \sum_i \tau_i \right)^{1/2} \text{poly}(k)$$

Taking Cauchy-Schwarz on the RHS we obtain

$$\rho \frac{1}{|\mathcal{F}|} \sum_i \tau_i^2 \leq \left( \frac{1}{|\mathcal{F}|} \sum_i \tau_i^2 \right)^{1/4} \text{poly}(k)$$

Noticing that  $\frac{1}{|\mathcal{F}|} \sum_i \tau_i^2$  appears in both LHS and RHS we rearrange to obtain

$$\frac{1}{|\mathcal{F}|} \sum_i \tau_i^2 \leq \frac{\text{poly}(k)}{\rho^{4/3}} \leq \epsilon$$

Where for  $\rho = \frac{\text{poly}(k)}{\epsilon^{3/4}}$  we have the average squared error of the constraints is upper bounded by  $\epsilon$ . Then via Markov's no more than  $\sqrt{\epsilon}$  fraction of the constraints can be violated by more than squared error  $\sqrt{\epsilon}$ . We label these 'grossly' violated constraints. The clauses involved in these grossly violated constraints contributes no more than  $\text{poly}(k)\sqrt{\epsilon}$  to the objective. On the other hand, the constraints that are violated by no more than squared error  $\sqrt{\epsilon}$  contributed no more than  $\text{poly}(k)\epsilon^{1/8}$  to the objective which follows from the robustness theorem Theorem F.2. Taken together we conclude that

$$\mathcal{L}_\rho(\tilde{\mathbf{v}}) - \text{SDP}(\Lambda) \leq \epsilon$$

For  $\rho = \text{poly}(k, \epsilon^{-1})$  as desired.  $\square$

Finally we show it's not hard to generalize our algorithm to alphabets of size  $[q]$ .

**Notation for General Alphabet.** For any predicate  $P \in \mathcal{P}$ , let  $\mathcal{D}(P)$  be the set of all variable assignment tuples indexed by a set of variables  $s \subseteq \mathcal{S}(P)$  and an assignment  $\tau \in [q]^{|s|}$ . Let  $x_{(i,a)}$  denote an assignment of value  $a \in [q]$  to variable  $x_i$ .

---

**SDP 2** SDP Vector Formulation for Max-k-CSP General Alphabet (Equivalent to UGC optimal)

---

SDP Vector Formulation General Alphabet  $\Lambda = (\mathcal{V}, \mathcal{P}, q)$ .

Pseudoexpectation formulation of the objective.

$$\min_{x_1, x_2, \dots, x_N} \sum_{P_z \in \mathcal{P}} \tilde{\mathbb{E}}_\mu[-P_z(X_z)] \quad (82)$$

$$\text{subject to: } \tilde{\mathbb{E}}_\mu[(x_{(i,a)}^2 - x_{(i,a)}) \prod_{(j,b) \in \phi} x_{(j,b)}] = 0 \quad \forall i \in \mathcal{V}, \forall a \in [q], \forall \phi \subseteq \mathcal{D}(P), \forall P \in \mathcal{P} \quad (83)$$

$$\tilde{\mathbb{E}}_\mu[(\sum_{a \in [q]} x_{ia} - 1) \prod_{(j,b) \in \phi} x_{(j,b)}] = 0 \quad \forall i \in \mathcal{V}, \forall \phi \subseteq \mathcal{D}(P), \forall P \in \mathcal{P}, \quad (84)$$

$$\tilde{\mathbb{E}}_\mu[x_{(i,a)} x_{(i,a')} \prod_{(j,b) \in \phi} x_{(j,b)}] = 0 \quad \forall i \in \mathcal{V}, \forall a \neq a' \in [q], \forall \phi \subseteq \mathcal{D}(P), \forall P \in \mathcal{P}, \quad (85)$$

$$\tilde{\mathbb{E}}[SoS_{2kq}(X_\phi)] \geq 0 \quad \forall \phi \subseteq \mathcal{D}(P), \forall P \in \mathcal{P}, \quad (86)$$

$$\tilde{\mathbb{E}}[SoS_2(\mathbf{x})] \geq 0. \quad (87)$$

First constraint corresponds to booleanity of each value in the alphabet.

Second constraint corresponds to a variable taking on only one value in the alphabet.

Third constraint corresponds to a variable taking on only one value in the alphabet.

Fourth constraint corresponds to local distribution on the variables in each predicate.

Fifth constraint corresponds to the positivity of every degree two sum of squares of polynomials.

---

**Lemma C.4.** There exists a message passing algorithm that computes in  $\text{poly}(\epsilon^{-1}, \Phi, \log(\delta^{-1}))$  iterations a set of vectors  $\mathbf{v} := \{\hat{v}_{(i,a)}\}$  for all  $(i, a) \in \phi$ , for all  $\phi \subseteq \mathcal{D}(P)$ , for all  $P \in \mathcal{P}$  that satisfy the constraints of Algorithm 2 to error  $\epsilon$  and approximates the optimum of Algorithm 2 to error  $\epsilon$  with probability  $1 - \delta$

$$\left| \sum_{P_z \in \mathcal{P}} \tilde{\mathbb{E}}_\mu[P_z(X_z)] - \text{SDP}(\Lambda) \right| \leq \epsilon$$

where  $\text{SDP}(\Lambda)$  is the optimum of Algorithm 2.

*Proof.* The proof is entirely parallel to the proof of Theorem C.1. We can write Algorithm 2 entirely in terms of the vector of its cholesky decomposition where once again we take advantage of the fact that SoS degree  $2kq$  distributions are actual distributions over subsets of  $kq$  variables over each predicate. Given the overparameterized vector formulation, we observe that once again we are faced with equality constraints that can be added to the objective with a quadratic penalty. Perturbed gradient descent induces a message passing algorithm over the constraint graph  $G_\Lambda$ , and in no more than  $\text{poly}(\epsilon^{-1}\Phi)$  iterations reaches an  $(\epsilon, \gamma)$ -SOSP. The analysis of optimality goes along the same lines as Lemma E.1. For sufficiently large penalty  $\rho = \text{poly}(\epsilon^{-1}, q^k)$  the error in satisfying the constraints is  $\epsilon$  and the objective is robust to small perturbations in satisfying the constraint. That concludes our discussion of generalizing to general alphabets.  $\square$

## C.1 DEFINITIONS

**Definition** (Message passing algorithm). Given a graph  $G = (V, E)$  with a set of vectors  $\mathbf{v} = \{v_i\}_{i \in V}$  a message passing algorithm for  $T$  iterations is an update of the form; for vector  $v_i$  in  $\mathbf{v}$  and for iteration  $t \in [T]$ ,

$$v_i^{t+1} = \text{UPDATE}(\{v_j^t\}_{j \in N(i)}, v_i^t)$$

For an arbitrary polynomial time computable function  $\text{UPDATE} : \mathbb{R}^{|N(i)|} \times \mathbb{R}^r \rightarrow \mathbb{R}^r$

## C.2 NEURAL CERTIFICATION SCHEME

An intriguing aspect of OptGNN is that the embeddings can be interpreted as the solution to a low rank SDP which leaves open the possibility that the embeddings can be used to generate a dual certificate i.e a lower bound on a convex relaxation. First, we define the primal problem

$$\text{Minimize: } \langle C, X \rangle \quad (88)$$

$$\text{Subject to: } \langle A_i, X \rangle = b_i \quad \forall i \in [\mathcal{F}] \quad (89)$$

$$X \succeq 0 \quad (90)$$

**Lemma C.5.** Let OPT be the minimizer of the SDP equation 88. Then for any  $\tilde{X} \in \mathbb{R}^{N \times N} \succeq 0$  and any  $\lambda^* \in \mathbb{R}^{|\mathcal{F}|}$ , we define  $F_{\lambda^*}(X)$  to be

$$F_{\lambda^*}(\tilde{X}) := \langle C, \tilde{X} \rangle + \sum_{i \in \mathcal{F}} \lambda_i^* (\langle A_i, \tilde{X} \rangle - b_i)$$

We require SDP to satisfy a bound on its trace  $\text{Tr}(X) \leq \mathcal{Y}$  for some  $\mathcal{Y} \in \mathbb{R}^+$ . Then the following is a lower bound on OPT.

$$\text{OPT} \geq F_{\lambda^*}(\tilde{X}) - \langle \nabla F_{\lambda^*}(\tilde{X}), \tilde{X} \rangle + \lambda_{\min}(\nabla F_{\lambda^*}(\tilde{X})) \mathcal{Y}$$

*Proof.* Next we introduce lagrange multipliers  $\lambda \in \mathbb{R}^k$  and  $Q \succeq 0$  to form the lagrangian

$$\mathcal{L}(\lambda, Q, X) = \langle C, X \rangle + \sum_{i \in \mathcal{F}} \lambda_i (\langle A_i, X \rangle - b_i) - \langle Q, X \rangle$$

We lower bound the optimum of OPT defined to be the minimizer of equation 88

$$\text{OPT} := \min_{X \succeq 0} \max_{\lambda \in \mathbb{R}, Q \succeq 0} \mathcal{L}(\lambda, Q, X) \geq \min_{V \in \mathbb{R}^{N \times N}} \max_{\lambda} \langle C, VV^T \rangle + \sum_{i \in \mathcal{F}} \lambda_i (\langle A_i, VV^T \rangle - b_i) \quad (91)$$

$$= \max_{\lambda} \min_{V \in \mathbb{R}^{N \times N}} \langle C, VV^T \rangle + \sum_{i \in \mathcal{F}} \lambda_i (\langle A_i, VV^T \rangle - b_i) \quad (92)$$

$$= \min_{V \in \mathbb{R}^{N \times N}} \langle C, VV^T \rangle + \sum_{i \in \mathcal{F}} \lambda_i^* (\langle A_i, VV^T \rangle - b_i). \quad (93)$$

Where in the first inequality we replaced  $X \succeq 0$  with  $VV^T$  which is a lower bound as every psd matrix admits a cholesky decomposition. In the second inequality we flipped the order of min and max, and in the final inequality we chose a specific set of dual variables  $\lambda^* \in \mathbb{R}^{|\mathcal{F}|}$  which lower bounds the maximization over dual variables. The key is to find a good setting for  $\lambda^*$ .

Next we establish that for any choice of  $\lambda^*$  we can compute a lower bound on inequality 93 as follows. Let  $F_{\lambda^*}(VV^T)$  be defined as the function in the RHS of 93.

$$F_{\lambda^*}(VV^T) := \langle C, X \rangle + \sum_{i \in \mathcal{F}} \lambda_i^* (\langle A_i, X \rangle - b_i)$$

Then equation 93 can be rewritten as

$$OPT \geq \min_{V \in \mathbb{R}^{N \times N}} F_{\lambda^*}(VV^T) := \langle C, X \rangle + \sum_{i \in \mathcal{F}} \lambda_i^* (\langle A_i, X \rangle - b_i)$$

Now let  $V^*$  be the minimizer of equation 93 and let  $X^* = V^*(V^*)^T$ . We have by convexity that

$$F_{\lambda^*}(X) - F_{\lambda^*}(X^*) \leq \langle \nabla F_{\lambda^*}(X), X - X^* \rangle = \langle \nabla F_{\lambda^*}(X), X \rangle + \langle -\nabla F_{\lambda^*}(X), X^* \rangle \quad (94)$$

$$\leq \langle \nabla F_{\lambda^*}(X), X \rangle - \lambda_{\min}(\nabla F_{\lambda^*}(X)) \text{Tr}(X^*) \quad (95)$$

$$\leq \langle \nabla F_{\lambda^*}(X), X \rangle - \lambda_{\min}(\nabla F_{\lambda^*}(X))N \quad (96)$$

In the first inequality we apply the convexity of  $F_{\lambda^*}$ . In the second inequality we apply a standard inequality of frobenius inner product. In the last inequality we use the fact that  $\text{Tr}(X^*) = N$ . Rearranging we obtain for any  $X$

$$OPT \geq F_{\lambda^*}(X^*) \geq F_{\lambda^*}(X) - \langle \nabla F_{\lambda^*}(X), X \rangle + \lambda_{\min}(\nabla F_{\lambda^*}(X))N \quad (97)$$

Therefore it suffices to upper bound the two terms above  $\langle \nabla F_{\lambda^*}(X), X \rangle$  and  $\lambda_{\min}(\nabla F_{\lambda^*}(X))$  which is an expression that holds for any  $X$ . Given the output embeddings  $\tilde{V}$  of OptGNN (or indeed any set of vectors  $\tilde{V}$ ) let  $\tilde{X} = \tilde{V}\tilde{V}^T$ . Then we have concluded

$$OPT \geq F_{\lambda^*}(X^*) \geq F_{\lambda^*}(\tilde{X}) - \langle \nabla F_{\lambda^*}(\tilde{X}), \tilde{X} \rangle + \lambda_{\min}(\nabla F_{\lambda^*}(\tilde{X}))N \quad (98)$$

as desired.  $\square$

Up to this point, every manipulation is formal proof. Subsequently we detail how to estimate the dual variables  $\lambda^*$ . Although any estimate will produce a bound, it won't produce a tight bound. To be clear, solving for the optimal  $\lambda^*$  would be the same as building an SDP solver which would bring us back into the expensive primal dual procedures that are involved in solving SDP's. We are designing quick and cheap ways to output a dual certificate that may be somewhat looser. Our scheme is simply to set  $\lambda^*$  such that  $\|\nabla F_{\lambda^*}(\tilde{X})\|$  is minimized, ideally equal to zero. The intuition is that if  $(\tilde{X}, \lambda^*)$  were a primal dual pair, then the lagrangian would have a derivative with respect to  $X$  evaluated at  $\tilde{X}$  would be equal to zero. Let  $H_{\lambda^*}(V)$  be defined as follows

$$H_{\lambda^*}(\tilde{V}) := \langle C, \tilde{V}\tilde{V}^T \rangle + \sum_{i \in \mathcal{F}} \lambda_i^* (\langle A_i, \tilde{V}\tilde{V}^T \rangle - b_i)$$

We know the gradient of  $H_{\lambda^*}(\tilde{V})$

$$\nabla H_{\lambda^*}(\tilde{V}) = 2 \left( C + \sum_{i \in \mathcal{F}} \lambda_i^* A_i \right) \tilde{V} = 2 \nabla F_{\lambda^*}(\tilde{V}\tilde{V}^T) \tilde{V}$$

Therefore it suffices to find a setting of  $\lambda^*$  such that  $\|\nabla F_{\lambda^*}(\tilde{X})\tilde{V}\|$  is small, ideally zero. This would be a simple task, indeed a regression, if not for the unfortunate fact that OptGNN explicitly projects the vectors in  $\tilde{V}$  to be unit vectors. This creates numerical problems such that minimizing the norm of  $\|\nabla F_{\lambda^*}(\tilde{X})\tilde{V}\|$  does not produce a  $\nabla F_{\lambda^*}(\tilde{X})$  with a large minimum eigenvalue.

To fix this issue, let  $R_{\eta, \rho}(V)$  denote the penalized lagrangian with quadratic penalties for constraints of the form  $\langle A_i, X \rangle = b_i$  and linear penalty  $\eta_i$  for constraints along the main diagonal of  $X$  of the form  $\langle e_i e_i^T, X \rangle = 1$ .

$$R_{\eta, \rho}(V) := \langle C, VV^T \rangle + \sum_{i \in \mathcal{F}} \rho (\langle A_i, VV^T \rangle - b_i)^2 + \sum_{i=1}^N \eta_i (\langle e_i e_i^T, VV^T \rangle - 1)$$

Taking the gradient of  $R_{\eta,\rho}(V)$  we obtain

$$\nabla R_{\eta,\rho}(V) := 2CV + \sum_{i \in \mathcal{J}} 2\rho(\langle A_i, VV^T \rangle - b_i)A_iV + \sum_{i=1}^N 2\eta_i e_i e_i^T V$$

Our rule for setting dual variables  $\delta_i$  for  $i \in \mathcal{J}$  is

$$\delta_i := 2\rho(\langle A_i, \tilde{V}\tilde{V}^T \rangle - b_i)$$

our rule for setting dual variables  $\eta_j$  for  $j \in [N]$  is

$$\eta_j := \frac{1}{2} \left\| e_j^T \left( C + \sum_{i \in \mathcal{F}} 2\rho(\langle A_i, VV^T \rangle - b_i)A_i \right) V \right\|$$

Then our full set of dual variables  $\lambda^*$  is simply the concatenation  $(\delta, \eta)$ . Writing out everything explicitly we obtain the following matrix for  $\nabla F_{\lambda^*}(\tilde{V}\tilde{V}^T)$

$$\nabla F_{\lambda^*}(\tilde{V}\tilde{V}^T) = C + \sum_{i \in \mathcal{F}} \rho(\langle A_i, \tilde{V}\tilde{V}^T \rangle - b_i)A_i + \sum_{j \in [N]} \frac{1}{2} \left\| e_j^T \left( C + \sum_{i \in \mathcal{F}} 2\rho(\langle A_i, \tilde{V}\tilde{V}^T \rangle - b_i)A_i \right) \tilde{V} \right\| e_i e_i^T$$

Plugging this expression into Lemma C.5 the final bound we evaluate in our code is

$$\begin{aligned} OPT &\geq \langle C, \tilde{V}\tilde{V}^T \rangle + \sum_{i \in \mathcal{F}} 2\rho(\langle A_i, \tilde{V}\tilde{V}^T \rangle - b_i)^2 \\ &- \left\langle C + \sum_{i \in \mathcal{F}} \rho(\langle A_i, \tilde{V}\tilde{V}^T \rangle - b_i)A_i + \sum_{j \in [N]} \frac{1}{2} \left\| e_j^T \left( C + \sum_{i \in \mathcal{F}} 2\rho(\langle A_i, \tilde{V}\tilde{V}^T \rangle - b_i)A_i \right) \tilde{V} \right\| e_i e_i^T, \tilde{V}\tilde{V}^T \right\rangle \\ &+ \lambda_{\min} \left( C + \sum_{i \in \mathcal{F}} \rho(\langle A_i, \tilde{V}\tilde{V}^T \rangle - b_i)A_i + \sum_{j \in [N]} \frac{1}{2} \left\| e_j^T \left( C + \sum_{i \in \mathcal{F}} 2\rho(\langle A_i, \tilde{V}\tilde{V}^T \rangle - b_i)A_i \right) \tilde{V} \right\| e_i e_i^T \right) N \end{aligned} \quad (99)$$

Which is entirely computed in terms of  $\tilde{V}$  the output embeddings of OptGNN. The resulting plot is as follows.

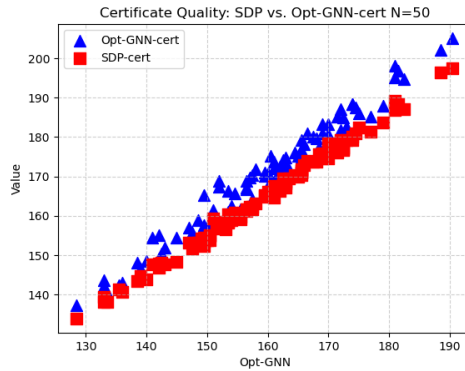


Figure 3: N=50 p=0.1 SDP vs OptGNN Dual Certificate

**Note:** The reason for splitting the set of dual variables is because the projection operator onto the unit ball is hard coded into the architecture of the lift network. Satisfying the constraint set via projection is different from the soft quadratic penalties on the remaining constraints and require separate handling.

**Max-Cut Certificate** For Max-Cut our dual variables are particularly simple as there are no constraints  $\langle A_i, X \rangle = b_i$  for  $b_i \neq 0$ . The dual variables for Max-Cut take on the form for all  $i \in [N]$

$$\lambda_i^* = \frac{1}{2} \left\| \sum_{j \in N(i)} w_{ij} v_j \right\|$$

It’s certainly possible to come up with tighter certification schemes which we leave to future work.

**Intuition:** Near global optimality one step of the augmented method of lagrange multipliers ought to closely approximate the dual variables. After obtaining a estimate for the penalized lagrange multipliers we estimate the lagrange multipliers for the norm constraint by approximating  $\nabla R_\lambda(V) = 0$ . The alternative would have been to solve the linear system for all the lagrange multipliers at once but this runs into numerical issues and degeneracies.

**Certificate Experiment:** We run our certification procedure which we name OptGNN-cert and compare it to the SDP certificate. Note, that mathematically we will always produce a larger (i.e inferior) dual certificate in comparison to the SDP because we are bounding the distance to the SDP optimum with error in the gradients and Hessians of the output embeddings of OptGNN. Our advantage is in the speed of the procedure. Without having to go through a primal dual solver, the entire time of producing OptGNN-cert is in the time required to feedforward through OptGNN. In this case we train an OptGNN-Max-Cut with 10 layers, on 1000 Erdos-Renyi graphs, with  $N = 100$  nodes and edge density  $p = 0.1$ . We plot the OptGNN Max-Cut value (an actual integer cut) on the x-axis and in the y-axis we plot the dual certificate value on the same graph where we compare the SDP certificate with the OptGNN-cert. See 3 for the  $N = 50$  graphs and 2 for the  $N = 100$  graphs.

Note of course the dual certificate for any technique must be larger than the cut value outputted by OptGNN so the scatter plot must be above the  $x = y$  axis of the plot. We see as is mathematically necessary, the OptGNN-cert is not as tight as the SDP certificate but certainly competitive and more importantly it is arrived at dramatically faster. Without any attempt at optimizing the runtime, the OptGNN feedforward and certification takes no more than 0.02 seconds whereas the SDP takes 0.5 seconds on  $N = 100$  node graphs.

## D EXPERIMENT DETAILS

In this section we give further details on our experimental setup.

**Datasets.** Our experiments span a variety of randomly generated and real-world datasets. Our randomly generated datasets contain graphs from several random graph models, in particular Erdős-Rényi (with  $p = 0.15$ ), Barabási-Albert (with  $m = 4$ ), Holme-Kim (with  $m = 4$  and  $p = 0.25$ ), Watts-Strogatz (with  $k = 4$  and  $p = 0.25$ ), and forced RB (with two sets of parameters, RB200 and RB500). Our real-world datasets are ENZYMES, PROTEINS, MUTAG, IMDB-BINARY, COLLAB (which we will together call **TU-small**), and REDDIT-BINARY, REDDIT-MULTI-5K, and REDDIT-MULTI-12K (which we will call **TU-REDDIT**).

We abbreviate the generated datasets using their initials and the range of vertex counts. For example, by ER (50,100) we denote Erdős-Rényi random graphs with a vertex count drawn uniformly at random from [50, 100]. In tables, we mark generated datasets with superscript <sup>a</sup>, **TU-small** with <sup>b</sup>, and **TU-REDDIT** with <sup>c</sup>.

For Table 3, we display results for forced RB instances drawn from two different distributions. For RB200, we select  $N$  uniformly in [6, 15] and  $K$  uniformly in [12, 21]. For RB500, we select  $N$  uniformly in [20, 34] and  $K$  uniformly in [10, 29].

In Table 2, random 3-SAT instances are generated by drawing three random variables for each clause and negating each variable with  $p = 0.5$ . We trained on instances with 100 variables and clause count drawn uniformly from the interval [400, 430], and tested on instances with 100 variables and 400, 415, and 430 clauses respectively.

**Baselines.** We compare the performance of our approach against known classical algorithms. In terms of classical baselines, we run Gurobi with varying timeouts and include SDP results on smaller datasets.

We also include a greedy baseline, which is the function `one_exchange` (for Max-Cut) or `min_weighted_vertex_cover` (for Min-Vertex-Cover) from `networkx` (Hagberg et al., 2008).



Parameter	ER, BA, WS, HK	RB200	RB500	3-SAT	TU-small	TU-REDDIT
Gradient steps	20,000	200,000	100,000	100,000	100,000	100,000
Validation freq	1,000	2,000	2,000	2,000	1,000	2,000
Batch size	16	32	32	32	16	16
Ranks	4, 8, 16, 32	32, 64	32, 64	32, 64	4, 8, 16, 32	4, 8, 16, 32
Layer counts	8, 16	16	16	16	8, 16	8, 16
Positional encodings	RW	none	none	none	LE, RW	RW
<b>Run count</b>	8	2	2	2	16	8

Figure 4: Hyperparameter range explored for each group of datasets. For each NN architecture, when training on a dataset, we explored every listed hyperparameter combination in the corresponding column.

**Validation and test splits.** For each dataset we hold out a validation and test slice for evaluation. In our generated graph experiments we set aside 1000 graphs each for validation and testing. Each step of training ran on randomly generated graphs. For **TU-small**, we used a train/validation/test split of 0.8/0.1/0.1. For **TU-REDDIT**, we set aside 100 graphs each for validation and testing.

**Scoring.** To measure a model’s score on a graph, we first run the model on the graph with a random initial vector assignment to generate an SDP output, and then round this output to an integral solution using 1,000 random hyperplanes. For the graph, we retain the best score achieved by any hyperplane.

We ran validation periodically during each training run and retained the model that achieved the highest validation score. Then for each model and dataset, we selected the hyperparameter setting that achieved the highest validation score, and we report the average score measured on the test slice. Please see D for further details on the hyperparameter ranges used.

In Table 3 and Table 4, at test time, we use 100 random initial vector assignments instead of just 1, and retain the best score achieved by any hyperplane on any random initial vector assignment. We use 1 random initial vector assignment for validation as in other cases.

**Hardware.** Our training runs used 20 cores of an Intel Xeon Gold 6248 (for data loading and random graph generation) and a NVIDIA Tesla V100 GPU. Our Gurobi runs use 8 threads on a Intel Xeon Platinum 8260. Our KaMIS runs use an Intel Core i9-13900H. Our LwD and DGL-TREESearch runs use an Intel Core i9-13900H and an RTX 4060.

**Hyperparameters.** We ran each experiment on a range of hyperparameters. See Figure 4 for the hyperparameter listing. For all training runs, we used the Adam optimizer Kingma & Ba (2014) with a learning rate of 0.001. We used Laplacian eigenvector Dwivedi et al. (2020) (LE) or random walk Dwivedi et al. (2021) (RW) positional encoding with dimensionality of half the rank, except for rank 32 where we used 8 dimensions. For Max-3-SAT, we set the penalty term  $\rho = 0.003$ .

#### D.1 MAX-3-SAT

**ErdősGNN.** The ErdősGNN baseline accepts as input a clause-variable bipartite graph of the SAT formula and the node degrees as input attributes. Each variable  $x_i$  is set to TRUE with probability  $p_i$ . A graph neural network (GatedGCNN) is trained until convergence ( $\sim 50k$  iterations) with randomly generated formulae with clause to variable ratio in the range  $[4, 4.3]$ . The neural network is trained to produce output probabilities  $p_i$  by minimizing the expected number of unsatisfied clauses. The exact closed form of the expectation can be found in (Karaliyas, 2023). At inference time, the probabilities are rounded to binary assignments using the method of conditional expectation.

**WalkSAT.** We use a publicly available python implementation of WalkSAT and we set the max number of variable flips to  $4 \times$  number of variables, for a total of 400 flips on the instances we tested.

**Autograd.** The autograd comparison measures the performance of autograd on the same loss as OptGNN. Starting with some initial node embeddings for the instance, the Lagrangian is computed for the problem and the node embeddings are updated by minimizing the Lagrangian using Adam. This process is run for several iterations. After it is concluded, the vectors are rounded with hyperplane rounding, yielding a binary assignment for the variables of the formula.

**Autograd parameters.** We use the Adam optimizer with learning rate 0.1 for 1000 epochs with penalty 0.01 and round with 10,000 hyperplanes, which is 10 times as many as that used by OptGNN.

## D.2 ADDITIONAL RESULTS

### D.2.1 COMPARISONS WITH GUROBI AND GREEDY

Table 6 and Table 5 contain comparisons on additional datasets with Gurobi and Greedy.

Dataset	OptGNN	Greedy	Gurobi 0.1s	Gurobi 1.0s	Gurobi 8.0s
BA <sup>a</sup> (50,100)	42.88 (27)	51.92	42.82	42.82	42.82
BA <sup>a</sup> (100,200)	83.43 (25)	101.42	83.19	83.19	83.19
BA <sup>a</sup> (400,500)	248.74 (27)	302.53	256.33	246.49	246.46
ER <sup>a</sup> (50,100)	55.25 (21)	68.85	55.06	54.67	54.67
ER <sup>a</sup> (100,200)	126.52 (18)	143.51	127.83	123.47	122.76
ER <sup>a</sup> (400,500)	420.70 (41)	442.84	423.07	423.07	415.52
HK <sup>a</sup> (50,100)	43.06 (25)	51.38	42.98	42.98	42.98
HK <sup>a</sup> (100,200)	84.38 (25)	100.87	84.07	84.07	84.07
HK <sup>a</sup> (400,500)	249.26 (27)	298.98	247.90	247.57	247.57
WC <sup>a</sup> (50,100)	46.38 (26)	72.55	45.74	45.74	45.74
WC <sup>a</sup> (100,200)	91.28 (21)	143.70	89.80	89.80	89.80
WC <sup>a</sup> (400,500)	274.21 (31)	434.52	269.58	269.39	269.39
MUTAG <sup>b</sup>	7.79 (18)	12.84	7.74	7.74	7.74
ENZYMES <sup>b</sup>	20.00 (24)	27.35	20.00	20.00	20.00
PROTEINS <sup>b</sup>	25.29 (18)	33.93	24.96	24.96	24.96
IMDB-BIN <sup>b</sup>	16.78 (18)	17.24	16.76	16.76	16.76
COLLAB <sup>b</sup>	67.50 (23)	71.74	67.47	67.46	67.46
REDDIT-BIN <sup>c</sup>	82.85 (38)	117.16	82.81	82.81	82.81
REDDIT-M-12K <sup>c</sup>	81.55 (25)	115.72	81.57	81.52	81.52
REDDIT-M-5K <sup>c</sup>	107.36 (33)	153.24	108.73	107.32	107.32

Table 5: Performance of OptGNN, Greedy, and Gurobi 0.1s, 1s, and 8s on Min-Vertex-Cover. For each approach and dataset, we report the average Vertex-Cover size measured on the test slice. Here, lower score is better. In parentheses, we include the average runtime in *milliseconds* for OptGNN.

### D.2.2 RATIO TABLES

In Figure 5 and Figure 6 we supply the performance of OptGNN as a ratio against the integral value achieved by Gurobi running with a time limit of 8 seconds. These tables include the standard deviation in the ratio. We note that for Maximum Cut, OptGNN comes within 1.1% of the Gurobi 8s value, and for Min-Vertex-Cover, OptGNN comes within 3.1%.

## D.3 MODEL ABLATION STUDY

Here we provide the evaluations of several models that were trained on the same loss as OptGNN. We see that OptGNN consistently achieves the best performance among different neural architectures. Note that while OptGNN was consistently the best model, other models were able to perform relatively well; for instance, GatedGCNN achieves average cut values within a few percent of OptGNN on nearly all the datasets (excluding COLLAB). This points to the overall viability of training using an SDP relaxation for the loss function.

Table 8 presents the performance of alternative neural network architectures on Min-Vertex-Cover.

## D.4 EFFECTS OF HYPERPARAMETERS ON PERFORMANCE

Figure 7 and Figure 8 present overall trends in model performance across hyperparameters.

Dataset	OptGNN	Greedy	Gurobi 0.1s	Gurobi 1.0s	Gurobi 8.0s
BA <sup>a</sup> (50,100)	351.49 (18)	200.10	351.87	352.12	352.12
BA <sup>a</sup> (100,200)	717.19 (20)	407.98	719.41	719.72	720.17
BA <sup>a</sup> (400,500)	2197.99 (66)	1255.22	2208.11	2208.11	2212.49
ER <sup>a</sup> (50,100)	528.95 (18)	298.55	529.93	530.03	530.16
ER <sup>a</sup> (100,200)	1995.05 (24)	1097.26	2002.88	2002.88	2002.93
ER <sup>a</sup> (400,500)	16387.46 (225)	8622.34	16476.72	16491.60	16495.31
HK <sup>a</sup> (50,100)	345.74 (18)	196.23	346.18	346.42	346.42
HK <sup>a</sup> (100,200)	709.39 (23)	402.54	711.68	712.26	712.88
HK <sup>a</sup> (400,500)	2159.90 (61)	1230.98	2169.46	2169.46	2173.88
WC <sup>a</sup> (50,100)	198.29 (18)	116.65	198.74	198.74	198.74
WC <sup>a</sup> (100,200)	389.83 (24)	229.43	390.96	392.07	392.07
WC <sup>a</sup> (400,500)	1166.47 (78)	690.19	1173.45	1175.97	1179.86
MUTAG <sup>b</sup>	27.95 (9)	16.95	27.95	27.95	27.95
ENZYMES <sup>b</sup>	81.37 (14)	48.53	81.45	81.45	81.45
PROTEINS <sup>b</sup>	102.15 (12)	60.74	102.28	102.36	102.36
IMDB-BIN <sup>b</sup>	97.47 (11)	51.85	97.50	97.50	97.50
COLLAB <sup>b</sup>	2622.41 (22)	1345.70	2624.32	2624.57	2624.62
REDDIT-BIN <sup>c</sup>	693.33 (186)	439.79	693.02	694.10	694.14
REDDIT-M-12K <sup>c</sup>	568.00 (89)	358.40	567.71	568.91	568.94
REDDIT-M-5K <sup>c</sup>	786.09 (133)	495.02	785.44	787.48	787.92

Table 6: Performance of OptGNN, Greedy, and Gurobi 0.1s, 1s, and 8s on Maximum Cut. For each approach and dataset, we report the average cut size measured on the test slice. Here, higher score is better. In parentheses, we include the average runtime in *milliseconds* for OptGNN.

Dataset	OptGNN
BA <sup>a</sup> (50,100)	0.998 ± 0.002
BA <sup>a</sup> (100,200)	0.996 ± 0.003
BA <sup>a</sup> (400,500)	0.993 ± 0.003
ER <sup>a</sup> (50,100)	0.998 ± 0.002
ER <sup>a</sup> (100,200)	0.996 ± 0.002
ER <sup>a</sup> (400,500)	0.993 ± 0.001
HK <sup>a</sup> (50,100)	0.998 ± 0.002
HK <sup>a</sup> (100,200)	0.995 ± 0.003
HK <sup>a</sup> (400,500)	0.994 ± 0.003
WC <sup>a</sup> (50,100)	0.998 ± 0.003
WC <sup>a</sup> (100,200)	0.995 ± 0.003
WC <sup>a</sup> (400,500)	0.989 ± 0.003
MUTAG <sup>b</sup>	1.000 ± 0.000
ENZYMES <sup>b</sup>	0.999 ± 0.003
PROTEINS <sup>b</sup>	1.000 ± 0.002
IMDB-BIN <sup>b</sup>	1.000 ± 0.001
COLLAB <sup>b</sup>	0.999 ± 0.002
REDDIT-BIN <sup>c</sup>	1.000 ± 0.001
REDDIT-M-12K <sup>c</sup>	0.999 ± 0.002
REDDIT-M-5K <sup>c</sup>	0.999 ± 0.002

Figure 5: Performance of OptGNN on Max-Cut compared to Gurobi running under an 8 second time limit, expressed as a ratio. For each dataset, we take the ratio of the integral values achieved by OptGNN and Gurobi 8s on each of the graphs in the test slice. We present the average and standard deviation of these ratios. Here, higher is better. This table demonstrates that OptGNN achieves nearly the same performance, missing on average 1.1% of the cut value in the worst measured case.

Dataset	OptGNN
BA <sup>a</sup> (50,100)	1.001 ± 0.005
BA <sup>a</sup> (100,200)	1.003 ± 0.005
BA <sup>a</sup> (400,500)	1.008 ± 0.011
ER <sup>a</sup> (50,100)	1.010 ± 0.015
ER <sup>a</sup> (100,200)	1.031 ± 0.012
ER <sup>a</sup> (400,500)	1.013 ± 0.006
HK <sup>a</sup> (50,100)	1.002 ± 0.007
HK <sup>a</sup> (100,200)	1.004 ± 0.013
HK <sup>a</sup> (400,500)	1.007 ± 0.011
WC <sup>a</sup> (50,100)	1.014 ± 0.016
WC <sup>a</sup> (100,200)	1.016 ± 0.013
WC <sup>a</sup> (400,500)	1.018 ± 0.007
MUTAG <sup>b</sup>	1.009 ± 0.027
ENZYMES <sup>b</sup>	1.000 ± 0.000
PROTEINS <sup>b</sup>	1.010 ± 0.021
IMDB-BIN <sup>b</sup>	1.002 ± 0.016
COLLAB <sup>b</sup>	1.001 ± 0.003
REDDIT-BIN <sup>c</sup>	1.000 ± 0.002
REDDIT-M-12K <sup>c</sup>	1.000 ± 0.001
REDDIT-M-5K <sup>c</sup>	1.000 ± 0.001

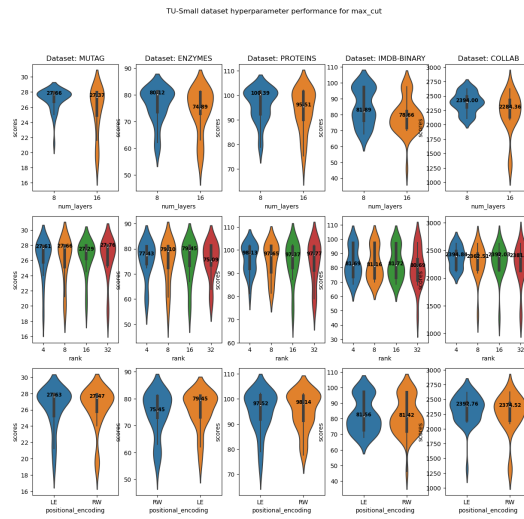
Figure 6: Performance of OptGNN on Min-Vertex-Cover compared to Gurobi running under an 8 second time limit, expressed as a ratio. For each dataset, we take the ratio of the integral values achieved by OptGNN and Gurobi 8s on each of the graphs in the test slice. We present the average and standard deviation of these ratios. Here, lower is better. This table demonstrates that OptGNN achieves nearly the same performance, producing a cover on average 3.1% larger than Gurobi 8s in the worst measured case.

Dataset	GAT	GCNN	GIN	GatedGCNN	OptGNN
ER <sup>a</sup> (50,100)	525.92 (25)	500.94 (17)	498.82 (14)	526.78 (14)	<b>528.95</b> (18)
ER <sup>a</sup> (100,200)	1979.45 (20)	1890.10 (26)	1893.23 (23)	1978.78 (21)	<b>1995.05</b> (24)
ER <sup>a</sup> (400,500)	16317.69 (208)	15692.12 (233)	15818.42 (212)	16188.85 (210)	<b>16387.46</b> (225)
MUTAG <sup>b</sup>	27.84 (19)	27.11 (12)	27.16 (13)	<b>27.95</b> (14)	<b>27.95</b> (9)
ENZYMES <sup>b</sup>	80.73 (17)	74.03 (12)	73.85 (16)	81.35 (9)	<b>81.37</b> (14)
PROTEINS <sup>b</sup>	100.94 (14)	92.01 (19)	92.62 (17)	101.68 (10)	<b>102.15</b> (12)
IMDB-BIN <sup>b</sup>	81.89 (18)	70.56 (21)	81.50 (10)	97.11 (9)	<b>97.47</b> (11)
COLLAB <sup>b</sup>	2611.83 (22)	2109.81 (21)	2430.20 (23)	2318.19 (18)	<b>2622.41</b> (22)

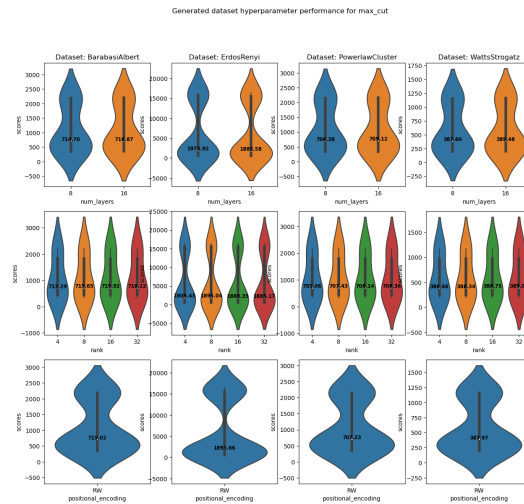
Table 7: Performance of various model architectures for selected datasets on Maximum Cut. Here, higher is better. GAT is the Graph Attention network (Veličković et al., 2018), GIN is the Graph Isomorphism Network (Xu et al., 2019), GCNN is the Graph Convolutional Neural Network (Morris et al., 2019), and GatedGCNN is the gated version (Li et al., 2015).

Dataset	GAT	GCNN	GIN	GatedGCNN	OptGNN
ER <sup>a</sup> (50,100)	58.78 (20)	64.42 (23)	64.18 (20)	56.17 (14)	<b>55.25</b> (21)
ER <sup>a</sup> (100,200)	129.47 (20)	141.94 (17)	140.06 (20)	130.32 (20)	<b>126.52</b> (18)
ER <sup>a</sup> (400,500)	443.93 (43)	444.12 (33)	442.11 (31)	440.90 (28)	<b>420.70</b> (41)
MUTAG <sup>b</sup>	<b>7.79</b> (19)	8.11 (16)	7.95 (20)	<b>7.79</b> (17)	<b>7.79</b> (18)
ENZYMES <sup>b</sup>	21.93 (24)	25.42 (18)	25.80 (28)	20.28 (14)	<b>20.00</b> (24)
PROTEINS <sup>b</sup>	28.19 (23)	31.07 (19)	32.28 (21)	<b>25.25</b> (19)	25.29 (18)
IMDB-BIN <sup>b</sup>	17.62 (21)	19.22 (19)	19.03 (23)	16.79 (15)	<b>16.78</b> (18)
COLLAB <sup>b</sup>	68.23 (23)	73.32 (17)	73.82 (26)	72.92 (13)	<b>67.50</b> (23)

Table 8: Performance of various model architectures compared to OptGNN for selected datasets on Min-Vertex-Cover. Here, lower is better.

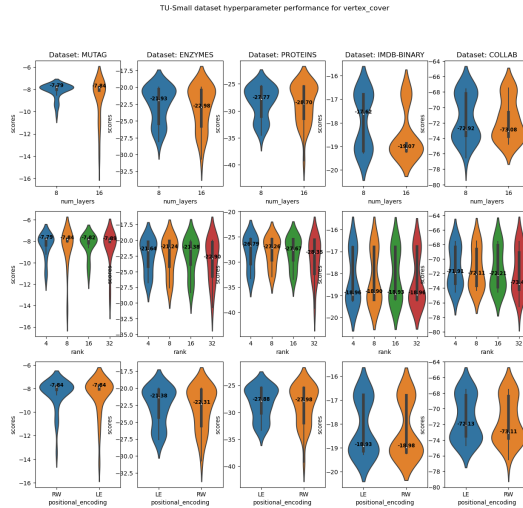


(a) On TU-small datasets.

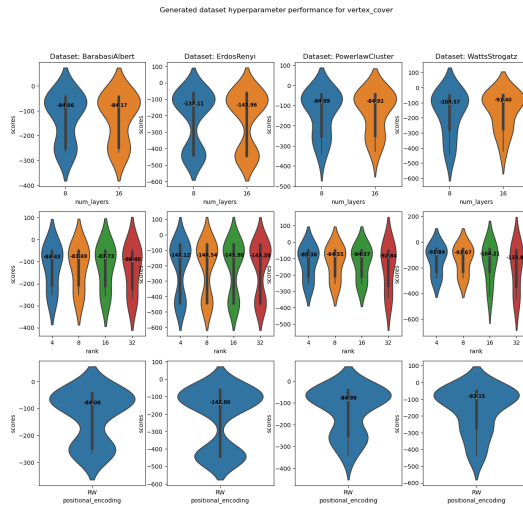


(b) On generated datasets.

Figure 8: Trends in model performance on Max-Cut with respect to the number of layers, hidden size, and positional encoding of the models.



(a) On TU-small datasets.



(b) On generated datasets.

Figure 7: Trends in model performance on Min-Vertex-Cover with respect to the number of layers, hidden size, and positional encoding of the models.

### D.5 OUT OF DISTRIBUTION TESTING

OptGNN trained on one dataset performed quite well on other datasets without any finetuning, suggesting that the model can generalize to examples outside its training distribution. For each dataset in our collection, we train a model and then test the trained model on a subset of datasets in the collection. The results are shown in Table 9. It is apparent from the results that the model performance generalizes well to different datasets. Interestingly, we frequently observe that the model reaches its peak performance on a given test dataset even when trained on a different one. This suggests that the model indeed is capturing elements of a more general process instead of just overfitting the training data.

### D.6 PSEUDOCODE FOR OPTGNN TRAINING AND INFERENCE

In algorithm 3, we present pseudocode for OptGNN in the Max-Cut case and in algorithm 4 pseudocode for the forward pass of a general SDP.

Train Dataset	MUTAG	ENZYMES	PROTEINS	IMDB-BIN	COLLAB
BA (50,100)	<b>7.74</b>	20.12	27.66	17.57	74.15
BA (100,200)	<b>7.74</b>	20.35	26.03	16.86	69.29
BA (400,500)	8.05	21.00	26.54	17.34	70.17
ER (50,100)	<b>7.74</b>	20.37	28.17	16.86	69.07
ER (100,200)	8.05	21.52	27.72	16.89	68.83
ER (400,500)	7.79	21.55	28.60	16.78	68.74
HK (50,100)	<b>7.74</b>	20.42	25.60	17.05	69.17
HK (100,200)	7.84	20.43	27.30	17.01	70.20
HK (400,500)	7.95	20.63	26.30	17.15	69.91
WC (50,100)	7.89	<b>20.13</b>	25.46	17.38	70.14
WC (100,200)	7.79	20.30	25.45	17.91	71.16
WC (400,500)	8.05	20.48	25.79	17.12	70.16
MUTAG	<b>7.74</b>	20.83	26.76	16.92	70.09
ENZYMES	<b>7.74</b>	20.60	28.29	16.79	68.40
PROTEINS	7.89	20.22	<b>25.29</b>	16.77	70.26
IMDB-BIN	7.95	20.97	27.06	<b>16.76</b>	68.03
COLLAB	7.89	20.35	26.13	<b>16.76</b>	<b>67.52</b>

Table 9: Models for Min-Vertex-Cover trained on "dataset" were tested on a selection of the TU datasets (ENZYMES, PROTEINS, MUTAG, IMDB-BINARY, and COLLAB). We observe that the performance of the models generalizes well even when they are taken out of their training context.

---

**Algorithm 3** OptGNN pseudocode for Max-Cut forward pass

---

**Require:** graph  $G$

- 1:  $\mathbf{v}^0 = \{v_1, v_2, \dots, v_N\}$  (random initial feature vectors and/or positional encodings)
  - 2: **for**  $t = 1, 2, 3, \dots, T$  **do**
  - 3:   **for**  $v_i^t \in \mathbf{v}^t$  **do**
  - 4:      $v_i^{t+1} \leftarrow v_i^t + \sum_{j \in N(i)} v_j^t$
  - 5:      $\hat{v}_i^{t+1} \leftarrow \text{Linear}\left(\frac{v_i^{t+1}}{|v_i^{t+1}|}\right)$
  - 6:   **end for**
  - 7: **end for**
- 

---

**Algorithm 4** OptGNN pseudocode for implementing a general SDP forward pass

---

**Require:** graph  $G$

- 1:  $\mathbf{v}^0 = \{v_1, v_2, \dots, v_N\}$  (random initial feature vectors and/or positional encodings)
  - 2: **for**  $t = 1, 2, 3, \dots, T$  **do**
  - 3:   **for**  $v_i^t \in \mathbf{v}^t$  **do**
  - 4:      $v_i^{t+1} \leftarrow v_i^t + \text{Autograd}(\mathcal{L}(\mathbf{v}_i^t; G))$
  - 5:      $\hat{v}_i^{t+1} \leftarrow \text{Linear}\left(\frac{v_i^{t+1}}{|v_i^{t+1}|}\right)$
  - 6:   **end for**
  - 7: **end for**
-

## E GENERALIZATION ANALYSIS

In this section we produce a generalization bound for OptGNN. First we restate our result that a penalized loss approximates the optimum of SDP 1. Our analysis follows from a standard perturbation argument where the key is to bound the lipschitzness of the OptGNN aggregation function. Here we will have to be more precise with the exact polynomial dependence of the lipschitzness of the gradient  $\nabla \mathcal{L}_\rho$  and the smoothness of the hessian  $\nabla^2 \mathcal{L}_\rho$ .

**Notation:** For the convenience of the proofs in this section, with a slight abuse of notation, we will define loss functions  $\mathcal{L}_\rho(V)$  that take matrix arguments  $V$  instead of collections of vectors  $\mathbf{v}$  where  $V$  is simply the vectors in  $\mathbf{v}$  concatenated row by row. We will also refer to rows of  $V$  by indexing them with set notation  $v_i \in V$  where  $v_i$  denotes the  $i$ 'th row of  $V$ . Furthermore, let every vector be bounded in norm by some absolute constant  $B$ .

We begin by recomputing precisely the number of iterations required for algorithm 2 to approximate the global optimum of SDP 1. Note that this was done in the proof of Theorem C.1 but we do it here with explicit polynomial dependence.

**Lemma E.1** (gradient descent lemma restated). Algorithm 2 computes in  $O(\Phi^4 \epsilon^{-4} \log^4(\delta^{-1}))$  iterations a set of vectors  $\mathbf{v} := \{\hat{v}_s\}$  for all  $s \subseteq \mathcal{S}(P)$  for all  $P \in \mathcal{P}$  that satisfy the constraints of SDP 1 to average error  $\epsilon$  and approximates the optimum of SDP 1 to error  $\epsilon$  with probability  $1 - \delta$

$$\left| \sum_{P_z \in \mathcal{P}} \tilde{\mathbb{E}}_{\hat{\mu}}[P_z(X_z)] - \text{SDP}(\Lambda) \right| \leq \epsilon$$

where  $\text{SDP}(\Lambda)$  is the optimum of SDP 1.

*Proof.* To apply the gradient descent lemma of Jin et al. (2017) Theorem F.1 we need a bound on the lipschitzness of the gradient and the smoothness of the hessian of the loss equation 73. By the lipschitz gradient Lemma E.2 we have that the loss is  $\ell := \text{poly}(B)\rho$  lipschitz, and by the smooth hessian Lemma F.1 we have the loss is  $\gamma := \text{poly}(B)\rho$  smooth. Then we have by Theorem F.1 that perturbed gradient descent in

$$O\left(\frac{(f(X_0) - f^*)\ell}{\epsilon'^2} \log^4\left(\frac{d\ell\Delta_f}{\epsilon'^2\delta}\right)\right)$$

iterations can achieve a  $(\gamma^2, \epsilon')$ -SOSP. In our setting  $|f(X_0) - f^*| \leq 1$  because the loss is normalized between  $[0, 1]$ . Our desired accuracy  $\epsilon'$  is  $\text{poly}(B^{-1}, \rho^{-1})\Phi^{-2} = \text{poly}(B^{-1}, \epsilon^{-1})\Phi^{-2}$  where we take  $\rho = \text{poly}(2^k, \epsilon^{-1})$  as in Lemma E.1. For these settings we achieve an  $\epsilon$  approximation in  $\tilde{O}(\Phi^4 \epsilon^{-4} \log^4(\delta^{-1}))$  iterations.  $\square$

Next we move on to prove the lipschitzness of the Max-CSP gradient. This is important for two reasons. First we need it to bound the number of iterations required in the proof of Lemma E.1. Secondly, the lipschitzness of the hessian will be the key quantity

**Lemma E.2** (Lipschitz Gradient Lemma Max-CSP). For a Max-CSP instance  $\Lambda$ , Let  $\mathcal{L}_\rho(\mathbf{v})$  be the normalized loss defined in equation 73. Then the gradient satisfies

$$\|\nabla \mathcal{L}_\rho(V) - \nabla \mathcal{L}_\rho(\hat{V})\|_F \leq O(B^4 \rho) \|V - \hat{V}\|_F$$

*Proof.* We begin with the form of the Max-CSP gradient.

$$\left\| \nabla \mathcal{L}_\rho(V) - \nabla \mathcal{L}_\rho(\hat{V}) \right\|_F = \sqrt{\sum_{w \in \mathcal{F}} \left\| \frac{\partial \mathcal{L}_\rho(V)}{\partial v_w} - \frac{\partial \mathcal{L}_\rho(\hat{V})}{\partial \hat{v}_w} \right\|_F^2} \quad (100)$$



Where recall

$$\begin{aligned} \frac{\partial \mathcal{L}_\rho(\mathbf{v})}{\partial v_w} &= \frac{1}{|\mathcal{P}|} \left[ \sum_{\substack{P_z \in \mathcal{P} \\ \text{s.t. } w \subseteq z} \sum_{\substack{s \subseteq z \\ \text{s.t. } w \subseteq s}} y_s \frac{1}{|\mathcal{C}(s)|} \sum_{\substack{w' \subseteq s \\ \text{s.t. } \zeta(w, w') = s}} v_{w'} \right. \\ &\quad + 2\rho \left[ \sum_{\substack{P_z \in \mathcal{P} \\ \text{s.t. } w \subseteq z} \sum_{\substack{w', h, h' \subseteq s \\ \text{s.t. } \zeta(w, w') = \zeta(h, h')}} (\langle v_w, v_{w'} \rangle - \langle v_h, v_{h'} \rangle) v'_w \right. \\ &\quad \left. \left. + (\|v_w\|^2 - 1)v_w \right] \right] \quad (101) \end{aligned}$$

We break the gradient  $\nabla \mathcal{L}_\rho(V)$  up into three terms  $\mathcal{T}_1(V), \mathcal{T}_2(V)$ , and  $\mathcal{T}_3(V)$  such that  $\partial \mathcal{L}_\rho(V)/\partial v_w = \mathcal{T}_1(V)|_w + \mathcal{T}_2(V)|_w + \mathcal{T}_3(V)|_w$  Where  $\mathcal{T}_1(V)|_w, \mathcal{T}_2(V)|_w, \mathcal{T}_3(V)|_w$  are defined as follows

$$\mathcal{T}_1(V)|_w := \frac{1}{|\mathcal{P}|} \left[ \sum_{\substack{P_z \in \mathcal{P} \\ \text{s.t. } w \subseteq z} \sum_{\substack{s \subseteq z \\ \text{s.t. } w \subseteq s}} y_s \frac{1}{|\mathcal{C}(s)|} \sum_{\substack{w' \subseteq s \\ \text{s.t. } \zeta(w, w') = s}} v_{w'} \right] \quad (102)$$

$$\mathcal{T}_2(V)|_w = \frac{2\rho}{|\mathcal{P}|} \left[ \sum_{\substack{P_z \in \mathcal{P} \\ \text{s.t. } w \subseteq z} \sum_{\substack{w', h, h' \subseteq s \\ \text{s.t. } \zeta(w, w') = \zeta(h, h')}} (\langle v_w, v_{w'} \rangle - \langle v_h, v_{h'} \rangle) v'_w \right] \quad (103)$$

$$\mathcal{T}_3(V)|_w := \frac{2\rho}{|\mathcal{P}|} (\|v_w\|^2 - 1)v_w \quad (104)$$

Such that by triangle inequality we have

$$\left\| \nabla \mathcal{L}_\rho(V) - \nabla \mathcal{L}_\rho(\hat{V}) \right\|_F \leq \left\| \mathcal{T}_1(V) - \mathcal{T}_1(\hat{V}) \right\|_F + \left\| \mathcal{T}_2(V) - \mathcal{T}_2(\hat{V}) \right\|_F + \left\| \mathcal{T}_3(V) - \mathcal{T}_3(\hat{V}) \right\|_F \quad (105)$$

Where the three terms in equation 105 are as follows.

$$\left\| \mathcal{T}_1(V) - \mathcal{T}_1(\hat{V}) \right\|_F = \frac{1}{|\mathcal{P}|} \sqrt{\sum_{w \in \mathcal{F}} \left\| \left[ \sum_{\substack{P_z \in \mathcal{P} \\ \text{s.t. } w \subseteq z} \sum_{\substack{s \subseteq z \\ \text{s.t. } w \subseteq s}} y_s \frac{1}{|\mathcal{C}(s)|} \sum_{\substack{w' \subseteq s \\ \text{s.t. } \zeta(w, w') = s}} (v_{w'} - \hat{v}_{w'}) \right] \right\|^2} \quad (106)$$

$$\left\| \mathcal{T}_2(V) - \mathcal{T}_2(\hat{V}) \right\|_F$$

$$(107)$$

$$:= \frac{2\rho}{|\mathcal{P}|} \sqrt{\sum_{w \in \mathcal{F}} \left\| \left[ \sum_{\substack{P_z \in \mathcal{P} \\ \text{s.t. } w \subseteq z} \sum_{\substack{w', h, h' \subseteq s \\ \text{s.t. } \zeta(w, w') = \zeta(h, h')}} \left[ (\langle v_w, v_{w'} \rangle - \langle v_h, v_{h'} \rangle) v'_w - (\langle \hat{v}_w, \hat{v}_{w'} \rangle - \langle \hat{v}_h, \hat{v}_{h'} \rangle) \hat{v}'_w \right] \right] \right\|^2} \quad (108)$$

$$\left\| \mathcal{T}_3(V) - \mathcal{T}_3(\hat{V}) \right\|_F := \frac{2\rho}{|\mathcal{P}|} \sqrt{\sum_{w \in \mathcal{F}} \left\| \left[ (\|v_w\|^2 - 1)v_w - (\|\hat{v}_w\|^2 - 1)\hat{v}_w \right] \right\|^2} \quad (109)$$

We bound the terms one by one. First we bound term 1.

**Term 1:**

$$\left\| \mathcal{T}_1(V) - \mathcal{T}_1(\hat{V}) \right\|_F = \frac{1}{|\mathcal{P}|} \sqrt{\sum_{w \in \mathcal{F}} \left\| \left[ \sum_{\substack{P_z \in \mathcal{P} \\ \text{s.t. } w \subseteq z} \sum_{\substack{s \subseteq z \\ \text{s.t. } w \subseteq s} y_s \frac{1}{|\mathcal{C}(s)|} \sum_{\substack{w' \subseteq s \\ \text{s.t. } \zeta(w, w') = s}} (v_{w'} - \hat{v}_{w'}) \right] \right\|^2} \quad (110)$$

We will need to define some matrices so that we can write the above expression as the frobenius inner product of matrices. First we define  $G_\Lambda$  to be the adjacency matrix of the constraint graph. In particular we denote the  $(w, w')$  entry of  $G_\Lambda$  as  $G_\Lambda|_{w, w'}$  defined as follows.

$$G_\Lambda|_{w, w'} := \begin{cases} 1, & \text{if there exists } P_z \in \mathcal{P} \text{ s.t. } \zeta(w, w') \subseteq z \\ 0, & \text{otherwise} \end{cases}$$

Furthermore, we define  $M_{y_s/\mathcal{C}(s)}$  to be a matrix comprised of a set of coefficients  $y_s/|\mathcal{C}(s)|$  corresponding to every edge in the constraint graph  $G_\Lambda$ . The  $(w, w')$  entry of  $M_{y_s/\mathcal{C}(s)}$  is denoted  $M_{y_s/\mathcal{C}(s)}|_{w, w'}$  and defined as follows.

$$M_{y_s/\mathcal{C}(s)}|_{w, w'} := \begin{cases} y_s/|\mathcal{C}(s)|, & \text{if there exists } P_z \in \mathcal{P} \text{ s.t. } \zeta(w, w') = s \subseteq z \\ 0, & \text{otherwise} \end{cases}$$

Then rewriting equation 110

$$\left\| \mathcal{T}_1(V) - \mathcal{T}_1(\hat{V}) \right\|_F = \frac{1}{|\mathcal{P}|} \sqrt{\sum_{w \in \mathcal{F}} \left\| \left[ e_w^T G_\Lambda \odot M_{y_s/\mathcal{C}(s)} (V - \hat{V}) \right] \right\|^2} \quad (111)$$

$$= \frac{1}{|\mathcal{P}|} \sqrt{\left\| (G_\Lambda \odot M_{y_s/\mathcal{C}(s)}) (V - \hat{V}) \right\|_F^2} \quad (112)$$

By Cauchy-Schwarz we obtain

$$\left\| \mathcal{T}_1(V) - \mathcal{T}_1(\hat{V}) \right\|_F \leq \frac{1}{|\mathcal{P}|} \|G_\Lambda \odot M_{y_s/\mathcal{C}(s)}\| \|V - \hat{V}\|_F \quad (113)$$

Next we move on to bound term 2.

**Term 2:**

$$\left\| \mathcal{T}_2(V) - \mathcal{T}_2(\hat{V}) \right\|_F = \quad (114)$$

$$\frac{2\rho}{|\mathcal{P}|} \sqrt{\sum_{w \in \mathcal{F}} \left\| \left[ \sum_{\substack{P_z \in \mathcal{P} \\ \text{s.t. } w \subseteq z} \sum_{\substack{w', h, h' \subseteq s \\ \text{s.t. } \zeta(w, w') = \zeta(h, h')}} \left[ (\langle v_w, v_{w'} \rangle v'_w - \langle v_h, v_{h'} \rangle v'_w) - (\langle \hat{v}_w, \hat{v}_{w'} \rangle \hat{v}'_w - \langle \hat{v}_h, \hat{v}_{h'} \rangle \hat{v}'_w) \right] \right\|^2} \quad (115)$$

Let the vector  $\delta_{w'} = v_w - v_{w'}$  and let the scalar  $\delta_{w, w'} = \langle v_w, v_{w'} \rangle - \langle \hat{v}_w, \hat{v}_{w'} \rangle$ . Then we have by plugging definitions that

$$(\langle v_w, v_{w'} \rangle v'_w - \langle \hat{v}_w, \hat{v}_{w'} \rangle \hat{v}'_w) = (\langle v_w, v_{w'} \rangle v'_w - ((\langle v_w, v_{w'} \rangle + \delta_{w, w'}) (v'_w + \delta_{w'}))) \quad (116)$$

Substituting equation 116 into equation 115 in the square root we obtain

$$= \frac{2\rho}{|\mathcal{P}|} \sqrt{\sum_{w \in \mathcal{F}} \left\| \sum_{\substack{P_z \in \mathcal{P} \\ \text{s.t. } w \subseteq z} \sum_{w' \subseteq s} -\langle v_w, v_{w'} \rangle \delta_{w'} - \delta_{w, w'} v'_w + \delta_{w, w'} \delta_{w'} \right\|^2} \quad (117)$$

Applying triangle inequality we obtain

$$\leq \frac{16\rho}{|\mathcal{P}|} \sqrt{\sum_{w \in \mathcal{F}} \left\| \sum_{\substack{P_z \in \mathcal{P} \\ s.t. w \subseteq z}} \sum_{w' \subseteq s} -\langle v_w, v_{w'} \rangle \delta_{w'} \right\|^2 + \sum_{w \in \mathcal{F}} \left\| \sum_{\substack{P_z \in \mathcal{P} \\ s.t. w \subseteq z}} \sum_{w' \subseteq s} -\delta_{w,w'} v'_w \right\|^2 + \sum_{w \in \mathcal{F}} \left\| \sum_{\substack{P_z \in \mathcal{P} \\ s.t. w \subseteq z}} \sum_{w' \subseteq s} \delta_{w,w'} \delta_{w'} \right\|^2} \quad (118)$$

Let  $M_{\langle v_w, v_{w'} \rangle} \in \mathbb{R}^{|\mathcal{P}|2^k \times |\mathcal{P}|2^k}$  be the matrix whose  $w, w'$  entry is  $\langle v_w, v_{w'} \rangle$ . Let  $M_{\delta_{w,w'}}$  be the matrix whose  $w, w'$  entry is  $\delta_{w,w'}$ . Let  $\odot$  denote the entrywise product of two matrices.

$$= \frac{16\rho}{|\mathcal{P}|} \sqrt{\|G_\Lambda \odot M_{\langle v_w, v_{w'} \rangle} (V - \hat{V})\|_F^2 + \|G_\Lambda \odot M_{\delta_{w,w'}} (V - \hat{V})\|_F^2 + \|G_\Lambda \odot M_{\delta_{w,w'}} (V - \hat{V})\|_F^2} \quad (119)$$

Applying Cauchy-Schwarz we obtain

$$= \frac{16\rho}{|\mathcal{P}|} \sqrt{\|G_\Lambda \odot M_{\langle v_w, v_{w'} \rangle}\|_F^2 \|V - \hat{V}\|_F^2 + \|G_\Lambda \odot M_{\delta_{w,w'}}\|_F^2 \|V - \hat{V}\|_F^2 + \|G_\Lambda \odot M_{\delta_{w,w'}}\|_F^2 \|V - \hat{V}\|_F^2} \quad (120)$$

We apply entrywise upper bound  $\langle v_w, v_{w'} \rangle \leq B^2$  which can be done because we're taking a frobenius norm so the sign of each entry does not matter. Likewise we apply a crude entrywise upper bound of  $\delta_{w,w'} \leq B^2$  again because the sign of each entry does not matter in the frobenius norm (for each row this is euclidean norm).

$$= \frac{16B^4\rho}{|\mathcal{P}|} \sqrt{\|G_\Lambda\|_F^2 \|V - \hat{V}\|_F^2 + \|G_\Lambda\|_F^2 \|V - \hat{V}\|_F^2 + \|G_\Lambda\|_F^2 \|V - \hat{V}\|_F^2} \quad (121)$$

Using the fact that  $\|G_\lambda\|_F \leq 2^k \sqrt{|\mathcal{P}|}$

$$= \frac{2^k B^4 \rho}{\sqrt{|\mathcal{P}|}} \|V - \hat{V}\|_F \leq 2^k B^4 \rho \|V - \hat{V}\|_F \quad (122)$$

Therefore we have established

$$\|\mathcal{T}_2(V) - \mathcal{T}_2(\hat{V})\|_F \leq 2^k B^4 \rho \|V - \hat{V}\|_F \quad (123)$$

Finally we move on to bound term 3.

**Term 3:**

$$\|\mathcal{T}_3(V) - \mathcal{T}_3(\hat{V})\|_F := \frac{2\rho}{|\mathcal{P}|} \sqrt{\sum_{w \in \mathcal{F}} \left\| \left[ (\|v_w\|^2 - 1)v_w - (\|\hat{v}_w\|^2 - 1)\hat{v}_w \right] \right\|^2} \quad (124)$$

$$= \frac{2\rho}{|\mathcal{P}|} \sqrt{\sum_{w \in \mathcal{F}} \left\| \left[ \|v_w\|^2 v_w - \|\hat{v}_w\|^2 \hat{v}_w + \hat{v}_w - v_w \right] \right\|^2} \quad (125)$$

Applying triangle inequality we obtain

$$\leq \frac{2\rho}{|\mathcal{P}|} \sqrt{\sum_{w \in \mathcal{F}} \left[ \left\| \|v_w\|^2 v_w - \|\hat{v}_w\|^2 \hat{v}_w \right\|^2 \right]} + \frac{2\rho}{|\mathcal{P}|} \sqrt{\sum_{w \in \mathcal{F}} \left[ \|\hat{v}_w - v_w\|^2 \right]} \quad (126)$$

Using the fact that  $\sum_{w \in \mathcal{F}} \left[ \|\hat{v}_w - v_w\|^2 \right] = \|V - \hat{V}\|_F$

$$= \frac{2\rho}{|\mathcal{P}|} \sqrt{\sum_{w \in \mathcal{F}} \left[ \left\| \|v_w\|^2 v_w - \|\hat{v}_w\|^2 \hat{v}_w \right\|^2 \right]} + \frac{2\rho}{|\mathcal{P}|} \|V - \hat{V}\|_F \quad (127)$$

Let  $\delta_{v_w} := v'_w - v_w$  then substituting the definition we obtain

$$= \frac{2\rho}{|\mathcal{P}|} \sqrt{\sum_{w \in \mathcal{F}} \left[ \left\| \|v_w\|^2 v_w - \|v_w + \delta_{v_w}\|^2 (v_w + \delta_{v_w}) \right\|^2 \right]} + \frac{2\rho}{|\mathcal{P}|} \|V - \hat{V}\|_F \quad (128)$$

expanding the expression in the square root we obtain

$$= \frac{2\rho}{|\mathcal{P}|} \sqrt{\sum_{w \in \mathcal{F}} \left[ \left\| -2\langle v_w, \delta_{v_w} \rangle v_w - \|\delta_{v_w}\|^2 v_w - \|v_w\|^2 \delta_{v_w} - 2\langle v_w, \delta_{v_w} \rangle \delta_{v_w} - \|\delta_{v_w}\|^2 \delta_{v_w} \right\|^2 \right]} \quad (129)$$

$$+ \frac{2\rho}{|\mathcal{P}|} \|V - \hat{V}\|_F \quad (130)$$

By triangle inequality we upper bound by

$$\leq \frac{2\rho}{|\mathcal{P}|} \sqrt{\sum_{w \in \mathcal{F}} \left[ \left\| -2\langle v_w, \delta_{v_w} \rangle v_w \right\|^2 \right]} + \frac{2\rho}{|\mathcal{P}|} \sqrt{\sum_{w \in \mathcal{F}} \left[ \left\| -\|\delta_{v_w}\|^2 v_w \right\|^2 \right]} + \frac{2\rho}{|\mathcal{P}|} \sqrt{\sum_{w \in \mathcal{F}} \left[ \left\| -\|v_w\|^2 \delta_{v_w} \right\|^2 \right]} + \frac{2\rho}{|\mathcal{P}|} \sqrt{\sum_{w \in \mathcal{F}} \left[ \left\| -2\langle v_w, \delta_{v_w} \rangle \delta_{v_w} \right\|^2 \right]} + \frac{2\rho}{|\mathcal{P}|} \sqrt{\sum_{w \in \mathcal{F}} \left[ \left\| -\|\delta_{v_w}\|^2 \delta_{v_w} \right\|^2 \right]} + \frac{2\rho}{|\mathcal{P}|} \|V - \hat{V}\|_F \quad (131)$$

For the first term consider by Cauchy-Schwarz

$$\left\| -2\langle v_w, \delta_{v_w} \rangle v_w \right\|^2 = 4\langle v_w, \delta_{v_w} \rangle^2 \|v_w\|^2 \leq 4B^4 \|\delta_{v_w}\|^2$$

Consider the second term which we upper bound via the norm bound on  $\|v_w\| \leq B$

$$\left\| \|\delta_{v_w}\|^2 v_w \right\|^2 = \|\delta_{v_w}\|^2 B^2$$

Consider the third term which we upper bound via the norm bound on  $\|v_w\| \leq B$

$$\left\| -\|v_w\|^2 \delta_{v_w} \right\|^2 = \|v_w\|^2 \|\delta_{v_w}\|^2 \leq B^2 \|\delta_{v_w}\|^2$$

Consider the fourth term which we upper bound via Cauchy-Schwarz

$$\left\| -2\langle v_w, \delta_{v_w} \rangle \delta_{v_w} \right\|^2 = 4\langle v_w, \delta_{v_w} \rangle^2 \|\delta_{v_w}\|^2 \leq 4B^4 \|\delta_{v_w}\|^2$$

Consider the fifth term. We apply a crude upper bound of  $\|\delta_{v_w}\|^2 \leq B^2$

$$\left\| -\|\delta_{v_w}\|^2 \delta_{v_w} \right\|^2 = \|\delta_{v_w}\|^2 \|\delta_{v_w}\|^2 \leq B^2 \|\delta_{v_w}\|^2$$

Therefore we conclude

$$131 \leq \frac{20B^2\rho}{|\mathcal{P}|} \sqrt{\sum_{w \in \mathcal{F}} \|\delta_{v_w}\|^2} + \frac{2\rho}{|\mathcal{P}|} \|V - \hat{V}\|_F \quad (132)$$

$$= \frac{20B^2\rho}{|\mathcal{P}|} \|V - \hat{V}\|_F + \frac{2\rho}{|\mathcal{P}|} \|V - \hat{V}\|_F \quad (133)$$

So we conclude our bound on term 3

$$\left\| \mathcal{T}_3(V) - \mathcal{T}_3(\hat{V}) \right\|_F \leq 20B^2\rho \left\| V - \hat{V} \right\|_F \quad (134)$$

as desired. Putting our bounds for terms 1, 2, and 3 into equation 105 we obtain

$$\left\| \nabla \mathcal{L}_\rho(V) - \nabla \mathcal{L}_\rho(\hat{V}) \right\|_F \leq O(B^2\rho) \left\| V - \hat{V} \right\|_F \quad (135)$$

as desired.  $\square$

**Lemma E.3** (Max-CSP gradient perturbation analysis). For any set of matrices  $M := \{M_1, M_2, \dots, M_T\} \in \mathbb{R}^{2r \times r}$  a perturbation  $U := \{U_1, U_2, \dots, U_T\} \in \mathbb{R}^{2r \times r}$  that satisfies  $\|U_i\|_{1,1} \leq \epsilon$  for all  $i \in [T]$ . Let  $M + U$  denote the elementwise addition of  $M$  and  $U$  as such  $M + U := \{M_1 + U_1, M_2 + U_2, \dots, M_T + U_T\}$ . Then for a matrix  $V \in \mathbb{R}^{r \times N}$  satisfying  $\|V\|_F \leq \sqrt{d}$  we define the aggregation function  $\text{AGG} : \mathbb{R}^{r \times N} \rightarrow \mathbb{R}^{2r \times N}$  as such

$$\text{AGG}(V) := \begin{bmatrix} V \\ \nabla \mathcal{L}_\rho(V) \end{bmatrix} \quad (136)$$

Furthermore, let  $\text{LAYER}_{M_i}(V)$  denote

$$\text{LAYER}_{M_i}(V) = M_i(\text{AGG}(V))$$

Finally, let  $\text{OptGNN}_M : \mathbb{R}^{r \times N} \rightarrow \mathbb{R}$  be defined as

$$\text{OptGNN}_M(V) = \mathcal{L}_\rho \circ \text{LAYER}_{M_T} \circ \dots \circ \text{LAYER}_{M_2} \circ \text{LAYER}_{M_1}(V)$$

Here we feed the output of the final layer  $\text{LAYER}_T$  to the loss function  $\mathcal{L} : \mathbb{R}^{r \times N} \rightarrow \mathbb{R}$ . Then

$$\left\| \text{OptGNN}_M(V) - \text{OptGNN}_{M+U}(V) \right\|_F \leq O(\epsilon B^{2T} \rho^{2T} r^{2T})$$

*Proof.* We begin by analyzing how much the gradient perturbs the input to a single layer. First we apply the definition of  $\text{LAYER}$  and  $\text{AGG}$  to obtain

$$\left\| \text{LAYER}_M(V) - \text{LAYER}_{M+U}(V) \right\|_F \quad (137)$$

$$\leq \left\| (M + U)V - MV \right\|_F + \left\| \nabla \mathcal{L}_\rho((M + U)V) - \nabla \mathcal{L}_\rho(MV) \right\|_F \quad (138)$$

$$= \left\| UV \right\|_F + \left\| \nabla \mathcal{L}_\rho((M + U)V) - \nabla \mathcal{L}_\rho(MV) \right\|_F \quad (139)$$

$$\leq \|U\|_F \|V\|_F + \left\| \nabla \mathcal{L}_\rho((M + U)V) - \nabla \mathcal{L}_\rho(MV) \right\|_F \quad (140)$$

$$\leq \epsilon r^{3/2} + \left\| \nabla \mathcal{L}_\rho((M + U)V) - \nabla \mathcal{L}_\rho(MV) \right\|_F \quad (141)$$

Here the first inequality follows by triangle inequality. The second inequality follows by Cauchy-Schwarz. Finally the frobenius norm of  $U$  is  $\epsilon r$  the frobenius norm of  $V$  is  $\sqrt{d}$ . Then applying the lipschitzness of the gradient Lemma E.2 we obtain.

$$\leq \epsilon r^{3/2} + O(B^2\rho) \left\| (M + U)V - MV \right\|_F = O(B^2\rho) \left\| UV \right\|_F \quad (142)$$

$$\leq \epsilon r^{3/2} + O(B^2\rho) \|U\|_F \|V\|_F \quad (143)$$

$$\leq \epsilon r^{3/2} + O(B^2\rho)\epsilon d \|V\|_F \quad (144)$$

$$= O(B^2\rho)\epsilon r^{3/2} \quad (145)$$

To conclude, we've established that

$$\left\| \text{LAYER}_M(V) - \text{LAYER}_{M+U}(V) \right\|_F = O(B^2\rho)\epsilon r^{3/2} \quad (146)$$

Next we upper bound the lipschitzness of the  $\text{LAYER}$  function by the frobenius norm of  $\|M\|_F \leq O(r)$  multiplied by the lipschitzness of  $\nabla \mathcal{L}_\rho$  which is  $O(B^2\rho)$ . Taken together we find the lipschitzness of  $\text{LAYER}$  is upper bounded by  $O(B^2\rho r)$ .

Note that  $\text{OptGNN}$  is comprised of  $T$  layers of  $\text{LAYER}$  functions followed by the evaluation of the loss  $\mathcal{L}$ . The  $T$  layers contribute a geometric series of errors with the dominant term being  $O(\epsilon r^{3/2} B^2\rho * (B^2\rho r)^T) = O(\epsilon (B^2\rho r)^{2T})$ . The smaller order terms contribute no more than an additional multiplicative factor of  $T$  leading to an error of  $O(T\epsilon (B^2\rho r)^{2T})$ . At any rate, the dominant term is the exponential dependence on the number of layers. Finally,  $\text{OptGNN}$ 's final layer is the

evaluation of the loss  $\mathcal{L}_\rho$ . The lipschitzness of the loss  $\mathcal{L}_\rho$  can be computed as follows. For any pair of matrices  $V$  and  $\hat{V}$  both in  $\mathbb{R}^{r \times r}$  we have

$$|\mathcal{L}_\rho(V) - \mathcal{L}_\rho(\hat{V})| \leq \frac{\rho 2^k}{|\mathcal{P}|} \|V - \hat{V}\|_F^2 \quad (147)$$

where we used the fact that the loss is dominated by its quadratic penalty term  $\rho$  times the square of the violations where each row in  $V$  can be counted in up to  $2^k$  constraints normalized by the number of predicates  $|\mathcal{P}|$ . Putting this together applying the LAYER function over  $T$  layers we obtain

$$\|\text{OptGNN}_{M+U}(V) - \text{OptGNN}_M(V)\| \leq O(\epsilon B^{2T} \rho^{2T} r^{2T}) \quad (148)$$

□

At this point we restate some elementary theorems in the study of PAC learning adapted for the unsupervised learning setting.

**Lemma E.4** (Agnostic PAC learnability (folklore)). Let  $x_1, x_2, \dots, x_N \sim \mathcal{D}$  be data drawn from a distribution  $\mathcal{D}$ . Let  $\mathcal{H}$  be any finite hypothesis class comprised of functions  $h \in \mathcal{H}$  where the range of  $h$  is bounded in  $[0, 1]$ . Let  $\hat{h} \in \mathcal{H}$  be the empirical loss minimizer

$$\arg \min_{h \in \mathcal{H}} \frac{1}{N} \sum_{i \in [N]} h(x_i)$$

Let  $\delta$  be the failure probability and let  $\epsilon$  be the approximation error. Then we say  $\mathcal{H}$  is  $(N, \epsilon, \delta)$ -PAC learnable if

$$\Pr\left[\frac{1}{N} \sum_{i \in [N]} \hat{h}(x_i) - \mathbb{E}_{x \sim \mathcal{D}}[h(x)] \geq \epsilon\right] \leq \delta$$

Furthermore,  $\mathcal{H}$  is  $(N, \epsilon, \delta)$ -PAC learnable so long as

$$N = O\left(\log |\mathcal{H}| \frac{\log(1/\delta)}{\epsilon^2}\right)$$

The proof is a standard epsilon net union bound argument which the familiar reader should feel free to skip.

*Proof.* For any fixed hypothesis  $h$  the difference between the distributional loss between  $[0, 1]$  and the empirical loss can be bounded by Hoeffding.

$$\Pr_{x_1, \dots, x_N \sim \mathcal{D}} \left[ \mathbb{E}_{x \sim \mathcal{D}}[h(x)] - \frac{1}{N} \sum_{i \in [N]} h(x_i) > \epsilon \right] \leq \exp(-N\epsilon^2)$$

Let  $\hat{h} \in \mathcal{H}$  be the empirical risk minimizer within the hypothesis class  $\mathcal{H}$  on data  $\{x_1, x_2, \dots, x_N\}$ . What is the probability that the empirical risk deviates from the distributional risk by greater than  $\epsilon$ ? i.e we wish to upper bound the quantity

$$\Pr_{x_1, \dots, x_N \sim \mathcal{D}} \left[ \mathbb{E}_{x \sim \mathcal{D}}[\hat{h}(x)] - \frac{1}{N} \sum_{i \in [N]} \hat{h}(x_i) > \epsilon \right]$$

Of course the biggest caveat is that  $\hat{h}$  depends on  $x_1, \dots, x_N$  and thus Hoeffding does not apply. Therefore we upper bound by the probability over draws  $x_1, \dots, x_N \sim \mathcal{D}$  that there exists ANY hypothesis in  $\mathcal{H}$  that deviates from its distributional risk by more than  $\epsilon$ .

$$\Pr_{x_1, \dots, x_N \sim \mathcal{D}} \left[ \mathbb{E}_{x \sim \mathcal{D}}[\hat{h}(x)] - \frac{1}{N} \sum_{i \in [N]} \hat{h}(x_i) > \epsilon \right] \leq \Pr_{x_1, \dots, x_N \sim \mathcal{D}} \left[ \bigcup_{h \in \mathcal{H}} \left[ \mathbb{E}_{x \sim \mathcal{D}}[h(x)] - \frac{1}{N} \sum_{i \in [N]} h(x_i) > \epsilon \right] \right] \quad (149)$$

This follows because the event that  $\hat{h}$  deviates substantially from its distributional loss is one of the elements of the union on the right hand side.

$$\left[ \mathbb{E}_{x \sim \mathcal{D}}[\hat{h}(x)] - \frac{1}{N} \sum_{i \in [N]} \hat{h}(x_i) > \epsilon \right] \subseteq \left[ \bigcup_{h \in \mathcal{H}} \left[ \mathbb{E}_{x \sim \mathcal{D}}[h(x)] - \frac{1}{N} \sum_{i \in [N]} h(x_i) > \epsilon \right] \right]$$

Then we have via union bound that

$$\begin{aligned} \Pr_{x_1, \dots, x_N \sim \mathcal{D}} \left[ \mathbb{E}_{x \sim \mathcal{D}}[\hat{h}(x)] - \frac{1}{N} \sum_{i \in [N]} \hat{h}(x_i) > \epsilon \right] &\leq \Pr_{x_1, \dots, x_N \sim \mathcal{D}} \left[ \bigcup_{h \in \mathcal{H}} \left[ \mathbb{E}_{x \sim \mathcal{D}}[h(x)] - \frac{1}{N} \sum_{i \in [N]} h(x_i) > \epsilon \right] \right] \\ &\leq \sum_{h \in \mathcal{H}} \Pr_{x_1, \dots, x_N \sim \mathcal{D}} \left[ \mathbb{E}_{x \sim \mathcal{D}}[h(x)] - \frac{1}{N} \sum_{i \in [N]} h(x_i) > \epsilon \right] \\ &\leq \sum_{h \in \mathcal{H}} \exp(-\epsilon^2 N) = |\mathcal{H}| \exp(-\epsilon^2 N) \quad (150) \end{aligned}$$

where the last line follows by Hoeffding. In particular if we want the failure probability to be  $\delta$  then

$$|\mathcal{H}| \exp(-\epsilon^2 N) \leq \delta \quad (151)$$

which implies

$$N \geq \frac{1}{\epsilon^2} \ln\left(\frac{|\mathcal{H}|}{\delta}\right)$$

Suffices for the  $\hat{h} \in \mathcal{H}$  to deviate from its empirical risk by less than  $\epsilon$ .  $\square$

Finally putting our perturbation analysis Lemma E.3 together with the agnostic PAC learnability Lemma E.4

**Lemma E.5.** Let  $\Lambda_1, \Lambda_2, \dots, \Lambda_\Gamma \sim \mathcal{D}$  be Max-CSP instances drawn from a distribution over instances  $\mathcal{D}$  with no more than  $|\mathcal{P}|$  predicates. Let  $M$  be a set of parameters  $M = \{M_1, M_2, \dots, M_T\}$  in a parameter space  $\Theta$ . Then for  $T = O(\Phi^4)$ , for  $\Gamma = O(\frac{1}{\epsilon^4} \Phi^6 \log^4(\delta^{-1}))$ , let  $\hat{M}$  be the empirical loss minimizer

$$\hat{M} := \arg \min_{M \in \Theta} \frac{1}{\Gamma} \sum_{i \in [\Gamma]} \text{OptGNN}_{(M, \Lambda_i)}(V)$$

Then we have that OptGNN is  $(\Gamma, \epsilon, \delta)$ -PAC learnable

$$\Pr \left[ \left| \frac{1}{\Gamma} \sum_{i \in [\Gamma]} \text{OptGNN}_{(\hat{M}, \Lambda_i)}(V) - \mathbb{E}_{\Lambda \sim \mathcal{D}} [\text{OBJ}(\Lambda)] \right| \leq \epsilon \right] \geq 1 - \delta$$

*Proof.* The result follows directly from the agnostic PAC learning Lemma E.4 and the perturbation analysis Lemma E.3. We have that for a net of interval size  $\frac{\epsilon}{r^{2T}}$  suffices for an  $\epsilon$  approximation. The cardinality of the net is then  $r^{2T}/\epsilon$  per parameter raised the power of the number of parameters required for OptGNN to represent an  $\epsilon$  approximate solution to  $\text{SDP}(\Lambda)$ . Each LAYER is comprised of a matrix  $M_i$  of dimension  $r \times 2r$  for  $r = \Phi$ . By Lemma E.1 we need a total of  $T = O(\Phi^4 \epsilon^{-4} \log^4(\delta^{-1}))$  layers to represent an  $\epsilon$  optimal solution with probability  $1 - \delta$ . Then the total number of parameters in the network is  $O(\Phi^6 \epsilon^{-4} \log^4(\delta^{-1}))$  as desired.  $\square$

## F HESSIAN LEMMAS

This section is to prove the hessian  $\nabla^2 \mathcal{L}_\rho$  is smooth. This is relevant for bounding the number of iterations required for algorithm 2.

**Lemma F.1** (Smooth Hessian Lemma). For a Max-CSP instance  $\Lambda$ , Let  $\mathcal{L}_\rho(\mathbf{v})$  be the normalized loss defined in equation 73. Then the hessian satisfies

$$\|\nabla^2 \mathcal{L}_\rho(\mathbf{v}) - \nabla^2 \mathcal{L}_\rho(\hat{\mathbf{v}})\| \leq 8B\rho \|V - \hat{V}\|_F$$

In particular for  $\rho = \text{poly}(k, \epsilon^{-1})$  we have that the hessian is  $\text{poly}(B, k, \epsilon^{-1})$  smooth.

*Proof.* Next we verify this for the Max-CSP hessian. The form of its hessian is far more complex. To simplify matters we first consider the hessian of polynomials of the form  $\mathcal{T}(v_i, v_j, v_k, v_\ell) = (\langle v_i, v_j \rangle - \langle v_k, v_\ell \rangle)^2$

$$\nabla^2 \mathcal{T}(v_i, v_j, v_k, v_\ell) := \begin{cases} \frac{\partial}{\partial v_{ia} \partial v_{kb}} \mathcal{T} = -2v_{ja}v_{\ell b}, & \text{for } a, b \in [r] \\ \frac{\partial}{\partial v_{ia} \partial v_{\ell b}} \mathcal{T} = -2v_{ja}v_{kb}, & \text{for } a, b \in [r] \\ \frac{\partial}{\partial v_{ja} \partial v_{kb}} \mathcal{T} = -2v_{ia}v_{\ell b}, & \text{for } a, b \in [r] \\ \frac{\partial}{\partial v_{ja} \partial v_{\ell b}} \mathcal{T} = -2v_{ia}v_{kb}, & \text{for } a, b \in [r] \\ \frac{\partial}{\partial v_{ia} \partial v_{jb}} \mathcal{T} = 2v_{ja}v_{ib}, & \text{for } a, b \in [r] \\ \frac{\partial}{\partial v_{ka} \partial v_{\ell b}} \mathcal{T} = 2v_{\ell a}v_{kb}, & \text{for } a, b \in [r] \\ \frac{\partial}{\partial v_{ia}^2} \mathcal{T} = v_{ja}^2, & \text{for } a \in [r] \\ \frac{\partial}{\partial v_{ja}^2} \mathcal{T} = v_{ia}^2, & \text{for } a \in [r] \\ \frac{\partial}{\partial v_{ka}^2} \mathcal{T} = v_{\ell a}^2, & \text{for } a \in [r] \\ \frac{\partial}{\partial v_{\ell a}^2} \mathcal{T} = v_{ka}^2, & \text{for } a \in [r] \\ 0, & \text{otherwise} \end{cases}$$

We can decompose the Hessian as a sum of 10 matrices corresponding to the cases enumerated above.

$$\begin{aligned} \nabla^2 \mathcal{T}(\mathbf{v}) &= \nabla^2 \mathcal{T}(\mathbf{v})|_{(i,k)} + \nabla^2 \mathcal{T}(\mathbf{v})|_{(i,\ell)} + \nabla^2 \mathcal{T}(\mathbf{v})|_{(j,k)} + \nabla^2 \mathcal{T}(\mathbf{v})|_{(j,\ell)} \\ &\quad + \nabla^2 \mathcal{T}(\mathbf{v})|_{(i,j)} + \nabla^2 \mathcal{T}(\mathbf{v})|_{(k,\ell)} \\ &\quad + \nabla^2 \mathcal{T}(\mathbf{v})|_{(i,i)} + \nabla^2 \mathcal{T}(\mathbf{v})|_{(j,j)} + \nabla^2 \mathcal{T}(\mathbf{v})|_{(k,k)} + \nabla^2 \mathcal{T}(\mathbf{v})|_{(\ell,\ell)} \end{aligned} \quad (152)$$

Then we can compute

$$\begin{aligned} \|\nabla^2 \mathcal{T}(\mathbf{v}) - \nabla^2 \mathcal{T}(\hat{\mathbf{v}})\|_F &\leq \\ &\|\nabla^2 \mathcal{T}(\mathbf{v})|_{(i,k)} - \nabla^2 \mathcal{T}(\hat{\mathbf{v}})|_{(i,k)}\|_F + \|\nabla^2 \mathcal{T}(\mathbf{v})|_{(i,\ell)} - \nabla^2 \mathcal{T}(\hat{\mathbf{v}})|_{(i,\ell)}\|_F \\ &+ \|\nabla^2 \mathcal{T}(\mathbf{v})|_{(j,k)} - \nabla^2 \mathcal{T}(\hat{\mathbf{v}})|_{(j,k)}\|_F + \|\nabla^2 \mathcal{T}(\mathbf{v})|_{(i,k)} - \nabla^2 \mathcal{T}(\hat{\mathbf{v}})|_{(j,\ell)}\|_F \\ &+ \|\nabla^2 \mathcal{T}(\mathbf{v})|_{(i,j)} - \nabla^2 \mathcal{T}(\hat{\mathbf{v}})|_{(i,j)}\|_F + \|\nabla^2 \mathcal{T}(\mathbf{v})|_{(k,\ell)} - \nabla^2 \mathcal{T}(\hat{\mathbf{v}})|_{(k,\ell)}\|_F \\ &+ \|\nabla^2 \mathcal{T}(\mathbf{v})|_{(i,i)} - \nabla^2 \mathcal{T}(\hat{\mathbf{v}})|_{(i,i)}\|_F + \|\nabla^2 \mathcal{T}(\mathbf{v})|_{(j,j)} - \nabla^2 \mathcal{T}(\hat{\mathbf{v}})|_{(j,j)}\|_F \\ &+ \|\nabla^2 \mathcal{T}(\mathbf{v})|_{(k,k)} - \nabla^2 \mathcal{T}(\hat{\mathbf{v}})|_{(k,k)}\|_F + \|\nabla^2 \mathcal{T}(\mathbf{v})|_{(\ell,\ell)} - \nabla^2 \mathcal{T}(\hat{\mathbf{v}})|_{(\ell,\ell)}\|_F \end{aligned} \quad (153)$$

Noticing that the first four terms have the same upper bound, terms 5 and 6 have the same upper bound, and terms 7 through 10 share the same upper bound we obtain

$$\begin{aligned} \|\nabla^2 \mathcal{T}(\mathbf{v}) - \nabla^2 \mathcal{T}(\hat{\mathbf{v}})\|_F &\leq 4\|\nabla^2 \mathcal{T}(\mathbf{v})|_{(i,k)} - \nabla^2 \mathcal{T}(\hat{\mathbf{v}})|_{(i,k)}\|_F \\ &\quad + 2\|\nabla^2 \mathcal{T}(\mathbf{v})|_{(i,j)} - \nabla^2 \mathcal{T}(\hat{\mathbf{v}})|_{(i,j)}\|_F \\ &\quad + 4\|\nabla^2 \mathcal{T}(\mathbf{v})|_{(i,i)} - \nabla^2 \mathcal{T}(\hat{\mathbf{v}})|_{(i,i)}\|_F \end{aligned} \quad (154)$$

Now consider the first term

$$\|\nabla^2 \mathcal{T}(\mathbf{v})|_{(i,k)} - \nabla^2 \mathcal{T}(\hat{\mathbf{v}})|_{(i,k)}\|_F^2 = 4 \left( \sum_{a,b \in [r]} (v_{ja}v_{\ell b} - \hat{v}_{ja}\hat{v}_{\ell b})^2 \right) \quad (155)$$



Let  $\delta_j = \hat{v}_j - v_j$  and  $\delta_\ell = \hat{v}_\ell - v_\ell$ . We expand equation 155 to obtain

$$\begin{aligned}
&= 2\|v_j v_\ell^T - \hat{v}_j \hat{v}_\ell^T\|_F = 2\|v_j v_\ell^T - (v_j + \delta_j)(v_\ell + \delta_\ell)^T\|_F^2 \\
&= 2\|v_j v_\ell^T - (v_j v_\ell^T + \delta_j v_\ell^T + v_j \delta_\ell^T + \delta_j \delta_\ell^T)\|_F^2 \\
&= 2\|(\delta_j v_\ell^T + v_j \delta_\ell^T + \delta_j \delta_\ell^T)\|_F^2 \\
&\leq 16(\|\delta_j\|^2 \|v_\ell\|^2 + \|v_j\|^2 \|\delta_j\|^2 + \|\delta_j\|^2 \|\delta_\ell\|^2) \leq 16B^2(\|\delta_j\|^2 + \|\delta_\ell\|^2)
\end{aligned}$$

Where we apply Cauchy-Schwarz as needed. The second term is bounded similarly. The last term can be bounded

$$\|\nabla^2 \mathcal{T}(\mathbf{v})|_{(i,i)} - \nabla^2 \mathcal{T}(\hat{\mathbf{v}})|_{(i,i)}\|_F \leq 2 \sqrt{\sum_{a \in [r]} (v_{ja}^2 - \hat{v}_{ja}^2)^2}$$

Upper bounding  $v_{ja} + \hat{v}_{ja} \leq 2B$  which applies for all  $a \in [r]$  we obtain

$$= 2 \sqrt{\sum_{a \in [r]} (v_{ja} - \hat{v}_{ja})^2 (v_{ja} + \hat{v}_{ja})^2} \leq 2 \sqrt{B^2 \sum_{a \in [r]} (v_{ja} - \hat{v}_{ja})^2} \leq 2\sqrt{\|v_j - \hat{v}_j\|^2 B^2}$$

Putting the terms together we obtain the following bound for

$$\begin{aligned}
\|\nabla^2 \mathcal{T}(\mathbf{v}) - \nabla^2 \mathcal{T}(\hat{\mathbf{v}})\|_F &\leq \\
&16B^2 \left[ (\|\delta_j\|^2 + \|\delta_\ell\|^2) + (\|\delta_j\|^2 + \|\delta_k\|^2) + (\|\delta_i\|^2 + \|\delta_\ell\|^2) + (\|\delta_i\|^2 + \|\delta_\ell\|^2) \right. \\
&\quad + (\|\delta_i\|^2 + \|\delta_j\|^2) + (\|\delta_k\|^2 + \|\delta_\ell\|^2) \\
&\quad \left. + (\|\delta_i\|^2 + \|\delta_j\|^2 + \|\delta_k\|^2 + \|\delta_\ell\|^2) \right] \quad (156)
\end{aligned}$$

Now we can perform the analysis for the hessian of the entire Max-CSP loss.

$$\begin{aligned}
\mathcal{L}_\rho(\mathbf{v}) &:= \frac{1}{|\mathcal{P}|} \left[ \sum_{P_z \in \mathcal{P}} \sum_{s \subseteq z} y_s \frac{1}{|\mathcal{C}(s)|} \sum_{\substack{g, g' \subseteq s \\ \zeta(g, g') = s}} \langle v_g, v_{g'} \rangle \right. \\
&\quad + \rho \left[ \sum_{P_z \in \mathcal{P}} \sum_{\substack{g, g', h, h' \subseteq z \\ \zeta(g, g') = \zeta(h, h')}} (\langle v_g, v_{g'} \rangle - \langle v_h, v_{h'} \rangle)^2 \right. \\
&\quad \left. \left. + \sum_{v_s \in \mathbf{v}} (\|v_s\|^2 - 1)^2 \right] \right] \quad (157)
\end{aligned}$$

We break the loss into three terms

$$\begin{aligned}
\mathcal{W}_1(\mathbf{v}) &:= \frac{1}{|\mathcal{P}|} \sum_{P_z \in \mathcal{P}} \sum_{s \subseteq z} y_s \frac{1}{|\mathcal{C}(s)|} \sum_{\substack{g, g' \subseteq s \\ \zeta(g, g') = s}} \langle v_g, v_{g'} \rangle \\
\mathcal{W}_2(\mathbf{v}) &:= \frac{\rho}{|\mathcal{P}|} \left[ \sum_{P_z \in \mathcal{P}} \sum_{\substack{g, g', h, h' \subseteq z \\ \zeta(g, g') = \zeta(h, h')}} (\langle v_g, v_{g'} \rangle - \langle v_h, v_{h'} \rangle)^2 \right] \\
\mathcal{W}_3(\mathbf{v}) &:= \frac{\rho}{|\mathcal{P}|} \sum_{v_s \in \mathbf{v}} (\|v_s\|^2 - 1)^2
\end{aligned}$$

Such that  $\mathcal{L}_\rho(\mathbf{v}) := \mathcal{W}_1(\mathbf{v}) + \mathcal{W}_2(\mathbf{v}) + \mathcal{W}_3(\mathbf{v})$ . We break the hessian apart into three terms

$$\begin{aligned}
\|\nabla^2 \mathcal{L}_\rho(\mathbf{v}) - \nabla^2 \mathcal{L}_\rho(\hat{\mathbf{v}})\|_F &\leq \|\nabla^2 \mathcal{W}_1(\mathbf{v}) - \nabla^2 \mathcal{W}_1(\hat{\mathbf{v}})\|_F \\
&\quad + \|\nabla^2 \mathcal{W}_2(\mathbf{v}) - \nabla^2 \mathcal{W}_2(\hat{\mathbf{v}})\| + \|\nabla^2 \mathcal{W}_3(\mathbf{v}) - \nabla^2 \mathcal{W}_3(\hat{\mathbf{v}})\| \quad (158)
\end{aligned}$$

The first term is zero as its the hessian of a quadratic which is a constant. The difference is then zero. We bound the second term as follows.

$$\begin{aligned} \|\nabla^2 \mathcal{W}_2(\mathbf{v}) - \nabla^2 \mathcal{W}_2(\hat{\mathbf{v}})\| &\leq \frac{\rho}{|\mathcal{P}|} \left\| \sum_{P_z \in \mathcal{P}} \sum_{\substack{g, g', h, h' \subseteq z \\ \zeta(g, g') = \zeta(h, h')}} (\nabla^2 \mathcal{T}_{(g, g', h, h')}(\mathbf{v}) - \nabla^2 \mathcal{T}_{(g, g', h, h')}(\hat{\mathbf{v}})) \right\|_F \\ &\leq \frac{\rho}{|\mathcal{P}|} \sqrt{\sum_{P_z \in \mathcal{P}} \sum_{\substack{g, g', h, h' \subseteq z \\ \zeta(g, g') = \zeta(h, h')}} 64B^2 (\|\delta_g\|^2 + \|\delta_{g'}\|^2 + \|\delta_h\|^2 + \|\delta_{h'}\|^2)} \end{aligned}$$

Noticing that each  $\delta_g$  can be involved in no more than  $|\mathcal{P}|$  sums by being variables in every single predicate.

$$\leq \frac{8B\rho}{|\mathcal{P}|} \sqrt{|\mathcal{P}| \|V - \hat{V}\|_F^2} \leq \frac{8B\rho}{\sqrt{|\mathcal{P}|}} \|V - \hat{V}\|_F$$

Now we move on to bound  $\mathcal{W}_3$

$$\begin{aligned} \|\mathcal{W}_3(\mathbf{v}) - \mathcal{W}_3(\hat{\mathbf{v}})\|_F &= \frac{\rho}{|\mathcal{P}|} \left\| \sum_{v_s \in \mathbf{v}} (\nabla^2 (\|v_s\|^2 - 1)^2 - \nabla^2 (\|\hat{v}_s\|^2 - 1)^2) \right\|_F \\ &\leq \frac{\rho B}{|\mathcal{P}|} \sqrt{\sum_{v_s \in \mathbf{v}} \|v_s - \hat{v}_s\|^2} = \frac{\rho B}{|\mathcal{P}|} \|V - \hat{V}\|_F \end{aligned}$$

Putting all three terms together we obtain the smoothness of the hessian is dominated by  $\mathcal{W}_2$ .

$$\|\nabla^2 \mathcal{L}_\rho(\mathbf{v}) - \nabla^2 \mathcal{L}_\rho(\hat{\mathbf{v}})\|_F \leq \left( \frac{8B\rho}{\sqrt{|\mathcal{P}|}} + \frac{B\rho}{|\mathcal{P}|} \right) \|V - \hat{V}\|_F \leq \frac{8B\rho}{\sqrt{|\mathcal{P}|}} \|V - \hat{V}\|_F$$

□

## F.1 MISCELLANEOUS LEMMAS

**Theorem F.1** (perturbed-gd Jin et al. (2017)). *Let  $f$  be  $\ell$ -smooth (that is, its gradient is  $\ell$ -Lipschitz) and have a  $\gamma$ -Lipschitz Hessian. There exists an absolute constant  $c_{max}$  such that for any  $\delta \in (0, 1)$ ,  $\epsilon \leq \frac{\ell^2}{\gamma}$ ,  $\Delta_f \geq f(X_0) - f^*$ , and constant  $c \leq c_{max}$ ,  $PGD(X_0, \ell, \gamma, \epsilon, c, \delta, \Delta_f)$  applied to the cost function  $f$  outputs a  $(\gamma^2, \epsilon)$  SOSP with probability at least  $1 - \delta$  in*

$$O\left(\frac{(f(X_0) - f^*)\ell}{\epsilon^2} \log^4\left(\frac{d\ell\Delta_f}{\epsilon^2\delta}\right)\right)$$

iterations.

**Definition.**  $[(\gamma, \epsilon)$ -second order stationary point] A  $(\gamma, \epsilon)$  second order stationary point of a function  $f$  is a point  $x$  satisfying

$$\begin{aligned} \|\nabla f(x)\| &\leq \epsilon \\ \lambda_{min}(\nabla^2 f(x)) &\geq -\sqrt{\gamma\epsilon} \end{aligned}$$

**Theorem F.2.** (Robustness Theorem 4.6 (Raghavendra & Steurer, 2009a) rephrased) *Let  $\mathbf{v}$  be a set of vectors satisfying the constraints of SDP 1 to additive error  $\epsilon$  with objective  $OBJ(\mathbf{v})$ , then*

$$SDP(\Lambda) \geq OBJ(\mathbf{v}) - \sqrt{\epsilon} \text{poly}(kq)$$

**Corollary 2.** Given a Max-k-CSP instance  $\Lambda$ , there is an  $\text{OptGNN}_{M, \Lambda}(\mathbf{v})$  with  $T = \text{poly}(\delta^{-1}, \epsilon^{-1}, |\mathcal{P}|q^k)$  layers,  $r = |\mathcal{P}|q^k$  dimensional embeddings, with learnable parameters  $M = \{M_1, \dots, M_T\}$  that outputs a set of vectors  $\mathbf{v}$  satisfying the constraints of SDP 1 and approximating its objective,  $SDP(\Lambda)$ , to error  $\epsilon$  with probability  $1 - \delta$ .

*Proof.* The proof is by inspecting the definition of  $\text{OptGNN}$  in the context of Theorem 3.1. □

**Corollary 3.** The  $\text{OptGNN}$  of Corollary 2, which by construction is equivalent to Algorithm 2, outputs a set of embeddings  $\mathbf{v}$  such that the rounding of Raghavendra & Steurer (2009a) outputs an integral assignment  $\mathcal{V}$  with a Max-k-CSP objective  $OBJ(\mathcal{V})$  satisfying  $OBJ(\mathcal{V}) \geq S_\Lambda(SDP(\Lambda) - \epsilon) - \epsilon$  in time  $\exp(\exp(\text{poly}(\frac{kq}{\epsilon})))$  which approximately dominates the Unique Games optimal approximation ratio.

---

*Proof.* The proof follows from the robustness theorem of Raghavendra & Steurer (2009a) which states that any solution to the SDP that satisfies the constraints approximately does not change the objective substantially Theorem F.2.  $\square$